Earth & Ocean Sciences
School of Natural Sciences
National University of Ireland, Galway

High-resolution habitat suitability modelling of vulnerable marine ecosystems in the deep sea

A thesis submitted for the degree of Doctor of Philosophy

Anna Maria Rengstorf (M.Sc.)

February 2013

Supervisors: Dr. Anthony Grehan
Prof. Colin Brown

Acknowledgements

This study was carried out within the framework of the European Community's Seventh Framework Programme (FP7/2007-2013) CoralFISH project (grant agreement n° 213144) and with the support of the Department of Communications, Energy and Natural Resources National Geoscience Programme 2007-2013 (Griffith Geoscience post-graduate fellowship). Additional travel funding, received from the Thomas Crawford Hayes trust fund and the Ron McDowell Student Support Award, was also greatly appreciated. My sincere gratitude goes to my project co-supervisors: Colin Brown for his unfailing enthusiasm, constructive comments and fruitful discussions throughout the course of this PhD; and Anthony Grehan for conceiving the project, for providing me with the opportunity of working on habitat suitability modelling of cold-water corals and of participating in numerous international research cruises, workshops and conferences. It was a pleasure to be part of the CoralFISH project, and I am thankful to all its members for their invaluable scientific input. Special thanks to Chris Yesson, who introduced me to the world of habitat suitability modelling, and whose contribution enhanced chapters 2 and 3 of this thesis. Particular thanks also to Christian Mohn for the productive, very interesting and fun collaboration on chapters 4 and 5.

It is a pleasure to express my gratitude to all staff members in Earth and Ocean Sciences, in particular Sadhbh Baxter for her effort with all CoralFISH related issues and her moral support throughout my PhD, Martin White for discussions on the oceanographic elements of this research, Garret Duffy for consultations on seabed surveys, Shane Rooney for technical support and Lorna Larkin for administrative support. I am also thankful to Inge van den Beld and Giulia Prato for their significant help in the video lab. Thanks to all postgraduates in the School of Natural Sciences past and present, for useful discussions and countless laughs throughout the last years.

I would like to express my cordial thanks to all involved in cruises CE0908 and CE10014, including engineers and pilots of ROV Holland I, Captain and crew of R.V. Celtic Explorer, all members of the shipboard scientific parties, and Anthony Grehan for providing me with subsequent access to the data and video collected during the cruises. Many thanks to Janine Guinan (GSI) and Louise Allcock (NUIG) for sharing the video footage of cruises CE0915 and CE10004 respectively, to Kieran Lyons (MI) for providing the Marine Institute's hydrodynamic model output, and to Xavier Monteys (GSI) for providing the INSS data.

I take this opportunity to thank my Galwegian friends and housemates, for keeping me sane throughout these years, and all my far away friends and family, for remaining close in spite of the geographical distance. I want to particularly thank my sister Isabel, my brother Philipp, and Nicolas, for their patience, understanding and encouragement, no matter what. Finally, this is for my parents; there are no words to express how grateful I am for your unconditional support, for letting me live my dreams whilst having my back, during the course of this PhD and always.

DECLARATION

This work has not previously been submitted for a degree in any university. To the best of my knowledge and belief, the thesis contains no material previously published or written by another person except where due reference is made in the thesis itself.

Anna M. Rengstorf

Abstract

Knowledge of the spatial distribution of species and habitats is crucial for effective management of marine resources. Data to support informed decision-making in the deep sea are often sparse or absent, as offshore sampling surveys are expensive, time-consuming, have limited coverage and are spatially biased. Habitat suitability models (HSMs) make use of the limited data available and are being applied increasingly to create continuous coverage maps of the potential distribution of species or habitats. Such maps have value as decision support tools for future survey planning, design of marine protected area networks and ultimately the implementation of marine spatial planning. In the deep sea, the quality of these maps is sub-optimal because of 1) the frequent lack of high-resolution ecologically relevant environmental variables, 2) species distribution data arising from opportunistic, spatially biased sampling, and 3) a lack of reliable species absence data. Therefore, this thesis has as its primary objective the development of repeatable and robust methods for deep-sea benthic HSM that take into account these issues.

Based on the case study of predicting suitable habitat for the cold-water coral *Lophelia pertusa* (Linnaeus 1758) in the north-east Atlantic, this thesis extends existing benthic HSM methodologies by 1) maximising the resolution and information content of environmental variables, 2) optimising the reliability of presence-only modelling methods, 3) investigating the predictive power of high-resolution environmental variables derived from 3D hydrodynamic models, 4) assessing the use of quantitative species occurrence proportion data for calibrating models, and 5) exploring the applicability of mixed models to account for spatially grouped transect data. The key outcome is the first reliable high-resolution HSM for *Lophelia pertusa* reef habitat as a tool for ecosystem-based management in Irish waters. The implications of HSMs for conservation, marine spatial planning and an understanding of ecosystem functioning and processes are discussed.

Contents

List of Figures

List of Tables

1. Introduction

1.1. General introduction and key concepts

From the beginnings to modern deep-sea research

The deep sea, as defined and used here, includes seabed areas and waters below the depth of 200 m and represents the largest biome of the global biosphere. It covers an area of approximately 360 million km^2, equivalent to 50% of the Earth's surface and 90% of the Earth's ocean area (UNEP 2007, Ramirez-Llodra *et al.* 2011). The exploration of the deep sea began about 150 years ago, stimulated by Forbes' infamous *azoic theory*, which postulated that the growing pressure, coldness and darkness with increasing water depth impeded the existence of living organisms below approximately 550 m (Forbes 1844). Surprisingly, this theory was widely accepted at the time. However, 25 years later, dredging activities from the *HMS Lightning* and the *HMS Porcupine* around the British Isles revealed the existence of life at water depths below 4000 m (Thomson 1873). These findings were the catalyst for the great *Challenger* expedition of 1872–1876, which explored and catalogued the deep-sea floor of the world's oceans and is considered to mark the birth of modern oceanography. Three quarters of a century later, the *Galathea* expedition (1950-1952) and Picard's and Walsh's submarine dive to the Challenger Deep (1960) proved that living organisms exist at all water depths, including the deepest parts of the ocean (>10 000 m).

Since then, technological developments and new discoveries have promoted a rapidly growing field of modern deep-sea research. In the 1960s and 1970s, increasingly sophisticated sampling equipment became available to researchers, ranging from trawls and dredges to a variety of coring and grabbing devices and finally video platforms which enable direct observations of deep-sea habitats and associated species (Gage & Bett 2005). Rapid advances in seabed mapping techniques using single-beam, multi-beam and side-scan sonars (Kenny *et al.* 2003, Anderson *et al.* 2008, Brown *et al.* 2011) have revealed previously unknown deep-sea habitat heterogeneity. A (non-exhaustive) list of known deep-sea benthic habitat

types includes open slopes, abyssal plains, seamounts, carbonate mounds, submarine canyons, cold-water coral habitats, cold seeps, hydrothermal vents, mud volcanoes and manganese-nodule provinces, all of which support a diverse and specialized fauna (UNEP 2007, Ramirez-Llodra *et al.* 2011). Developments in submarine technology and robotics, such as remotely operated vehicles (ROVs) and autonomous underwater vehicles (AUVs), now increasingly allow scientists to access and sample these remote regions of the ocean.

We have come a long way since Forbes' *azoic theory*. International research programmes, such as INDEEP (International network for scientific investigation of deep-sea ecosystems, http://www.indeep-project.org/), the Census of Marine Life (www.coml.org/) and EU-funded projects like HERMES (www.eu-hermes.net), HERMIONE (www.eu-hermione.net/) and CoralFISH (www.eu-fp7-coralfish.net/), are rapidly expanding our knowledge. We are improving our understanding of deep-sea ecosystem functions and processes, and we have taken first steps to value their goods and services (Armstrong *et al.* 2012). Yet, the deep sea remains the least studied ecosystem on Earth. Merely 5% of the deep-sea floor has been explored remotely and less than 0.01% has been sampled (Ramirez-Llodra *et al.* 2010). Given the deep sea's enormous size, its value in providing important goods and services, and its vulnerability to the ever-increasing anthropogenic impacts, there is an urgent need to deepen our knowledge on vulnerable deep-sea ecosystems, to map their spatial distribution, and to ensure their sustainable management and conservation.

Services and threats of deep-sea ecosystems

Ecosystem goods and services are the benefits human populations derive from ecosystem functions (Armstrong *et al.* 2012). The deep sea is a reservoir of a wide range of living and non-living resources. Commonly exploited goods include commercially important fin- and shellfish, genetic resources and chemical compounds for pharmaceuticals, oil, gas and minerals, and the provision of sites for waste disposal and CO_2 storage (Davies *et al.* 2007, UNEP 2007, Armstrong *et al.* 2012). The deep sea also provides important supporting and regulating services, including the provision of habitat to a highly diverse fauna, nutrient and water

cycling, chemosynthetic primary production, carbon sequestration and storage, gas and climate regulation, amongst others (UNEP 2007, Armstrong *et al.* 2012).

Due to diminishing resources on land and in shallow waters, the anthropogenic foot print in the deep sea is expanding at alarming rates (Halpern *et al.* 2008b, Benn *et al.* 2012). Advances in technology now facilitate exploitation of previously inaccessible resources of economic value. Adverse and sometimes cumulative impacts of deep-sea fisheries, oil and gas exploitation, cable and pipeline laying, littering and dumping, deep-sea mining, carbon capture and storage seriously threaten the health of deep-sea ecosystems (Glover & Smith 2003, Davies *et al.* 2007, Ramirez-Llodra *et al.* 2011, Benn *et al.* 2012). These effects are superimposed by climate-induced changes in ocean temperature, circulation and stratification, nutrient input and primary production, oxygen content, and ocean acidification (Smith *et al.* 2009, Doney *et al.* 2012). The latter is likely to have fatal consequences for some deep-sea habitats and species, especially for calcifying fauna such as bivalves and scleractinian corals (Orr *et al.* 2005, Guinotte & Fabry 2008, Feely *et al.* 2009).

Vulnerable marine ecosystems

High longevity and slow growth rates make certain deep-sea species (e.g. orange roughy, *Hoplostethus atlanticus*) and habitats (e.g. cold-water coral reefs and coral gardens) especially vulnerable to adverse impacts (Rogers *et al.* 2008, Auster *et al.* 2011). A rapid implementation of effective and precautionary measures is required to hinder their unsustainable exploitation or destruction. Criteria for identifying vulnerable marine ecosystems (VMEs) include their rarity or uniqueness, their functional significance, fragility, structural complexity as well as life histories that limit the probability of recovery (Rogers *et al.* 2008). Common examples include cold-water coral and sponge habitats, chemosynthetic ecosystems around hydrothermal vents and geophysical features such as seamounts. The scleractinian cold-water coral *Lophelia pertusa* (Linnaeus 1758), for example, forms fragile three-dimensional frameworks and reefs, that are easily destroyed by bottom fishing gear. Several known coral reef habitats have already been damaged by bottom trawling, resulting in severe loss of habitat complexity and a reduction of local biodiversity (Hall-Spencer *et al.* 2002, Grehan *et al.* 2005, Wheeler *et al.* 2005). Trawling

impacts have been found to be long lasting (Althaus *et al.* 2009) and to affect the reproductive biology and therefore the resilience of framework-building cold-water corals (Waller & Tyler 2005).

Policy context

Over the last decades, the United Nations, international conventions and organisations have developed a number of legal instruments and regulations in order to protect marine biodiversity, to sustainably manage offshore marine resources, and to control activities impacting the deep oceans (Table 1-1).

Table 1-1: Examples of international frameworks relevant for the protection and conservation of marine biodiversity and vulnerable marine ecosystems (VMEs) in the north-east Atlantic.

Framework	Main objectives
Convention on Biological Diversity	To conserve biodiversity To use biological diversity in a sustainable fashion To share benefits of genetic resources fairly and equitably
UNGA Resolutions 61/105 and 64/72	To assess the impact of bottom fishing on VMEs To identify/map VMEs through improved scientific research To close such areas to bottom fishing
United Nations Convention on the Law of the Sea (UNCLOS)	To define the rights and responsibilities of nations in their use of the oceans To protect and preserve the marine environment, including rare and fragile ecosystems and the habitats of threatened or endangered species
United Nations Fish Stocks Agreement (1995)	To impose obligations on coastal and fishing nations with respect to their management of highly migratory and straddling fish stocks in national and international waters
OSPAR Convention	To protect the maritime area against adverse effects of human activities in order to ensure human health and to conserve or restore marine ecosystems
EU Habitats Directive (92/43/EEC)	To promote the maintenance of biodiversity by requiring EU Member States to maintain, restore and monitor natural habitats and wild species listed in Annexes I and II at a "favourable conservation status"
EU Strategic Environmental Assessment Directive (2001/42/EC)	To enforce integration of environmental considerations into preparation and adoption of plans and programmes of industrial sectors in order to protect listed habitats from potential adverse impacts.
EU Marine Strategy Framework Directive (2008/56/EC)	To establish a framework within which EU member States shall take necessary measures to achieve or maintain "good environmental status" in the marine environment by the year 2020
EU Water Framework Directive (2000/60/EC)	To establish a framework for the protection of inland surface waters, transitional waters, coastal waters and groundwater
Bern Convention on the Conservation of European Wildlife and Natureal Habitats	To conserve wild flora and fauna and their natural habitats To promote cooperation between states To monitor and control endangered and vulnerable species To provide assistance concerning legal and scientific issues

In late 2006, the United Nations General Assembly Resolution 61/105 called upon States "to take action immediately, individually and through regional fisheries

management organizations and arrangements, and consistent with the precautionary approach and ecosystem approaches, to sustainably manage fish stocks and protect vulnerable marine ecosystems, including seamounts, hydrothermal vents and cold-water corals, from destructive fishing practices, recognizing the immense importance and value of deep-sea ecosystems and the biodiversity they contain" (UNGA 2006). In response, some Regional Fisheries Management Organizations, such as the North-East Atlantic Fisheries Commission (NEAFC), have adopted spatial conservation measures for existing and future bottom-fishing areas (NEAFC 2010), as well as (rather ineffective) move-on rules and environmental impact assessments for exploratory fisheries in order to protect VMEs (Weaver *et al.* 2011)

On a European level, the EU Habitats and Species Directive (92/43/EEC) requires member states to implement Special Areas of Conservation (SACs) for listed habitats (92/43/EEC Annex I) and species (Annex V) within their areas of national jurisdiction (200 nm limit). Four offshore SACs have been designated within Irish waters which are protecting *Lophelia pertusa* reefs (Annex I, category Reefs - Code 1170) from bottom fishing: the Belgica Mound Province (SAC 002327, 410.94 km^2), the Hovland Mound Province (SAC 002328, 1086.63 km^2), the South West Porcupine Bank (SAC 002329, 329.31 km^2) and the North West Porcupine Bank (SAC 002330, 716.43 km^2).

Within the north-east Atlantic region, the OSPAR Convention for the Protection of the Marine Environment of the north-east Atlantic (1992) requires the establishment of a network of marine protected areas (MPAs) for the protection, management and restoration of certain species and habitats listed under the OSPAR List of Threatened and/or Declining Species and Habitats (OSPAR 2010). The World Conservation Union (IUCN) has defined a marine protected area as "any area of intertidal or subtidal terrain together with its overlying water and associated flora, fauna, historical and cultural features, which has been reserved by law or other effective means to protect part or all of the enclosed environment." Depending on the objectives, the regulation levels within an MPA may vary greatly, ranging from managed multiple use areas to areas of restricted access. By the publication of the status report on the OSPAR network of MPAs in 2010, a total of 159 sites were

adopted, collectively covering ~150 000 km² of the OSPAR maritime area. However, only 22% of these designated OSPAR sites were located in offshore areas, resulting in an unbalanced distribution of MPAs within the respective exclusive economic zones (EEZs) as well as within the overall OSPAR region. Shortly after publication of the OSPAR status report, which highlighted the international need to overcome the network gaps in offshore areas, the OSPAR convention established the world's first network of MPAs in the high seas, covering approximately 286 200 km^2 of the North-East Atlantic (O'Leary *et al.* 2012).

Ecosystem-based management

The environmental legislations and initiatives summarised in Table 1-1 demonstrate an increasing effort at regional and global level to shift towards an ecosystem-based management of marine resources. Ecosystem-based management is a fundamentally place-based, holistic and integrative approach, that aims to effectively move away from traditional sector-based management and to incorporate the associated human population as an integral part of the ecosystem (Curtin & Prellezo 2011, Katsanevakis *et al.* 2011, UNEP 2011). The core objectives of ecosystem-based management include i) recognising connections among marine, coastal and terrestrial systems, including human societies; ii) utilizing an ecosystem services perspective that recognizes the value of important ecosystem functions; iii) considering cumulative adverse impacts of multiple stressors affecting an ecosystem; iv) managing and balancing multiple and sometimes conflicting objectives; and v) embracing change, learning, and adapting throughout the management process (UNEP 2011).

Marine spatial planning (MSP) is an essential tool for the practical implementation of ecosystem-based management (Douvere 2008). Ehler & Douvere (2009) describe MSP as "analysing and allocating parts of three-dimensional marine space to specific uses or non-use, to achieve ecological, economic, and social objectives that are usually specified through political process". Within this context, marine protected area networks provide a means for emphasised protection of features and processes within the ecosystem to be managed (OSPAR 2010, Katsanevakis *et al.* 2011). Ocean Zoning can be applied to partition a larger region into zones designed to allow

or prohibit certain activities (Halpern *et al.* 2008a, Katsanevakis *et al.* 2011). Geographic information systems (GIS) are commonly used to store, process, integrate, analyse and visualise relevant spatial data (Longley *et al.* 2005). A large range of GIS-based decision support tools for ecosystem-based management exist, for example Marxan (Ball & Possingham 2000) or Marxan with Zones (Watts *et al.* 2009), which assist managers in systematic spatial planning.

The concept of ecosystem-based marine spatial planning has been adopted by multiple governments, ranging from Western European countries and the United States to China and Australia, which have developed and implemented first MSP initiatives of different spatial and integrative dimensions (Ehler & Douvere 2009, Foley *et al.* 2010). In the high seas, MSP is hampered by a range of factors, including serious gaps in authority and scarcity of comprehensive data describing biological patterns (Ardron *et al.* 2008).

Marine habitat mapping

Marine habitat mapping is a powerful tool for ecosystem-based management and has recently become a standard practice in national and international marine spatial planning initiatives (Cogan *et al.* 2009). Holistic marine habitat mapping is a complex process that requires the integration of state of the art technology and statistical tools with data and scientific expertise from a range of disciplines including geology, biology, chemistry and oceanography (Figure 1-1). The standard mapping procedure usually involves the combination of full coverage, remotely sensed (e.g. using multibeam echosounders) or modelled (e.g. using ocean circulation models) data with in situ ("groundtruth") data derived from video surveys, sediment samples and oceanographic measurements within a GIS framework (Foster-Smith *et al.* 2007, Brown *et al.* 2011). Terrain geomorphology and substratum type can be readily obtained from multibeam bathymetry and backscatter data, and may act as surrogates for biological assemblages on the seafloor (Wilson *et al.* 2007, Degraer *et al.* 2008, Holmes *et al.* 2008, Verfaillie *et al.* 2008, Howell *et al.* 2011, Reiss *et al.* 2011). Full coverage habitat maps may be obtained by extrapolating the observed species-surrogate relationships over larger areas. In this sense, a habitat map does not necessarily reflect reality, but "is a

statement of our best estimate of habitat distribution at a point in time making best use of the knowledge we have available at that time" (Foster-Smith *et al.* 2007).

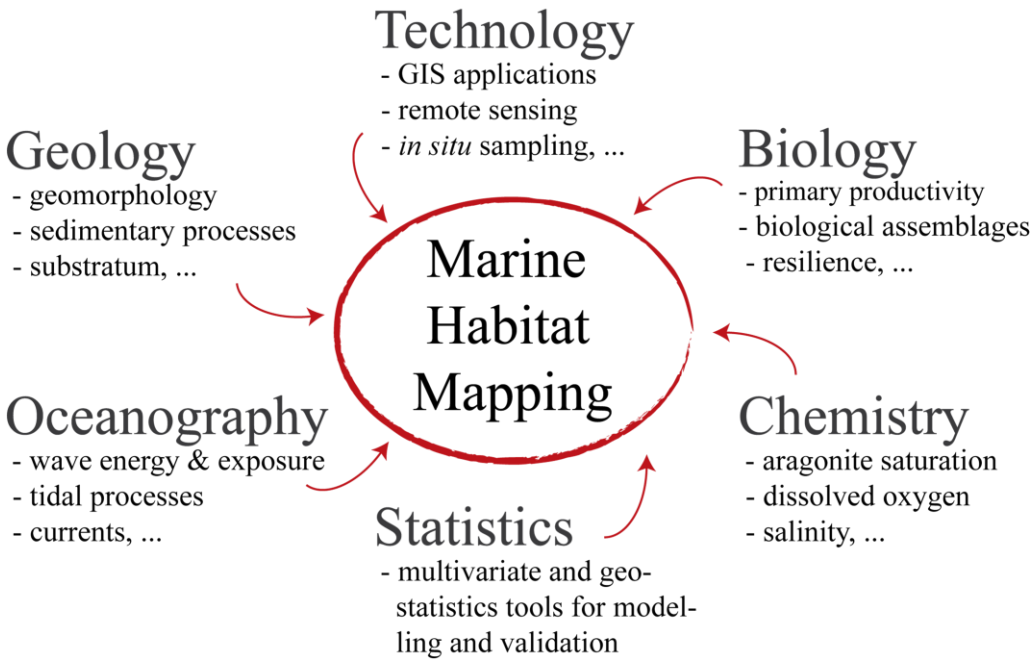

Figure 1-1: Summary of the main elements and disciplines related to benthic habitat mapping.

Habitat suitability modelling

An approach aimed at estimating single species or community distributions in geographic space is a central research tool in theoretical and applied ecology (Guisan & Zimmermann 2000, Elith & Leathwick 2009b). Habitat suitability models (HSMs), also referred to as species distribution models (Elith & Leathwick 2009b), environmental niche models (Hirzel *et al.* 2002) or resource selection functions (Boyce *et al.* 2002) statistically relate species occurrence data with environmental predictor variables to estimate full-coverage potential species distribution in geographic space (Guisan & Zimmermann 2000, Elith & Leathwick 2009b, Franklin 2009). Marine HSMs have been generally under-utilized compared to the terrestrial realm, but are recently receiving growing interest because of the increasing availability of relevant datasets and the international commitments to map and sustainably manage marine resources (Robinson *et al.* 2011). Useful marine applications include the prediction of the potential distribution of invasive species (Tyberghein *et al.* 2012), the estimation of impact of a changing climate on future

distributions (Lima *et al.* 2007, Tittensor *et al.* 2010a), to assess patterns of marine biodiversity (Tittensor *et al.* 2010b) and to aid conservation planning (Brown *et al.* 2012, Marshall 2012), amongst others.

A large range of algorithms is available for HSM (Table 1-2) and several comprehensive reviews of model types have been provided over the last decade (Guisan & Zimmermann 2000, Segurado & Araújo 2004, Guisan & Thuiller 2005, Elith *et al.* 2006, Franklin 2009). Methods range from relatively simple environmental envelopes using presence-only data (e.g. BIOCLIM, Busby 1991) to statistical models such as generalized linear models (GLMs) and generalized additive models (GAMs) using presence-absence data (Guisan *et al.* 2002) to machine learning algorithms such as Maxent (Phillips *et al.* 2006), Boosted Regression Trees (BRT, Elith *et al*. 2008) and Artificial Neural Networks (ANN, Lek & Guègan 1999).

Table 1-2: Common HSM algorithms, key features and references. Table modified from Elith & Leathwick (2009a).

Algorithm	Algorithm category [1]	Response variable [2]	Complexity of response [3]	Type of prediction [4]	Predictive performance [3]	Reference
BIOCLIM	Envelope	P	L	R	L	(Busby 1991)
DOMAIN	Envelope	P	L-M	C	L	(Carpenter *et al.* 1993)
ENFA	Factor analysis	P	L-M	C	M	(Hirzel *et al.* 2002)
GARP	Genetic algorithm	P	L-H	R	L-M	(Stockwell & Peters 1999)
Maxent	ML/maximum entropy	P	H	C	H	(Phillips *et al.* 2006)
GLM	Regression	PA, CT	L-H	C	M-H	(Guisan *et al.* 2002)
GAM	Regression	PA, CT	L-H	C	M-H	(Guisan *et al.* 2002)
CART	ML/Tree	PA, CT	L-M	C/B	L-M	(De'Ath & Fabricius 2000)
MARS	ML/Regression	PA, CT	L-H	C	M-H	(Friedman 1991)
BRT	ML/Regression/Tree	PA, CT	M-H	C	H	(Elith *et al.* 2008)
ANN	ML/Regression	PA	L-H	C	M-H	(Lek & Guègan 1999)
Bayesan	Bayesan	PA, CT	L-H	C	M-H	(Wade 2000)

[1] ML = machine learning
[2] P = presence-only; PA = presence-absence (or presence-pseudo-absence); CT = count data
[3] L = low, M = medium, H = high
[4] C = continuous, R = rank, B = binary

The appropriate model choice usually depends on 1) the amount and type (continuous or categorical) of the environmental predictor variables, 2) the complexity of the response curves and possible interactions between predictors, 3) the type of response variable (i.e. presence-only, presence-absence or count data), and 4) what one attempts to model (e.g. realized vs. potential distribution, Jiménez-Valverde *et al*. 2008). Table 1-2 summarises important attributes for a range of commonly used HSM algorithms.

HSM requires a number of steps including 1) ecological conceptualization (e.g. literature research), 2) collecting new or existing species occurrence data and filtering this data for useful, representative records, 3) developing new or collating existing environmental predictor variables, 4) selecting an appropriate model

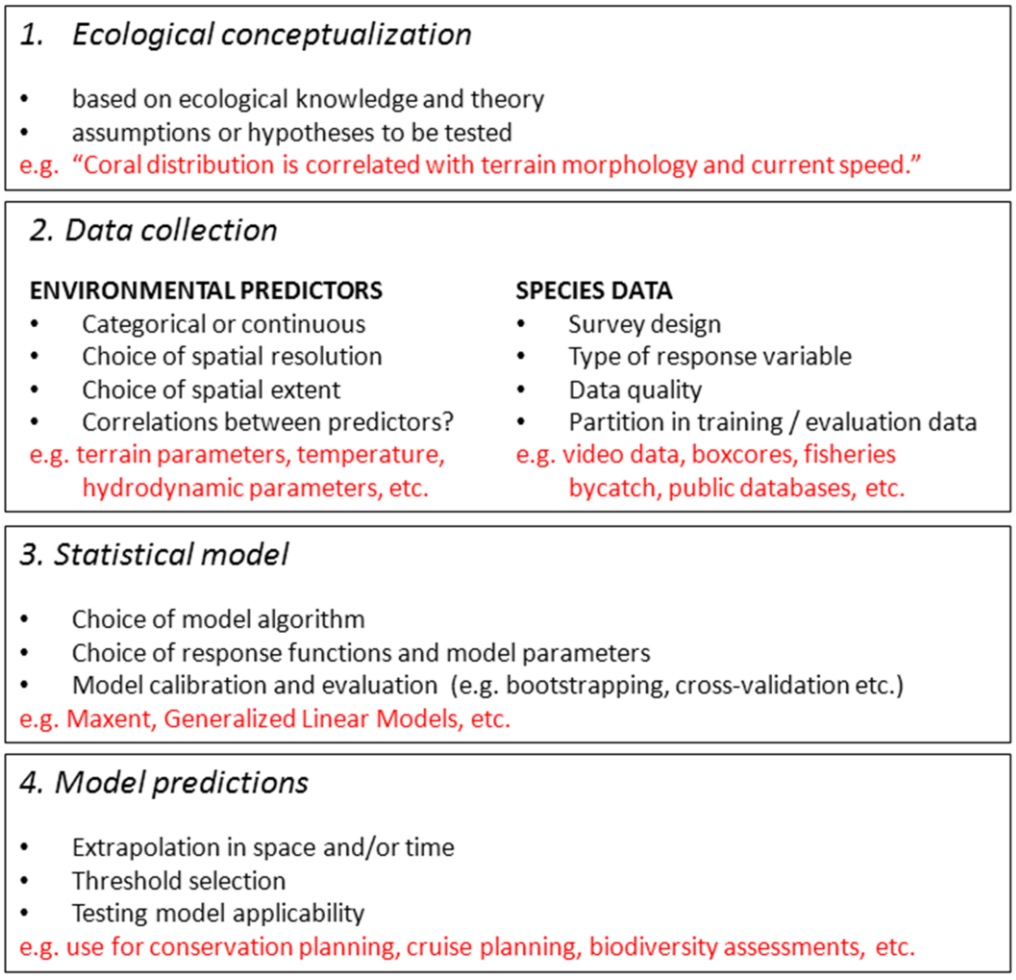

Figure 1-2: Key steps and considerations in Habitat Suitability Modelling (HSM). Examples are given for modelling suitable habitat for cold-water corals (in red).

algorithm, 5) calibrating and evaluating the model, 6) projecting predictions onto the entire study area, and 7) selecting a threshold to transform the continuous model result into a binary presence-absence map. The key steps of HSM and important data considerations are summarized in Figure 1-2. The Introduction and Method sections of Chapters 3 and 5 give relevant details in the context of *Lophelia pertusa* habitat preferences and HSM for cold-water corals.

1.2. Scope of thesis

The FP7 EU-Project CoralFISH consists of an international and interdisciplinary consortium of deep-sea scientists, modellers, oceanographers, economists and the fishing industry, with the ambition to assess the interaction between cold-water corals, deep-sea fish and fisheries, and to develop tools to assist ecosystem-based management in the deep waters of Europe and beyond (http://www.eu-fp7-coralfish.net/). This work was developed and conducted within the context of Work Package 6, which aims to "produce habitat suitability maps both regionally and for OSPAR region V to identify areas likely to contain vulnerable habitat". This Ph.D. thesis focuses on the Irish study region and aims to understand and predict the present-day spatial distribution of the framework-building cold-water coral *Lophelia pertusa* (Linnaeus 1758). Relationships between the species and a range of terrain-based and oceanographic predictor variables are analysed and modelled at regional (within the limits of the Irish extended continental shelf claim) and local (within selected carbonate mound provinces) scales (Figure 1-3).

It is noteworthy that other vulnerable marine ecosystems are present within Irish waters, including scleractinian, antipatharian and gorgonian corals as well as deep-sea sponge aggregations (Le Danois 1948). While the cold-water coral *Lophelia pertusa* serves as a single focal species throughout this thesis, the methods developed and described here can be easily adapted to estimate the distribution of other species or habitats, provided that distribution data and ecologically relevant predictor variables are available.

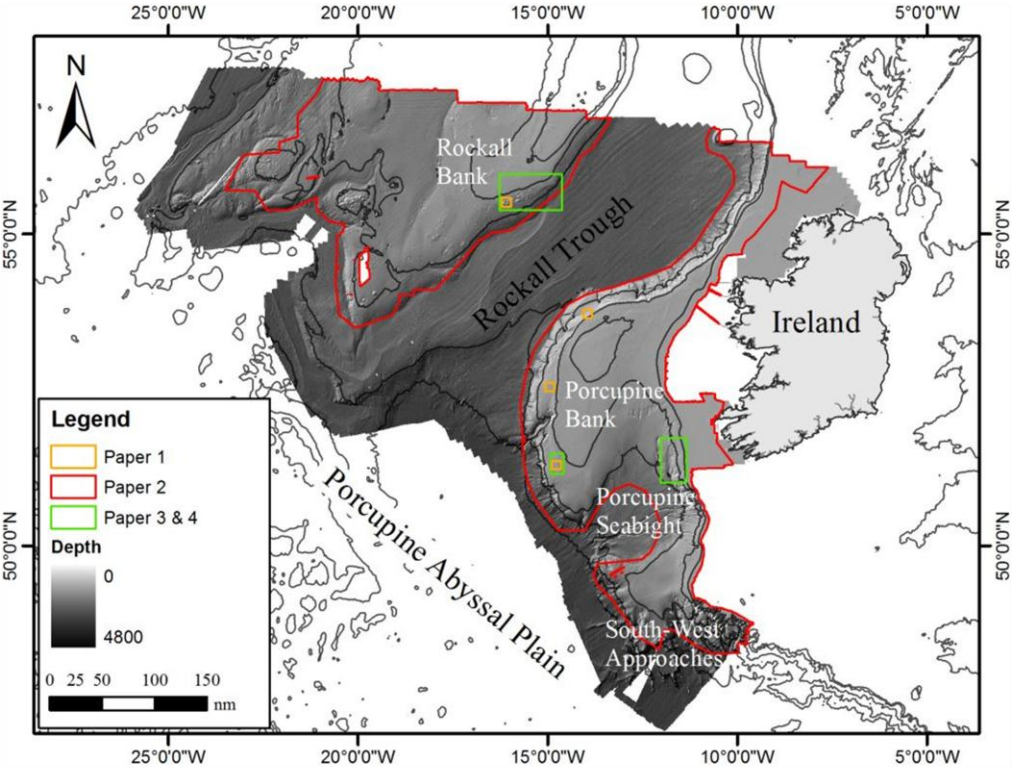

Figure 1-3: Study areas of each of the four research papers that constitute this thesis.

Working in the relatively remote deep-sea environment means that compromises have to be made, for example, related to quality, resolution and spatial coverage of data available for model development. Available deep-sea species distribution data frequently arise from opportunistic sampling and commonly lack (reliable) absence records. The application of deep-sea HSMs is also hindered by the general trade-off between spatial resolution and coverage of environmental predictor variables. Therefore, this thesis is also concerned with a number of methodological issues, such as making best possible use of available data, collecting new data in a standardized and efficient manner, and testing model approaches which incorporate spatial structure in sampling data.

Table 1-3 shows an overview of data and model algorithms tested within the four research papers that constitute this thesis.

Table 1-3: Overview of data and algorithms used within the research papers that constitute this thesis.

	Paper 1 (Chapter 2)	**Paper 2 (Chapter 3)**	**Paper 3 (Chapter 4)**	**Paper4 (Chapter 5)**
Environmental Predictors	Terrain	Terrain Hydrodynamics Chemistry	Hydrodynamics	Terrain Hydrodynamics
Distribution data	Presence-only	Presence-only	Presence-absence	Presence-absence Proportion
Algorithm	Maxent	Maxent	Only exploratory (box plots)	GLM[1] GLMM[2]
Spatial Resolution	50 – 1000 m	200 m	250 m	50 m

[1]GLM: Generalised linear model
[2]GLMM> Generalised linear mixed model

The theory applied to accomplish this research is highly interdisciplinary by nature and includes aspects of biology, ecology, geology, chemistry and oceanography, as well as a profound understanding of statistical modelling. Necessary methodologies to develop the HSMs include processing of multibeam data and terrain analysis, the design of ROV-based sampling surveys, the analysis of video data and the use of software and code to process and analyse large datasets (e.g. R project for Statistical Computing, www.r-project.org), amongst others. Instead of focusing in too much detail on any of these areas, the objective and challenge of this Ph.D. was to recognize and understand the relevant aspects of each discipline, become familiar with the respective concepts and methodologies, and to integrate them in an innovative, applied and productive manner. The strong focus towards applied research and the development of existing HSM methodologies for benthic deep-sea species are reflected throughout the research papers that constitute this thesis.

Specifically this thesis aims to

1. Identify the effect of initial bathymetry grid resolution on terrain-parameters and habitat suitability model predictions (Paper 1),
2. Identify environmental factors influencing the spatial distribution of the cold-water coral *Lophelia pertusa* by means of habitat suitability modelling at local and regional scales (Papers 2 and 4),
3. Develop a regional high-resolution habitat suitability map for *Lophelia pertusa* reefs within the limits of the Irish extended continental shelf claim as a tool for ecosystem-based management (Paper 2),

4. Assess relationships between coral distribution and local scale hydrodynamic regimes in three Irish carbonate mound provinces (Paper 3),
5. Develop local-scale habitat suitability models for *Lophelia pertusa* reefs within three Irish carbonate mound provinces (Paper 4), and
6. Improve existing methods for estimating deep-sea benthic species distributions by testing novel approaches, particularly the use of species distribution proportion data and generalized linear mixed models (Paper 4).

1.3. Summary of Papers

This thesis is structured around the following research papers:

Paper 1 (Chapter 2): Lead author – major role

Rengstorf A., Yesson C., Brown C. & Grehan A. (2012) Towards high-resolution habitat suitability modelling of vulnerable marine ecosystems in the deep sea: resolving terrain attribute dependencies. Marine Geodesy 35:4, 343-361.

This paper addresses the effect of bathymetric grid resolution on terrain parameters and demonstrates the inherited consequences for terrain-based HSMs developed for three cold-water coral carbonate mound areas and one control area off the west coast of Ireland. The raw data of the Irish National Seabed Survey (INSS) were used to generate bathymetric grids of 50 m x 50 m spatial resolution using Fledermaus gridding software. Aggregation and interpolation methods in ArcGIS were used to generate grids of varying spatial resolution and information content. Quantitative and distributional differences between terrain parameters resulting from varying bathymetry grids were assessed visually, by means of Pearson correlation coefficients and by means of descriptive summary statistics. Preliminary HSMs were generated employing Maxent (v3.3.1) using the limited cold-water coral distribution data available at that time (247 occurrence records from Guinan *et al.* 2009a). The study reveals the strong dependency of terrain parameters and HSM results on initial bathymetry grid resolution. It highlights the need for high-resolution (< 250 m) bathymetry data to ensure a realistic representation of the often relatively small carbonate mounds which provide a significant proportion of cold-water coral reefs in Irish waters.

The author was responsible for generating the high-resolution bathymetry grids from the raw INSS data, for bathymetry grid manipulations and terrain analyses, all statistical analyses using R, calibration of the Maxent models, computation of threshold-dependent presence-absence maps, all tables, maps and figures and a major part of the writing.

Paper 2 (Chapter 3): Lead author – major role

Rengstorf A., Yesson C., Brown C. & Grehan A., High-resolution habitat suitability modelling can improve conservation of vulnerable marine ecosystems in the deep sea. Journal of Biogeography (in press)

This paper builds on the suggestions of Paper 1 and integrates terrain parameters derived from the INSS multibeam bathymetry data with a large range of interpolated environmental data to develop a regional high-resolution (0.002° or ~ 200 m) HSM for *Lophelia pertusa* reefs, covering the extended Irish continental shelf claim. Environmental predictor variables were produced by depth-based re-sampling of global oceanographic datasets and a regional ocean circulation model. Multi-scale terrain parameters were computed from the INSS multibeam bathymetry using Landserf and ArcGIS software. A database of *L. pertusa* occurrences was compiled from an extensive review of existing records, as well as from analysis of video data collected during two CoralFISH research cruises. A rigorous quality control ensured that only records were used for analyses that represented living *L. pertusa* reefs. Investigations using Maxent (v3.3.3) revealed high predictive power for local-scale terrain variability (standard deviation of slope: 54 %), followed by near-bottom water temperature (28 %), and near-bottom hydrodynamic settings (bottom stress: 9 %). Suitable coral habitat was predicted on mound features and in canyon areas along a narrow band following the slopes of the Irish continental margin, the Rockall Bank and the Porcupine Bank. The detailed distribution map shows a significant reduction in habitat compared to a recent global scale analysis, and provides the first realistic estimate of *L. pertusa* distribution in Irish waters. The implications for marine spatial management are discussed.

The author was responsible for generating multi-scale terrain parameters, processing of hydrodynamic model output, video acquisition, processing and annotation, development of the *L. pertusa* database and data filtering, environmental variable selection, calibration and spatial cross-validation of the Maxent models, computation of the binary coral distribution map, all tables, maps and figures and a major part of the writing.

Paper 3 (Chapter 4): Second co-author – moderate role

Mohn C., Rengstorf A., Grehan A., White M., Duineveld G. & Soetart K., Linking benthic dynamics and cold-water coral occurrences: Results from a high-resolution modelling study at three cold-water coral provinces in the north-east Atlantic. Journal of Geophysical Research – Oceans (in prep.)

This paper describes the development and results of high-resolution (250 m x 250 m), three-dimensional ocean circulation models developed for three cold-water coral carbonate mound areas off the west coast of Ireland. The ROMS-AGRIF (v3) model was used with a nested model grid to describe benthic currents and a number of key oceanographic parameters for a one month observation period (April 15th – May 15th 2010). The predicted benthic currents and temperature values were validated against in-situ measurements where available. The hydrodynamic model results were placed in an ecological context by overlaying individual records of *Lophelia pertusa* presences and absences derived from ROV-based video transects. The results confirm the intensified benthic dynamics previously observed at individual coral sites. Living corals can mostly be found in areas of dominant downwelling. The 3D hydrodynamic models provide a high-resolution, spatially coherent picture of the distribution and variability of oceanographic key parameters over the full extent of each coral province and beyond.

The author provided ecological guidance, high-resolution bathymetry data and geo-referenced *L. pertusa* presence-absence data. The author conducted all analyses linking coral distribution and hydrodynamic key parameters using ArcGIS and R, prepared Table 4.1, Figures 4.2, 4.6 and 4.9, and had a moderate part in the writing.

Paper 4 (Chapter 5): Lead author – major role

Rengstorf A., Mohn C., Brown C., Wisz M. & Grehan A., Important considerations on the methodology for predicting deep-sea benthic species distributions using high-resolution environmental variables. A shortened version of this material is being prepared for submission to Deep Sea Research.

This paper starts with an overview of available data and methodologies for benthic HSM and illustrates emerging issues related to spatial and thematic data resolution. Using a case study for the prediction of *Lophelia pertusa* in three carbonate mound provinces along the Irish margin, the paper assesses the 1) usefulness of high-resolution hydrodynamic variables to improve HSMs, 2) advantages or otherwise of species occurrence proportion data compared to presence-absence data, 3) use of mixed effect models as an approach to deal with spatially grouped (i.e. pseudo-replicated) transect data, and 4) ability to transfer local scale HSMs generated in one region in order to predict species occurrence in another region. Generalised linear models (GLMs) were employed in the study, as they are flexible and descriptive modelling tools, allow for the use of presence-absence and proportion data, and can be extended to generalised linear mixed models (GLMMs) in R. Models including terrain and hydrodynamic variables performed significantly better than models using terrain variables only. However, inclusion of hydrodynamic variables reduced model transferability, due to the large differences in hydrodynamic settings between study areas. The preliminary results suggest that proportion models perform slightly better than presence-absence models. The usefulness of GLMM was probably mitigated due to the small number of independent transects available.

The author was responsible for most of the intellectual content in the paper, for generating terrain variables from the INSS bathymetry, post-processing of hydrodynamic model output, acquisition, annotation and processing of video data, all statistical analyses, manipulation of the R code to run the GLMs and GLMMs using presence-absence and proportion data, model projections and transferability assessments, all tables, maps and figures and a major part of the writing.

2. Towards high-resolution habitat suitability modelling of vulnerable marine ecosystems in the deep sea: resolving terrain attribute dependencies

Abstract

Recent habitat suitability models used to predict the occurrence of vulnerable marine species, particularly framework building cold-water corals, have identified terrain attributes such as slope and bathymetric position index as important predictive parameters. Due to their scale dependent nature, a realistic representation of terrain attributes is crucial for the development of reliable habitat suitability models. In this paper, three known coral areas and a non-coral control area off the west coast of Ireland were chosen to assess quantitative and distributional differences between terrain attributes derived from bathymetry grids of varying resolution and information content. Correlation analysis identified consistent changes of terrain attributes as grain size was altered. Response characteristics and dimensions depended on terrain attribute types and the dominant morphological length-scales within the study areas. The subsequent effect on habitat suitability maps was demonstrated by preliminary models generated at different grain sizes. This study demonstrates that high-resolution habitat suitability models based on terrain parameters derived from multi-beam generated bathymetry are required to detect many of the topographical features found in Irish waters that are associated with coral. This has implications for marine spatial planning in the deep sea.

Keywords: carbonate mounds, cold-water coral, ecosystem-based management, habitat suitability modelling, spatial resolution, terrain analysis

2.1. Introduction

In late 2006, the UN General Assembly resolution 61/105 highlighted the major need to identify, map and protect vulnerable marine ecosystems including cold-water corals from anthropogenic impacts such as bottom trawling (UNGA 2006). In order to facilitate the design and implementation of effective marine protected areas (MPAs), extensive knowledge of habitat distribution and species-habitat relationships is needed. However, information on deep-sea habitats is generally limited, since ROV- or submarine-based surveys are expensive and time-consuming. In the absence of complete surveys, habitat suitability modelling (HSM) can be applied to predict full coverage distribution of key species based on available presence-only point data (Hirzel *et al.* 2002, Phillips *et al.* 2006). Resulting species distribution maps can provide useful and cost-effective support for future survey planning and the design of MPAs (Galparsoro *et al.* 2009).

There has been a rapid increase in the development and relevance of HSM in terrestrial ecology and natural resource management (Guisan & Thuiller 2005, Elith *et al.* 2006). More recently, advances in seabed mapping technologies (Kenny *et al.* 2003, Anderson *et al.* 2008) and benthic sampling and surveying techniques (Gage & Bett 2005) have facilitated the application of HSM in the marine environment (Davies *et al.* 2008, Degraer *et al.* 2008, Dolan *et al.* 2008, Galparsoro *et al.* 2009, Guinan *et al.* 2009a). In the deep sea, much of the development of HSM approaches has centred on cold-water corals, both because they are an emblematic vulnerable marine ecosystem, and because our understanding of cold-water corals, and particularly *Lophelia pertusa*, habitat requirements are now well constrained (Roberts *et al.* 2009). Cold-water corals were also one of the few mentioned types of vulnerable marine ecosystems in the FAO Guidelines to Management of Fisheries in the High Seas (FAO 2009). Table 2-1 summarises cold-water coral HSMs developed at different spatial scales and using different modelling techniques. Analogous with the experience of terrestrial studies (MacKey & Lindenmayer 2001, Pearson & Dawson 2003) the dominant environmental factors for coral growth appear to vary over scales of investigation. In global HSMs for example, cold-water coral distribution is determined by the availability of suitable temperatures, oxygen and

aragonite saturation state, as well as enhanced surface productivity (Clark *et al.* 2006, Davies *et al.* 2008, Tittensor *et al.* 2009). In regional and local HSMs, bathymetric terrain attributes such as slope and bathymetric position index (BPI, Weiss 2001) have shown good potential as environmental predictors as they act as proxies indicating areas of enhanced currents and food supply for the suspension-feeding corals (Wilson *et al.* 2007, Dolan *et al.* 2008, Guinan *et al.* 2009a). The summary of HSMs in Table 2-1 further demonstrates the frequently encountered trade-off between spatial (cell size) and thematic (range of environmental variables) resolution (Guisan & Thuiller 2005, Kendall & Miller 2008). Indeed, the lack of extensive high-resolution environmental datasets has been identified to be one of the major restrictions to the reliability and applicability of cold-water coral HSMs (Bryan & Metaxas 2007, Etnoyer & Morgan 2007, Davies *et al.* 2008, Tittensor *et al.* 2009). For example, a 1º x 1º temperature grid was shown to be too coarse to accurately resolve rapid changes in water temperature, leading to a mismatch between coral occurrences and temperature values beyond the species' thermal tolerance limit (Davies *et al.* 2008). A precise spatial matching between presence data and environmental variables is necessary in order to avoid an artificial expansion of the species niche width, especially when modelling the distribution of sessile organisms (Guisan & Thuiller 2005).

Terrain attributes are increasingly applied in habitat classification and modelling studies, and seabed morphology has been shown to play a crucial role in the distribution of benthic biota (Kostylev *et al.* 2001, Lundblad *et al.* 2006, Wilson *et al.* 2007, Dolan *et al.* 2008, Holmes *et al.* 2008, Verfaillie *et al.* 2008, Guinan *et al.* 2009a, Guinan *et al.* 2009b). These attributes are frequently derived from readily available global bathymetry grids which combine quality-controlled ship depth soundings with satellite-derived gravity data (Marks & Smith 2006). While such hybrids provide full coverage of the world's ocean bathymetry, they are not reliable in resolving discrete morphological features on the seafloor. The global 1º x 1º resolution GEBCO grid (GEBCO 2009) for example proved to be too coarse to resolve many of the ocean's seamounts, which are known to be ecologically important biodiversity hotspots (Clark *et al.* 2006, Davies *et al.* 2008). By employing

Table 2-1: Local, regional and global scale habitat suitability models for cold-water corals.

	Target Taxon	Predictive Model	Environmental Data	Cell Size	Source
GLOBAL	Cold-water corals on Seamounts	ENFA	Alkalinity; Aragonite saturation state; Bathymetry; Current velocity; Dissolved inorganic carbon; Dissolved oxygen; Export primary Productivity; Productivity; Salinity; Seamount location; Temperature; % oxygen saturation	1°	Clark *et al.* 2006
	Scleractinian corals *(Lophelia pertusa)*	ENFA	Alkalinity; Aragonite saturation state; Bathymetry; Aspect; Dissolved inorganic carbon; Dissolved oxygen; Hydrocarbon seeps/Pockmarks; Nitrate; Phosphate; Productivity; Salinity; Silicate; Slope; Temperature	1°	Davies *et al.* 2008
	Scleractinian corals on seamounts	ENFA; MAXENT	Alkalinity; Aragonite saturation state; Bathymetry; Current velocity; Dissolved inorganic carbon; Dissolved oxygen; Export primary productivity; Nitrate; Phosphate; Productivity; Salinity; Seamount location; Silicate; Temperature; % oxygen saturation	1°	Tittensor *et al.* 2009
	Scleractinian corals	MAXENT	Alkalinity; Apparent oxygen utilisation; Aragonite; Bathymetry; BPI; Calcite; Carbonate ion concentration; Current velocity; Dissolved inorganic carbon; Dissolved oxygen; Eastness /Northness; Nitrate; pH; Phosphate; Productivity; Salinity; Silicate; Slope; Rugosity; Temperature; Vertical flow; % oxygen saturation	0.0083°	Guinotte *et al.* 2009
REGIONAL	Gorgonian corals *(Paragorgia arbore, Orimnoa resedaeformis)*	ENFA	Bathymetry; Current speed; Productivity; Slope; Substrate; Temperature	9km	Leverette & Metaxas 2005
	Gorgonian corals (Paragorgiidae, Primnoidae)	ENFA	Bathymetry; Current velocity; Productivity; Slope; Temperature	a)0.03° b)0.08°	Bryan & Metaxas 2007
	Scleractinian corals *(Lophelia pertusa)*	ENFA; GARP	Aspect; BPI; Current velocity; Curvature; Rugosity; Salinity; Slope; Temperature	550m	Guinan *et al.* 2009a
	Scleractinian corals *(Lophelia pertusa)*	ENFA	Aspect; Bathymetry; Current speed; Iceberg ploughmark areas; Productivity, Salinity, Slope, Temperature	0.25°	Davies *et al.* 2008
	Cold-water corals	Logistic regression	Bathymetry, Rugosity, Slope	15-50m	Woodby *et al.* 2009
LOCAL	Scleractinian corals *(Lophelia pertusa)*	ENFA; GARP	Aspect; BPI; Current velocity; Curvature; Rugosity; Salinity; Slope; Temperature	30m	Guinan *et al.* 2009a
	Scleractinian corals *(Lophelia pertusa)*	ENFA	Aspect; BPI; Curvature; Fractal Dimension; Rugosity; Slope; TRI	0.5m	Dolan *et al.* 2008

the GEBCO bathymetry with a 30 arc-second resolution, Guinotte *et al*. (2009) significantly improved the terrain detail in their global model, revealing suitable coral habitat on thousands of previously undetected seamounts.

In Irish waters, cold-water corals such as *Lophelia pertusa* and *Madrepora occulata* are often associated with areas of raised topography known as carbonate mounds. These are discrete morphological features of varying shape with heights ranging from tens to hundreds of metres (Wheeler *et al.* 2007). In this study, we investigate the effect of initial bathymetric grid resolution in the production of terrain attribute maps for carbonate mound areas on the Irish continental margin. The Irish National Seabed Survey bathymetric dataset was re-gridded at a grain size of 50 m x 50 m, to provide a high-resolution benchmark to measure the quality of terrain attributes derived from coarser resolutions. A grain size of 1000 m was chosen to be the upper limit of investigation, as it roughly corresponds to the 30 arc-second GEBCO grid used in the Guinotte *et al*. (2009) global model. The effects of terrain attribute resolution on the applicability of HSM are explored by means of preliminary "terrain suitability models" (i.e. habitat suitability models based on terrain parameters only) for cold-water corals.

2.2. Methods

Study Areas

Four study areas were chosen to represent large, medium and small carbonate mounds as well as a mound-less gently sloped area on the Irish continental margin in the depth range 550-1100 metres (Figure 2-1a). Study areas A, B and D measure 15 km x 15 km while study area C measures 10 km x 9 km. The main topographical features in the study areas are shown in Figure 2-1b. Study area A (55°28.21'N 16°6.23'W) is situated within the Logachev mound province, a belt of giant carbonate mounds stretching between 16°30'W and 15°15'W along the southern margin of the Rockall bank. The area's morphology and geology have been described in detail (Kenyon *et al.* 2003, Mienis *et al.* 2006, Wheeler *et al.* 2007). Mounds are predominantly arranged in down-slope oriented clusters, which may reach lengths of several kilometres and heights of up to 380 meters (Mienis *et al.*

2006). A large sediment wave field runs upslope and parallel to the mound belt. Previous video and photographic surveys revealed high densities of live corals on the summits and terraced flanks of the mounds (Olu-Le Roy *et al.* 2002, Mienis *et al.* 2006). Study area B (55°19.56'N 14°45.74'W) comprises the Arc Mound province on the western Porcupine Bank. This area is characterized by a north-south oriented carbonate mound chain in the east, and east-west oriented mound chains in the in the north. Some mound flanks drop into a channel or local depressions, resulting in steep slopes and larger mound flanks on one side of the mounds. The mounds reach between 50 and 100 m in height and base lengths seldom exceed 500 m. Video surveys have revealed the existence of high density cold-water coral assemblages on the flanks and tops of the mounds (Grehan *et al*. 2009). Study area C (53°46.47'N 13°58.24'W) in the southeast Rockall Trough covers the R1 area investigated by Guinan *et al*. (2009b). Carbonate mounds are aligned along a northeast–southwest trend. The tallest mound reaches approximately 200 m in height and has a base length of 1500m. Multi-scale relationships between coral presence points and terrain attributes in this area were studied by Guinan *et al*. (2009b). Study area D (52°36.82'N 14°57.74'W) is situated approximately 140 km north of the Arc mound province on the Western Porcupine Bank. It is a mound-less, relatively smooth area and serves as a control area.

Generation of terrain attribute maps

Multibeam data covering the study areas were acquired as part of the Irish National Seabed Survey. The employed multibeam system was a Kongsberg Simrad EM120 multibeam system mounted to the hull of the survey vessel S.V. Bligh. Multibeam data were processed to hydrographic standards (GOTECH 2002). The clean *.xyz ASCII data were acquired from the Geological Survey of Ireland by the authors and Fledermaus v.7 gridding software was used to produce a digital elevation model (DEM) with a grain size of 0.0005º x 0.0005º (WGS84). The DEM was imported into ArcGIS v.9 and projected in UTM Zone 28N with a grain size of 50 m x 50 m. This original bathymetry grid (B_{50}) contained the maximum amount of information and served as a source and benchmark for all further produced grids.

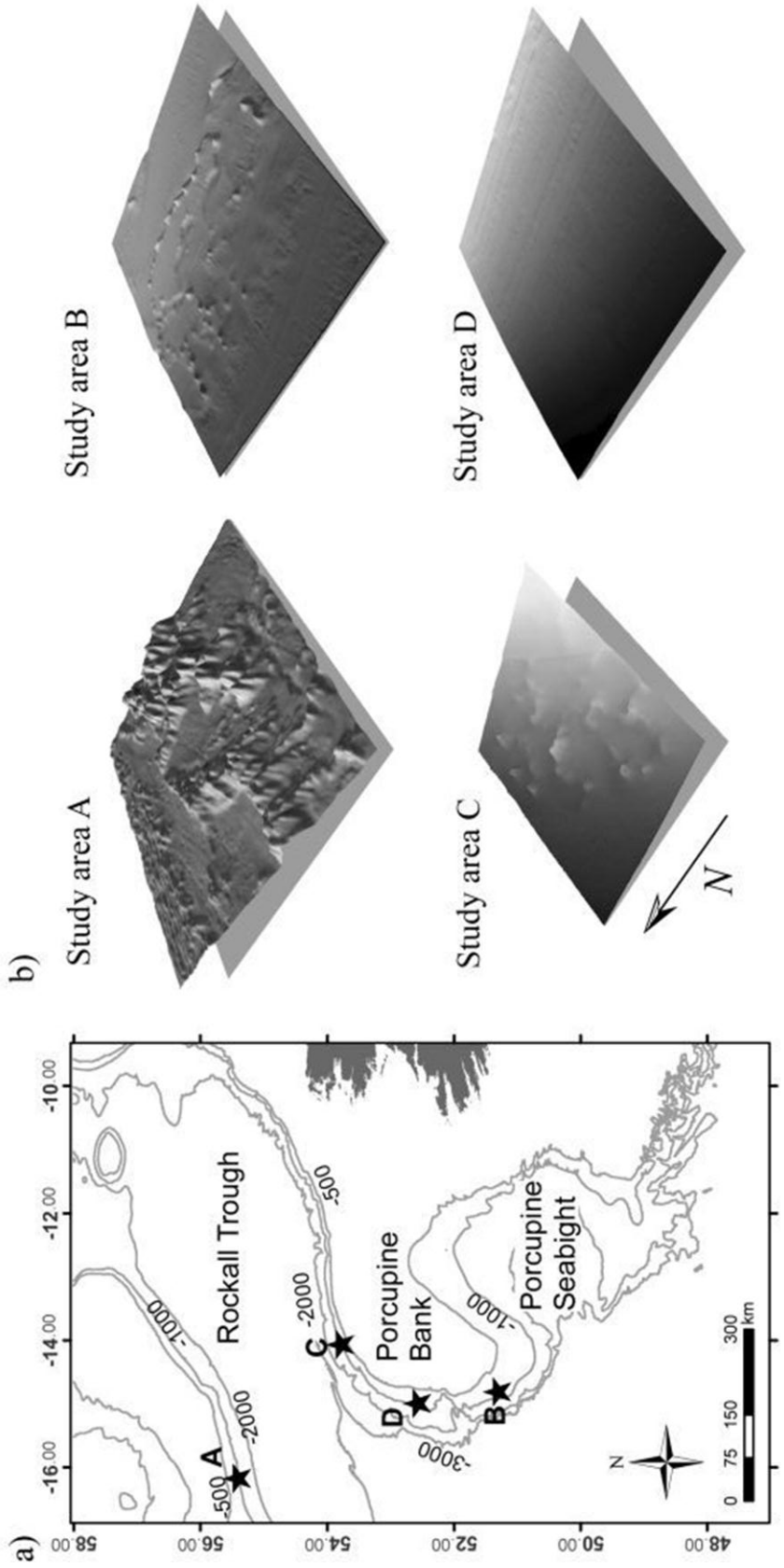

Figure 2-1: a) Overview of the study areas on the Irish continental margin: study area A (Logachev Mound Province), study area B (Arc Mound Province), study area C (R1 area) and study area D (control area). b) Terrain visualization of the study areas at 5 × vertical exaggeration based on INSS multibeam bathymetry at 50 m resolution. Study areas A, B and D measure 15 km x 15 km while study area C measures 10 km x 9 km. Projection is UTM Zone 28N (WGS84).

The Mean Aggregation strategy in ArcGIS v.9 was used to coarsen B_{50} to 100, 250, 500 and 1000 m spatial resolution (B_{100}, B_{250}, B_{500} and B_{1000} respectively). Re-sampling by bilinear interpolation (ArcGIS v.9) was then applied to the B_{1000} grid in order to obtain bathymetry grids of 500, 250, 100 and 50 m spatial resolution (I_{500}, I_{250}, I_{100} and I_{50} respectively), but with low information content. The purpose of these interpolated grids was to assess the utility of up-scaling coarse global bathymetry models such as GEBCO to finer spatial resolutions. Additionally one can derive information on how much of the variation between terrain attributes is due to the changing grid resolution (i.e. discretization effect) and how much is due to varying terrain information content (i.e. smoothing effect) (Gallant & Hutchinson 1996, Wolock & McCabe 2000, Sørensen & Seibert 2007).

We calculated slope, aspect (as eastness and northness values), plan and profile curvatures, bathymetric position index (BPI), roughness and rugosity for all bathymetry grids (B_{50}-B_{1000} and I_{50},-I_{500}) using ArcGIS v.9 and following parameter computation methods described by Wilson *et al*. (2007). The Benthic Terrain Modeller extension (Lundblad *et al.* 2006) was employed for the computation of terrain rugosity. A default neighbourhood of 3 x 3 grid cells was employed for all terrain attributes and for consistency in analyses no annulus was used for the computation of the BPI. To avoid including edge artefacts, the map borders for each study areas were clipped after terrain analysis. Cells per grid totalled 90 000, 22 500, 3 600, 900 and 225 for study areas A, B and D and 36 000, 9 000, 1 440, 360 and 90 for study area C at grid cell sizes of 50, 100, 250, 500 and 1 000 m respectively.

Terrain attribute analyses

Terrain attributes of varying resolution and terrain information content were compared in three different ways:

1) Maps were visually evaluated within ArcGIS v.9.

2) Pearson correlation coefficients (r) between the terrain attributes of the 50 m benchmark (B_{50}) and coarser resolutions (B_{100}-B_{1000}) were calculated in order to assess the effects of decreasing resolution on a cell-by-cell basis. This analysis gave information on the spatial agreement between maps.

3) For each study area, 500 random point locations were generated. These points were used to sample all underlying terrain attribute maps. The randomised sampling procedure was chosen because it simulated potential species presence data with minimal spatial autocorrelation. Box plots were computed for each set of sample points to obtain information on quantitative variations between terrain attribute maps of different resolutions and information content.

Generation of preliminary terrain suitability models

To investigate the effects of decreasing resolution and terrain information loss on HSM of cold-water corals, preliminary terrain suitability models were generated employing Maxent (Phillips *et al.* 2006). This modelling software estimates the distribution of a certain species by relating known species occurrences with a series of environmental variables via a machine learning maximum entropy algorithm. Maxent provides a user-friendly interface and has shown good performance in recent comparative modelling studies (Elith *et al.* 2006, Phillips *et al.* 2006, Guisan *et al.* 2007). Default parameters (convergence threshold of 10^{-5}, a maximum of 500 iterations and a regularization multiplier of 1) of Maxent version 3.31 (http://www.cs.princeton.edu/~schapire/maxent) were applied. Terrain suitability models for study area C were generated for each set of the above described terrain attributes (50, 100, 250, 500 and 1000 m resolution). The species sample data in this area consisted of 247 geo-referenced video-derived coral presence points provided by Guinan *et al*. (2009a). Maxent removed duplicate presence points within the grid cells, resulting in a reduction of sample points with increasing cell size (203 at 50 m, 44 at 100 m, 22 at 250 m, 13 at 500 m and 6 at 1000 m). The trained model was then projected onto all study areas. Maxent produces logistically scaled habitat suitability maps for each study area, with each pixel estimating the probability of species presence. Values close to zero indicate low probability, values close to one suggest high probability of species presence.

For many HSM applications, continuous predictions need to be reduced to binary maps indicating species presence and absence. In order to assess the effect of grid resolution on the total area predicted suitable coral habitat (i.e. coral presence), all produced HSMs were converted into binary maps based on a range of habitat

suitability index thresholds (0.4, 0.5, 0.6 and 0.7). All grid cells with habitat suitability values above the respective threshold were counted and the total area was computed by multiplying the cell count with the respective grid cell size.

2.3. Results

Visual evaluation of computed terrain attributes

The generated terrain attribute maps varied considerably with resolution and terrain information content. Figure 2-2 shows the distribution of slope values in study area A as an example for the general pattern found. Even though dominant features were roughly preserved over a range of resolutions, terrain detail and smaller features were gradually lost with increasing cell size. For example steep slopes were not resolved at coarse resolutions as they were increasingly aggregated with the adjacent valley bottom. The loss of high slope values was also visualized by the reduction of map contrast. Smaller features such as sediment waves in study area A or the Arc mounds in study area B entirely dissolved with coarsening resolution.

Lost terrain detail could not visibly be recovered by upscaling B_{1000} to finer resolutions. While I_{500} grid-based terrain attribute maps appeared to be smoother versions of the B_{1000} terrain attribute maps, further interpolation resulted in artefacts reflecting the cell structure of the underlying B_{1000} bathymetry grid (Figure 2-2b). These square-shaped structures are most visible in the I_{50} and I_{100} maps and are probably a consequence of the bilinear interpolation method applied. Virtually constant attribute values within the original 1000 m x 1000 m window and rapidly changing values at the window borders resulted in a grate-like grid appearance.

Increasing the grid cell sizes also led to an emergence of new distributional properties within terrain attribute maps. Figure 2-3 shows BPI, eastness, profile curvature and rugosity computed for study area B at 50, 250 and 1000 m resolution. While the grey-scales employed are map-specific and cannot be used as a basis for comparison between resolutions, it is clear that attribute maps based on B_{1000} fail to represent the terrain in a realistic manner. Frequently, an alternation between positive and negative terrain attribute values could be observed.

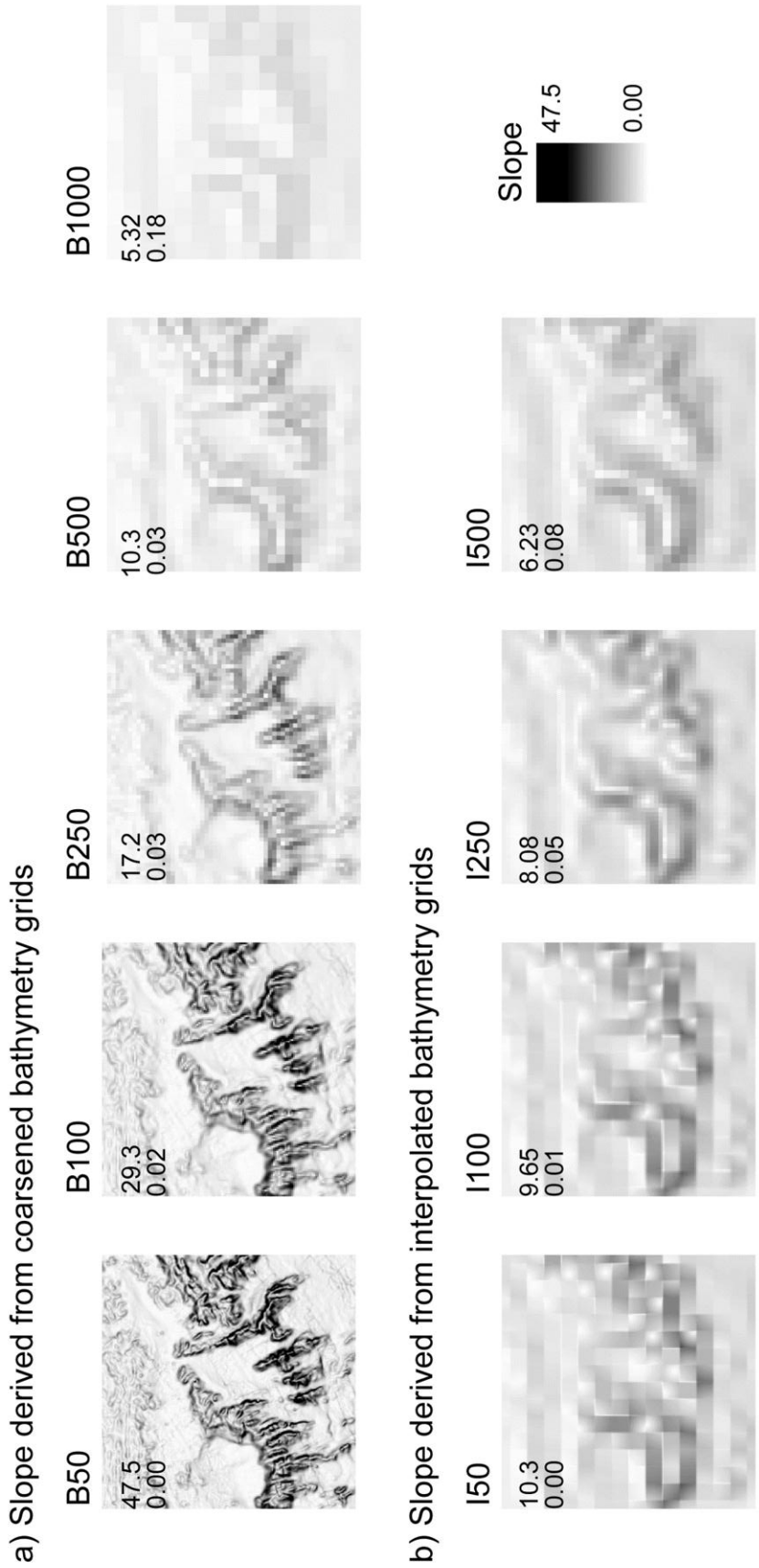

Figure 2-2: Slope maps of study area A derived from coarsened (a) and interpolated (b) bathymetry grids at 50, 100, 250, 500, and 1000 m resolutions The minimum and maximum slope values of each individual map are indicated.

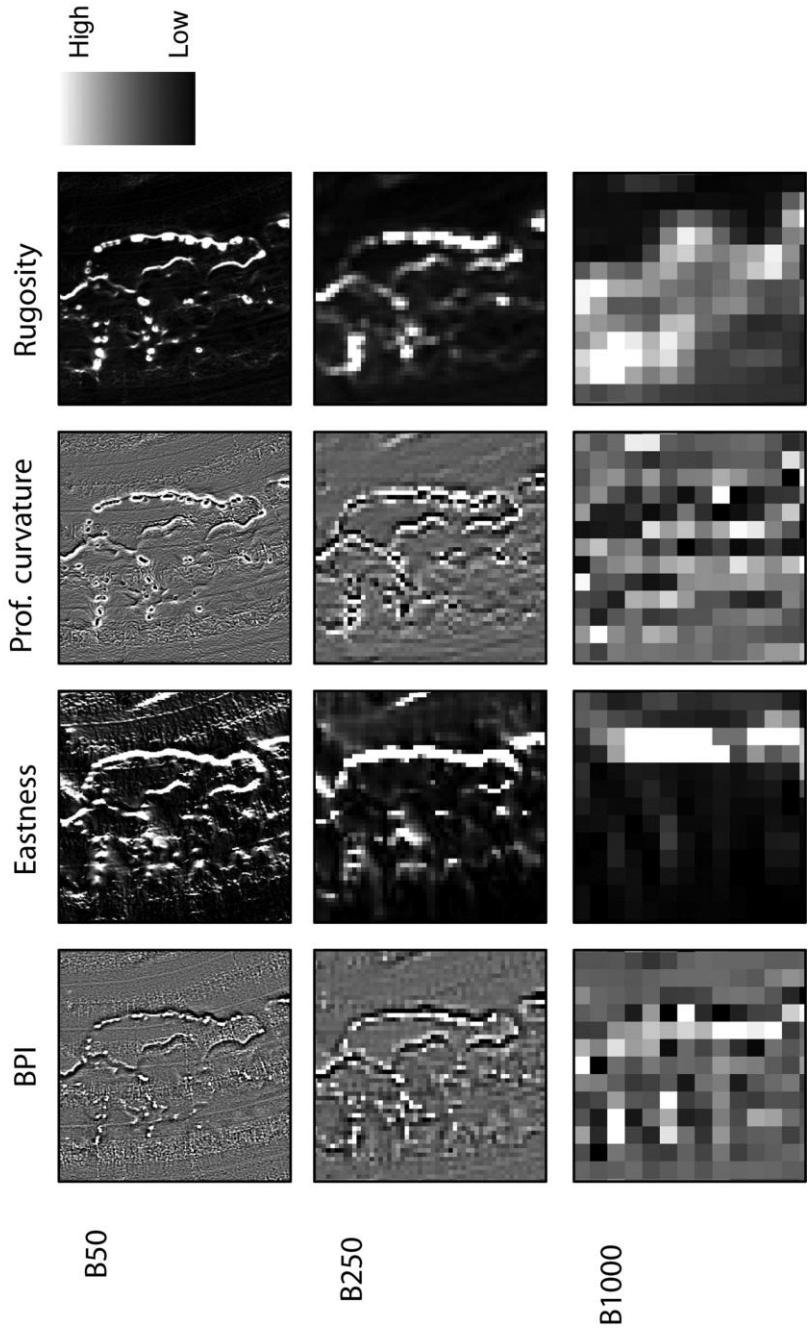

Figure 2-3: BPI, eastness, profile curvature, and rugosity maps computed for study area B based on varying initial grid resolutions. Grey-tone scale is computed individually for each parameter and resolution; range is too great to allow a common representation of changes within each parameter for all resolutions.

Spatial agreement of terrain attributes across resolutions

The Pearson correlation coefficient (*r*) was used to describe the nature (i.e. positive or negative) and strength of spatial agreement between terrain attributes of 50 m and coarser resolutions. High *r* values (close to 1) indicated that the terrain attribute based on a certain grid resolution represented the respective 50 m benchmark grid well, while low values (close to 0) indicated a poor correlation. Correlation coefficients consistently decreased with coarsening resolutions (Figure 2-4). This suggests a general decrease of spatial agreement between terrain attribute values with increasing grid cell size, along with a decrease in predictability of the manner of change. An abrupt drop in *r* values mostly between 100 and 250 m resolution indicated the potential crossing of a threshold, possibly reflecting dominant morphological length scales in the study areas. Interestingly, this drop was also observed for the BPI and curvatures in the mound-less control area (study area D), suggesting that these attributes might be sensitive to artefacts which are commonly existent in multibeam derived bathymetry. Slope, roughness and rugosity within the control area showed generally higher correlations, with *r* values of ~0.7 throughout resolutions. Averaged over all resolutions and study areas, slope, rugosity and roughness were the terrain attributes most robust to resolution changes (*r* means and standard deviations of 0.62±0.24, 0.61±0.25 and 0.60±0.25 respectively), while BPI, plan curvature and profile curvature were the most sensitive (0.34±0.28, 0.27±0.26 and 0.24±0.27 respectively).

Quantitative variations in terrain attribute values

All terrain attribute values varied dramatically with change in resolution and information content. Box plots for all study areas followed the same patterns and only results for study area A are presented here (Figure 2-5), the figures for the remaining study areas are included in the appendix S1. However, the dimensions of the y-axes were throughout highest for study areas A and C, followed by area B. Within the control area changes in attribute values remained negligible.

Effects of bathymetry grid coarsening ($B_{50} - B_{1000}$)

While the summary statistics of bathymetry remained generally constant throughout all grids, mean slope values decreased slowly and maximum values decreased

sharply with increasing cell size. The underestimations of maximum slope values when calculated at 1000 m resolution reached as high as ~80% (study areas A & C).

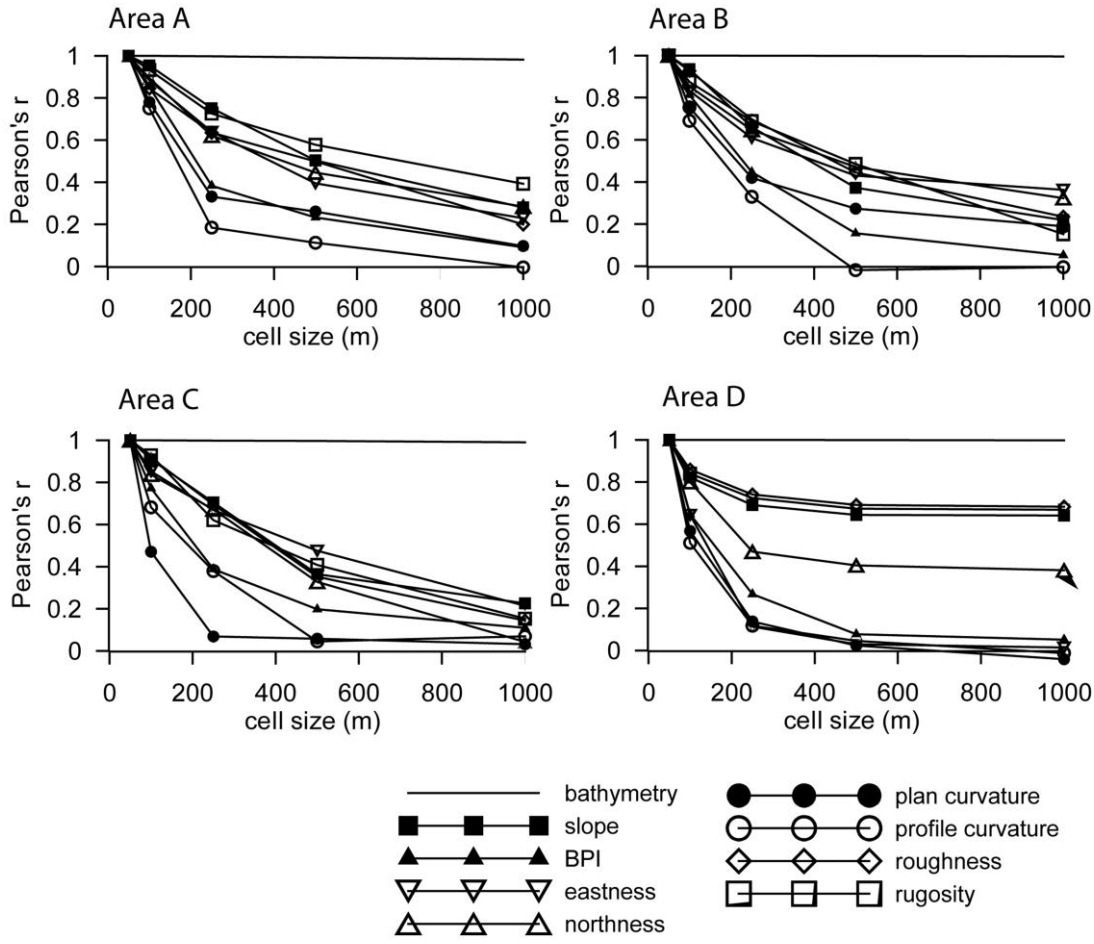

Figure 2-4: Pearson's correlation coefficient (*r*) between terrain attributes of 50 m (B_{50}) and coarser resolutions ($B_{100} - B_{1000}$).

Aspect (orientation) was transformed into eastness and northness for a better quantification of the parameter (Wilson *et al.* 2007). Mean values of both parameters were largely preserved across resolutions and mirrored the overall orientation of the study areas; e.g. study area C was dominated by negative eastness values (~ -0.7) and positive northness values (~ +0.8), reflecting the north-west facing slope of the continental margin in this area (Figure 2-1b). Generally, upper and lower percentiles converged towards the mean with coarsening resolution, reflecting the same terrain "smoothing" effect observed for slope.

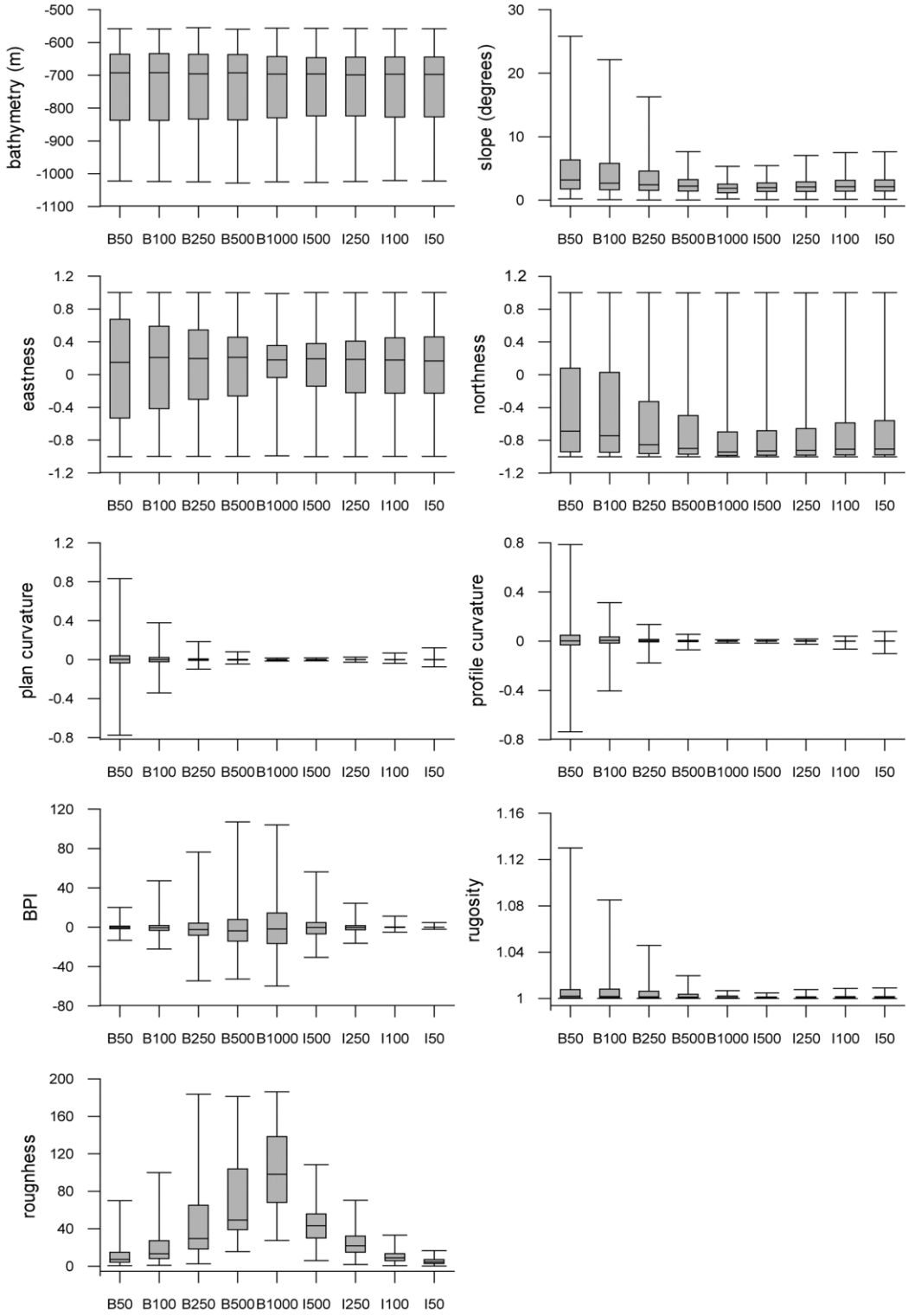

Figure 2-5: Box plots for the study area A illustrating the range, the median, and the upper and lower percentiles of terrain attribute values derived from grids of varying resolution (B_{50}-B_{1000}) and information content (I_{500}-I_{50}). The figures for study areas B-D are included in the appendix S1.

Plan and profile curvature showed strong resolution sensitivity as positive and negative values converged towards zero with increasing grid cell size. Again the same pattern was found for all study areas, however curvature values in study area D (control area) remained comparatively low and never exceeded +/- 0.2. Generally, mean values remained close to zero throughout resolutions, indicating that approximately the same level of convexity and concavity occurs in the study areas.

The BPI is a measure of the relative position (above or below) of an individual pixel in relation to its surrounding terrain (Weiss 2001). Coarsening grid resolution led to a strong overestimation of both positive and negative BPI values. Generally, the range of the percentiles expanded slowly while extreme values expanded rapidly with increasing grid cell size. Again the same qualitative differences between areas could be observed, with BPI values expanding most in study area A, followed by area C and finally area B.

All statistical measures of roughness increased with decreasing resolution while maximum rugosity values sharply decreased and converged towards one.

Effects of bathymetry grid interpolation ($I_{500} - I_{50}$)

The box plots derived from the up-scaled bathymetry grids of low terrain information content (I_{50}, I_{100}, I_{250}, I_{500}) replicated a similar pattern as plots derived from original grids of same resolution (B_{50}, B_{100}, B_{250}, B_{500}), even without reaching the extreme values observed for the higher resolution data. This similarity between box plots suggests that resolution-dependent differences can partly be attributed to the change in grid cell size (i.e. discretizaton effect). However, a substantial part of the differences remains due to the actual loss of information content (i.e. smoothing effect) and cannot be recovered by bilinear interpolation to higher resolution.

Preliminary terrain suitability models

Preliminary terrain suitability maps produced by Maxent clearly reflect the resolution-effects observed during terrain analysis (Figure 2-6). Only models of higher resolution (i.e. $B_{50} - B_{250}$) successfully identified areas of small-scale terrain complexity as suitable coral habitat. The control area (area D) was predicted to be unsuitable at all resolutions. It is noteworthy that the degree of resolution sensitivity

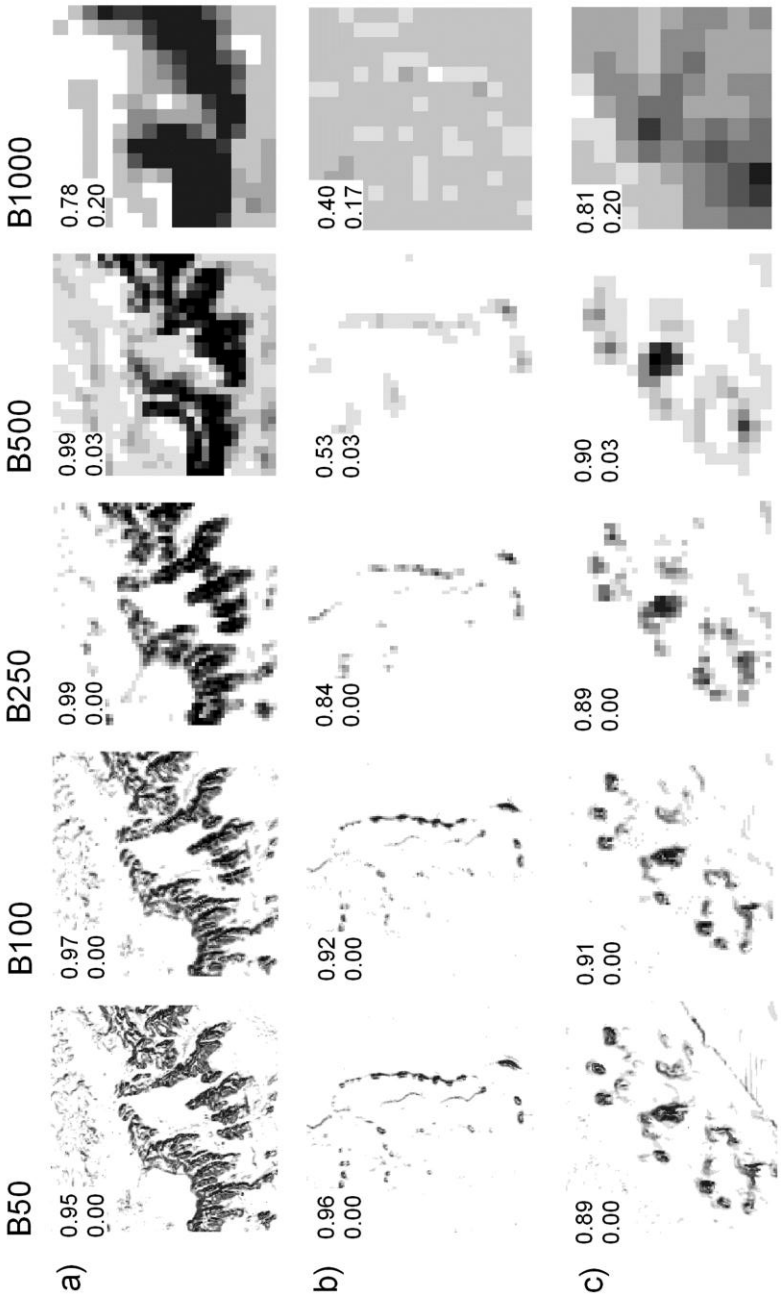

Figure 2-6: Continuous terrain suitability maps based on a set of 247 training data points provided by Guinan *et al.* 2009a. Models were trained within study area C (c) and projected to the study areas A (a), B (b) and D (not displayed) employing terrain variables based on B_{50}–B_{1000} bathymetry grids. Terrain suitability ranges from low (0, white) to high (1, black). Maximum and minimum suitability values are indicated in each map.

varied between study areas depending on average length-scales of the dominant morphological features (i.e. study area A shows less decrease in maximum habitat suitability values than study area B). Changes in extreme habitat suitability values further affected the total extent of area predicted suitable when different habitat suitability thresholds were applied. Interestingly, these responses were inconsistent between study areas (Figure 2-7). Study area A showed a constant pattern of over-prediction of suitable habitat with increasing cell size at all tested thresholds. Based on a threshold of 0.5, the predicted coral habitat increased from 35 km^2 at 50 m resolution to 77 km^2 at 1000 m resolution. Study area B on the other hand showed a pronounced under-prediction as grid cell size was increasing, with potentially suitable habitat decreasing from 3 km^2 at 50 m to 0 km^2 at 1000 m resolution. These contradicting trends are due to the above discussed qualitative differences in the study areas. Due to the large mound features in study area A, suitable coral habitat is detected throughout resolutions and the increasing cell size leads to an increase in predicted suitable area. Within study area B however, the smaller mound features become less distinguished at increasing cell sizes, and less suitable habitat can be detected by the HSM. The pattern observed in study area C suggests the existence of a cell size threshold between 500 and 1000 m resolution, above which a marked over-prediction will take place. Most of this over-prediction could be attributed to an increase in area predicted suitable based on lower thresholds (0.4 and 0.5).pobre po

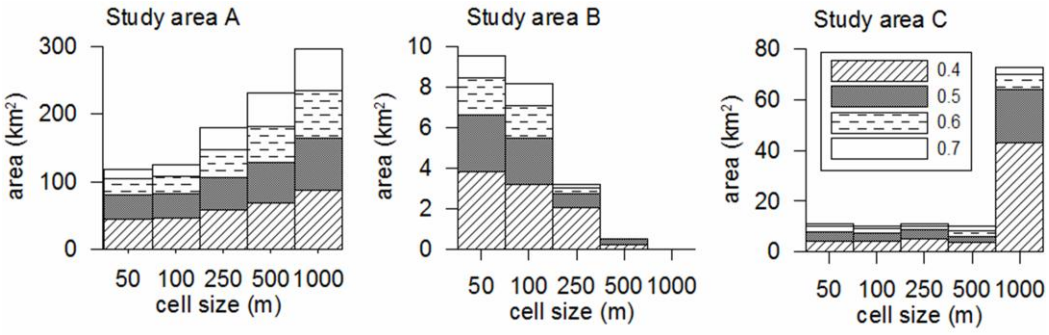

Figure 2-7: Stacked columns display the area (km^2) predicted to be suitable coral habitat based on binary maps resulting from a range of habitat suitability thresholds (from bottom to top: 0.4, 0.5, 0.6, and 0.7). Study area D is not displayed as less than 0.01 km^2 was predicted to be suitable.

2.4. Discussion

Terrain analysis

Terrain attributes, by their nature, are scale-dependent. Numerous authors have addressed the issues of initial grid resolution (Wolock & McCabe 2000, Kienzle 2004, Deng *et al.* 2007) and analysis window size (Albani *et al.* 2004, Schmidt & Andrew 2005, Wilson *et al.* 2007) in terrain analysis. Our results corroborate findings of studies investigating resolution dependency of topography-derived terrain attributes (Wolock & McCabe 2000, Kienzle 2004, Deng *et al.* 2007, Sørensen & Seibert 2007), in spite of differences in the grid resolution coarsening techniques applied. Sørensen & Seibert (2007) employed pixel thinning methods implemented in Idrisi software (www.clarklabs.org). Other authors re-sampled the high-resolution grids at every nth grid point to ensure exact matching between grid points on the coarse resolution grids with grid points on high-resolution grid (Wolock & McCabe 2000, Deng *et al.* 2007). We tested the latter approach in a preliminary study and did not find any significant differences to the results presented here. Grid coarsening by means of the Mean Aggregation method was chosen because resulting grids better represented coarse bathymetry models such as the GEBCO grid. Terrain attribute distributions of interpolated grids (I_{50} – I_{500}) partially reproduced the ones of the original grids (B_{50} –B_{500}). From this one could conclude that up-scaling coarse bathymetry to higher grid resolution is a way to obtain higher resolution terrain attribute maps. However, visual evaluation indicated significant differences between the coarsened and interpolated terrain attribute maps, including grate-like artefacts at the highest resolutions. Different upscaling methods should be considered if it is aimed to apply coarse bathymetry grids to terrain analysis of higher resolution. Interpolation techniques such as inverse distance weighing or kriging might prove more promising for such purpose, however the evaluation of and comparison between interpolation methods is beyond the scope of this study.

A detailed review of novel methods and trends in terrain analysis is given by Deng (2007). One promising example to overcome the scale problem in terrain analysis could be the incorporation of fuzzy logic to produce multi-scale parameters (Wood 1996) and multi-scale fuzzy objects (Fisher *et al.* 2004). An alternative approach

involves changing the analysis window size while maintaining a constant bathymetry grid resolution (Albani *et al.* 2004, Wilson *et al.* 2007). The applicability of the multi-scale terrain analysis approach to benthic mapping and habitat suitability modelling has recently been explored and seen promising results (Wilson *et al.* 2007, Dolan *et al.* 2008, Verfaillie *et al.* 2008, Guinan *et al.* 2009a). It is important to note that, while the multi-scale analysis approach is useful, it is only feasible when high-resolution bathymetric data are available in the first place.

Terrain resolution effects on HSM for cold-water corals

All terrain attributes tested within this study (slope, eastness, northness, plan and profile curvature, BPI, roughness and rugosity) varied dramatically with change in resolution of the underlying bathymetry (Figure 2-5). This may affect HSM results in different ways.

Slope has been identified as important predictive parameter in virtually all published cold-water coral HSM studies (Table 2-1 and references therein). Guinan *et al.* (2009b) found high cold-water coral coverage percentage to be directly associated with steep slope values. The underestimation of maximum (steep) slope values at coarse resolutions therefore has the effect of reducing the width of the slope-specific niche output by an HSM. In addition, the observed convergence of extreme values towards the mean (i.e. the loss in map contrast observed in Figure 2-2a) is likely to result in a loss of predictive power. Terrain aspect is intrinsically linked to slope and provides information on the exposure of seabed terrain to local and regional currents. We observed a substantial change of eastness and northness distributions with changing resolutions, as well as a resolution-dependent alternation between positive and negative values. Cold-water corals have been associated with positive BPI values corresponding to bathymetric highs such as crests and ridges (Dolan *et al.* 2008, Guinan *et al.* 2009a, Guinan *et al.* 2009b). We found the BPI to be highly resolution dependent, with a pronounced over-estimation of extreme values at coarser resolutions. Recent HSM studies approached the scale-sensitivity of the BPI by computing both a small-scale BPI (calculated over a small analysis window size), and a large-scale BPI (calculated with a large analysis window size) (Lundblad *et al.* 2006, Guinotte *et al.* 2009).

Preliminary terrain suitability models

The results presented in this study suggest that habitat suitability models employing terrain parameters based on bathymetry of 1000 m (~30 Arc-seconds) resolution fail to detect many of the small carbonate mounds found in Irish waters. Bathymetry data of at least 250 mx 250 m resolution are required to identify these areas as suitable coral habitat. Care must be taken if the available bathymetric data does not reflect local surface variability, as matching between the target species presence points and flawed terrain attribute values is likely to occur. This mismatch might skew the species' niche width as well as the resulting habitat suitability maps, ultimately leading to ill-informed management decisions.

Binary coral habitat maps based on different thresholds have been shown to highly depend on terrain attribute resolution, and care must be taken when making assumptions on total area coverage of species predictions when coarse bathymetry grids are being used. Besides the resolution factor discussed here, the choice of threshold will further influence the total area predicted suitable. Several methods for choosing an appropriate threshold are discussed in the literature (Liu *et al.* 2005, Jiménez-Valverde & Lobo 2007), but up to date no consensus for a best method has been reached and different thresholds are being used to respond to different management issues. Further research will be necessary to better describe and understand the effect of terrain attribute resolution and HSM thresholds for the generation of binary habitat suitability maps for the purpose of ecosystem-based management.

Besides the effects of original bathymetry resolution discussed above, HSMs also show an intrinsic sensitivity to changes in grid cell size (Guisan *et al.* 2007, Seo *et al.* 2009). Increasing model resolution may potentially influence a species' presence-absence pattern (Wiens 2002) and may affect the relevance of the output for management applications. Seo *et al.* (2009) reported a threefold increase in suitable area when models were run at 64 km x 64 km resolution compared to models run at 1 km x 1 km resolution. While the present study did not incorporate an evaluation of model performance, as more species sample data would be required from all study areas to compute reliable model evaluation indices, the generation of preliminary

terrain suitability models did illustrate the sensitivity of the model outcomes to initial bathymetry grid resolution.

The need for further information on local environmental drivers of cold-water coral distribution in order to improve their management has been identified by Duran Munoz *et al.* (2009) amongst others. In future work, we will use high-resolution hydrodynamic models to help identify whether regional and local oceanographic processes contribute to habitat optimisation in Irish waters. Where 3D oceanographic models of sufficient resolution are unavailable, a hierarchical modelling framework (MacKey & Lindenmayer 2001, Pearson & Dawson 2003) should be employed, combining high-resolution terrain information with lower resolution oceanographic parameters. Such hierarchical models would ensure the identification of suitable habitat on small morphological features while highlighting areas of unsuitable terrain in areas otherwise indicated as suitable by the oceanography. A hierarchical modelling framework could therefore improve estimates of actual coral coverage and the identification of vulnerable marine ecosystems at scales that support management decision making, particularly marine spatial planning.

2.5. Supporting Information

Appendix S1a: Box plots for the study area B illustrating the range, the median, and the upper and lower percentiles of terrain attribute values derived from grids of varying resolution (B_{50}-B_{1000}) and information content (I_{500}-I_{50}).

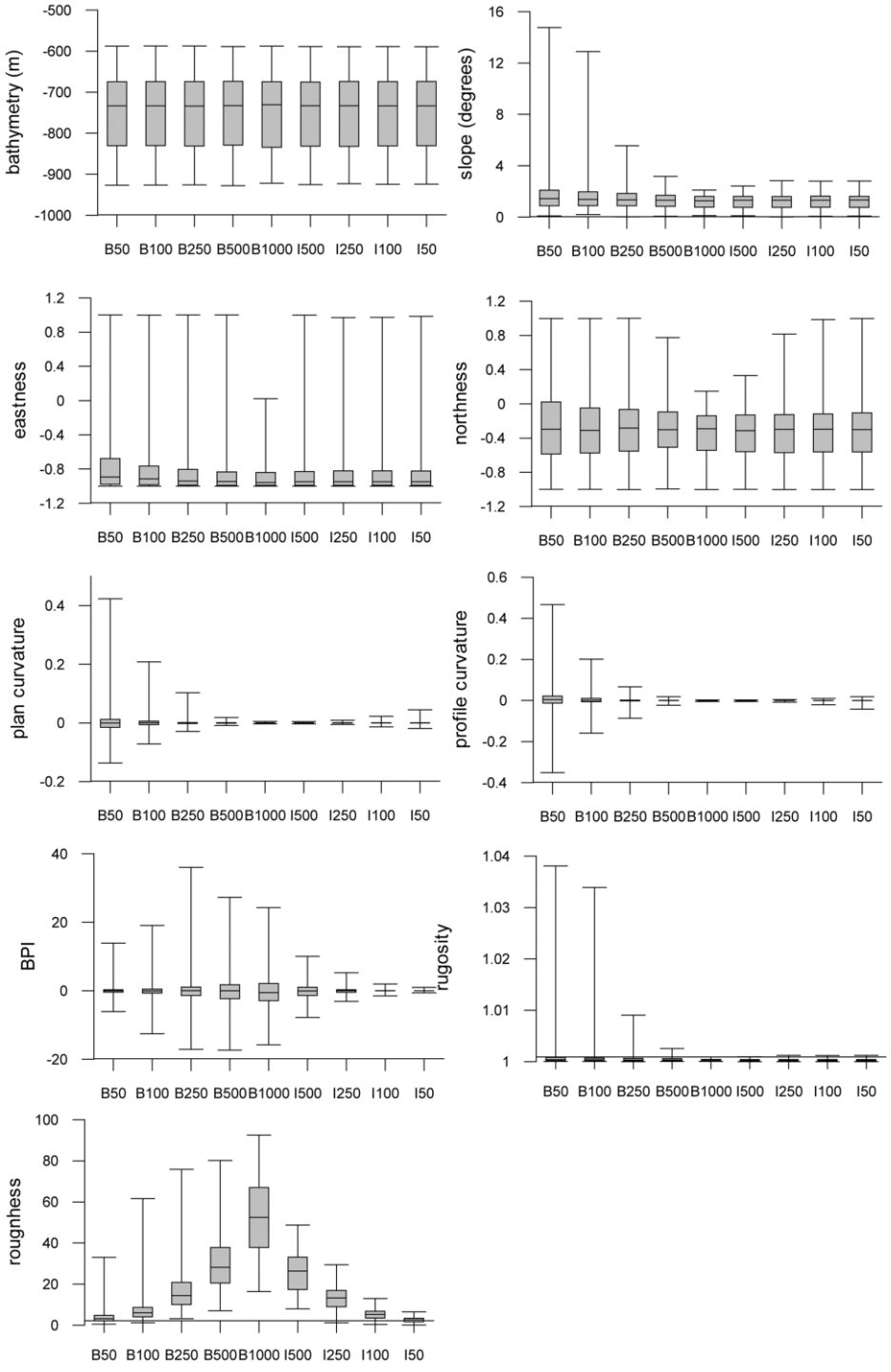

Appendix S1b: Box plots for the study area C illustrating the range, the median, and the upper and lower percentiles of terrain attribute values derived from grids of varying resolution (B_{50}-B_{1000}) and information content (I_{500}-I_{50}).

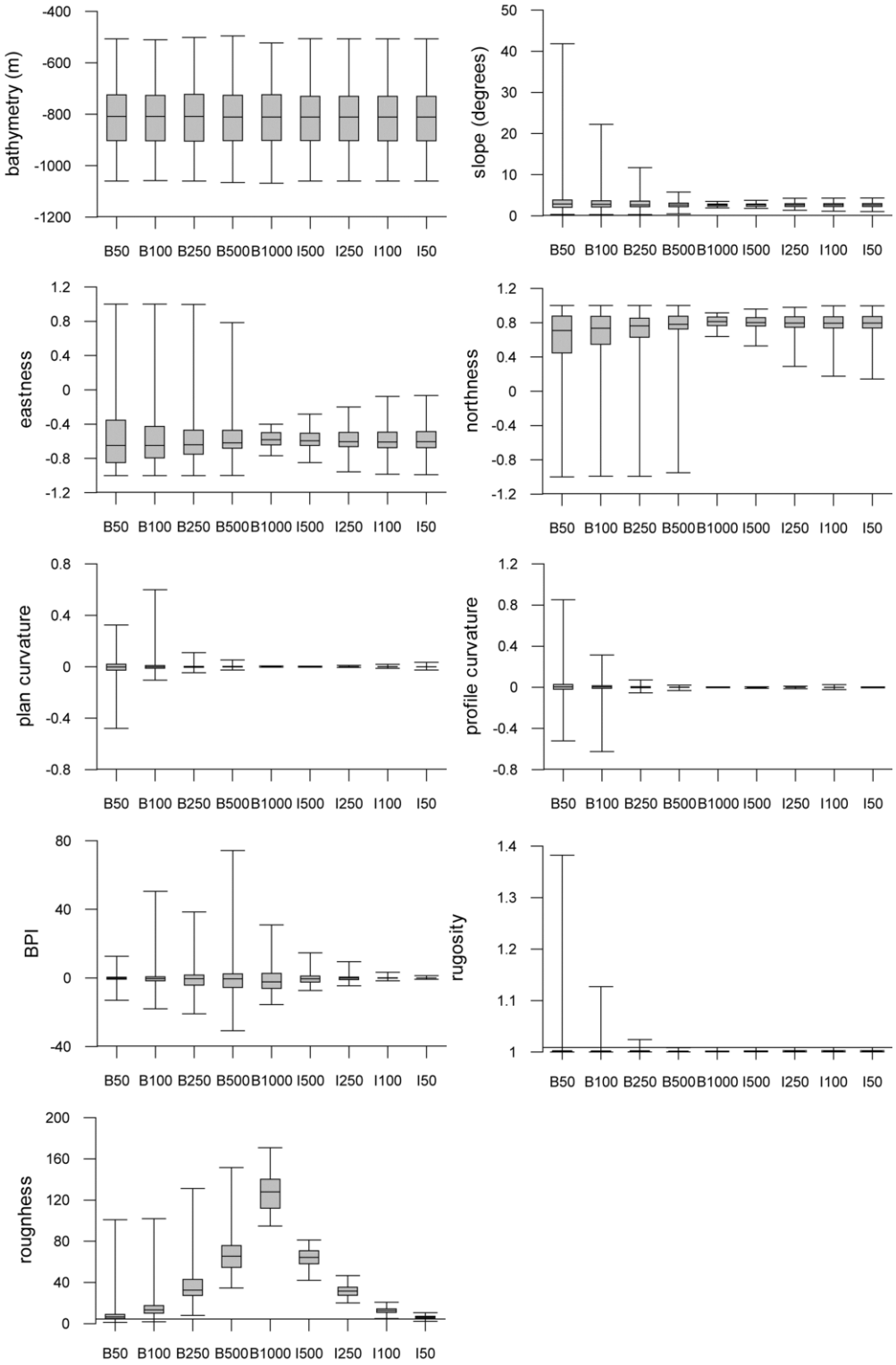

Appendix S1c: Box plots for the study area D illustrating the range, the median, and the upper and lower percentiles of terrain attribute values derived from grids of varying resolution (B_{50}-B_{1000}) and information content (I_{500}-I_{50}).

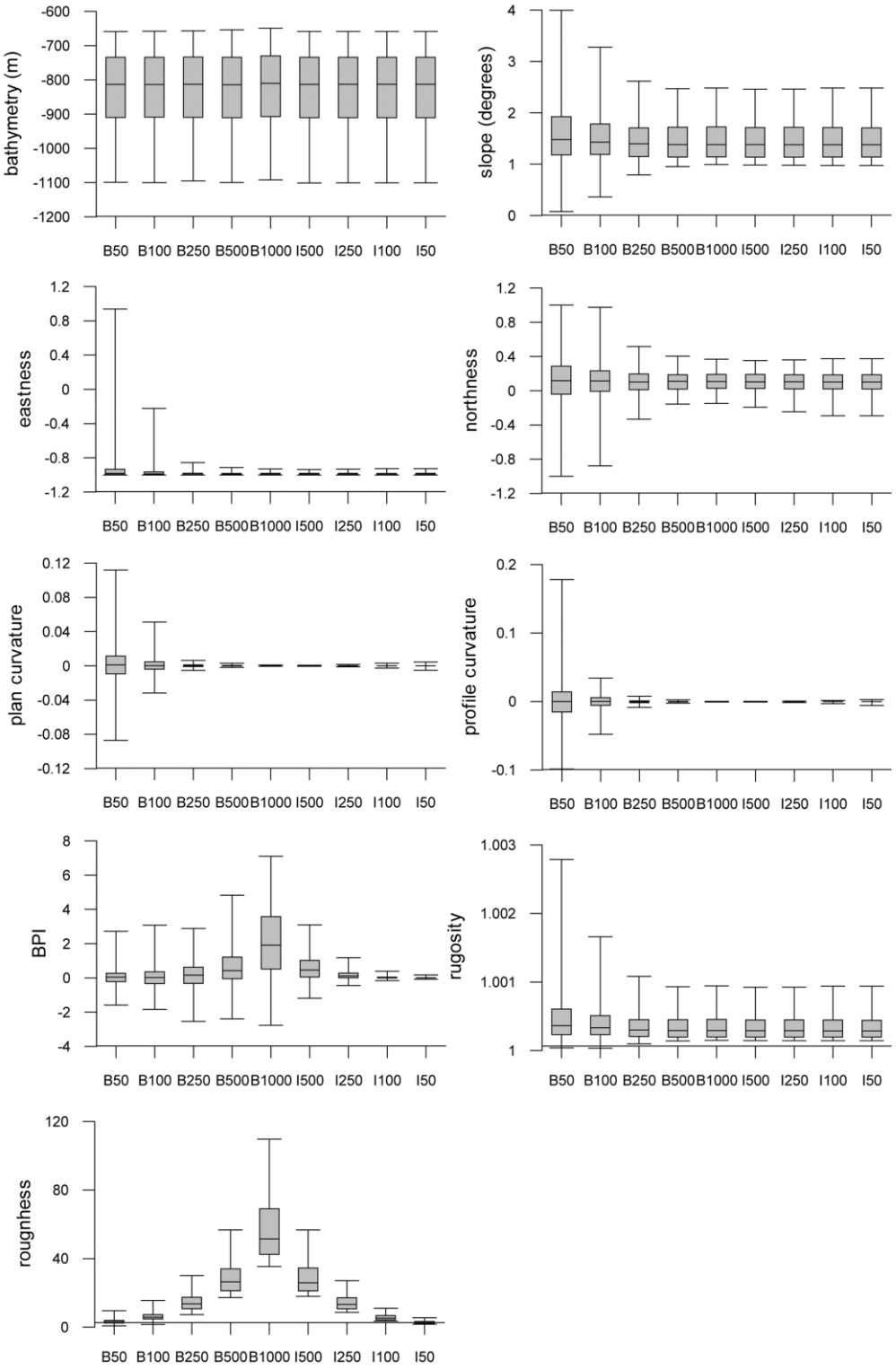

3. High-resolution habitat suitability modelling can improve conservation of vulnerable marine ecosystems in the deep sea

Abstract

Aim: The distribution of vulnerable marine ecosystems in the deep sea is poorly understood. This has led to the emergence of modelling methods to predict the occurrence of suitable habitat for conservation planning in data sparse areas. Recent global analyses for cold-water corals predict a high probability of occurrence along the slopes of continental margins, offshore banks and seamounts in the north-east Atlantic, but tend to over-estimate the extent of the habitat and do not provide the detail needed for finer-scale assessments and protected area planning. Using *Lophelia pertusa* reefs as an example, this study integrates multibeam bathymetry with a wide range of environmental data to produce a regional high-resolution habitat suitability map relevant for marine spatial planning.

Location: Irish continental margin (extended continental shelf claim)

Methods: Maximum entropy modelling was used to predict *L. pertusa* reef distribution at a spatial resolution of 0.002°. Coral occurrences were assembled from public databases, publications and video footage and filtered for quality. Environmental predictor variables were produced by re-sampling of global oceanographic datasets and a regional ocean circulation model. Multi-scale terrain parameters were computed from multibeam bathymetry.

Results: Suitable habitat was predicted on mound features and in canyon areas along a narrow band following the slopes of the Irish continental margin, the Rockall Bank and the Porcupine Bank. Standard deviation of the seabed slope was the most important variable to predict coral distribution (54%), followed by temperature (28%) and bottom shear stress (9%).

Main conclusion: This is the first regional cold-water coral habitat suitability modelling study to incorporate full coverage multibeam bathymetry over a wide

variety of deep-sea morphological features. The use of high-resolution environmental data and quality control of distribution data significantly reduce habitat over estimation demonstrated by global scale analyses. We provide a robust, coherent and transferrable methodology to generate detailed distribution maps of deep-sea benthic species and discuss implications for marine protected area network design.

Keywords: cold-water coral, deep sea, ecosystem-based management, habitat, *Lophelia pertusa*, Maxent, marine spatial planning, predictive modelling

3.1. Introduction

There is growing anthropogenic pressure on marine ecosystems in the deep sea as fisheries, mining, oil and gas exploration now occur in depths > 1500 m (Davies *et al.* 2007, Grehan *et al.* 2009). One of the biggest problems facing planners charged with developing comprehensive networks of marine protected areas to protect vulnerable marine ecosystems (cf. Rogers *et al*. 2008) in the deep sea is the lack of knowledge of the true distributional extent of the species and habitats. This is exacerbated in the case of framework building cold-water corals, because the composition of associated reef communities can change over relatively short distances (Rogers 1999).

While vulnerable marine ecosystems can occur at the scale of ocean basins, conservation efforts are generally undertaken within national jurisdictions where legislation provides the legal framework for the establishment of marine protected areas. More recently, a number of marine protected areas have been created in Areas Beyond National Jurisdiction where regional conservation conventions or fisheries management organisations have agreed such measures amongst their contracting parties. In 2010, the Oslo Paris Convention for the Protection of Biodiversity in the north-east Atlantic established the world's first High Seas marine protected areas: namely, the Mid-Atlantic Ridge north of the Azores, around the Milne, Altair, Antialtair and Josephine Seamounts and Charlie-Gibbs South MPA (OSPAR 2010).

Identification and mapping of vulnerable marine ecosystems at the scale of ocean basins is a challenge. As extensive surveys in the deep sea are time-consuming and expensive, there is an interest in using habitat suitability models (HSMs) to produce continuous coverage habitat maps in data sparse areas. HSMs statistically relate species distribution data with a set of environmental variables to understand and predict potential species distributions (Guisan & Zimmermann 2000, Elith *et al.* 2006). Existing approaches include environmental envelopes (e.g. BIOCLIM, Busby 1991), statistical models such as generalized regressions and non-parametric smoothing functions (Guisan *et al.* 2002), machine learning algorithms fitting complex responses and interactions (Elith *et al.* 2006), as well as hybrids of these. In the case of unavailable (e.g. museum collections and databases, Ross *et al*. 2012) or unreliable (e.g. in the deep oceans, Davies & Guinotte 2011) absence data, presence-only methods are commonly used which contrast presence records to randomly selected background data or pseudo-absence data (Elith *et al.* 2006, Pearce & Boyce 2006, Phillips *et al.* 2009). In a comparative study evaluating 16 algorithms using presence-only records of 226 terrestrial species from 6 regions of the world, Elith *et al*. (2006) found that machine learning methods (e.g. Maxent, Phillips *et al*. 2006) performed best, followed by regression-based methods, while environmental envelopes performed worst. Similar rankings were reported from comparative studies in marine benthic environments (Huang *et al.* 2011, Reiss *et al.* 2011).

Scleractinian cold-water corals, especially the framework-building species *Lophelia pertusa* (Linnaeus 1758), have been a popular target for HSM development in the deep sea (Guinan *et al.* 2009a, Tittensor *et al.* 2010a, Davies & Guinotte 2011, Howell *et al.* 2011). They form emblematic vulnerable marine ecosystems (Rogers *et al.* 2008) and their biology and ecology are now well described (Rogers 1999, Roberts *et al.* 2009). *Lophelia pertusa* reefs are "hot spots of biomass and carbon cycling along continental margins" (van Oevelen *et al.* 2009). Their associated faunal abundance and diversity are consistently higher than in neighbouring non-coral areas and they support a "characteristic reef fauna" (Henry & Roberts 2007, Roberts *et al.* 2008). A pan-European research project (Roberts *et al.* 2006) reported > 1300 species associated with *L. pertusa* reefs and this number is increasing as new

reefs are discovered and new species are described. These cold-water coral reefs also have an important role as feeding, breeding and nursery grounds for fish, including commercially important species (Costello *et al.* 2005).

Lophelia pertusa is widely distributed globally and has been reported from depths between ~ 40 - 3800 m (Freiwald *et al.* 2004). This suspension feeding species prefers areas with enhanced currents that ensure plentiful food supply and prevent sediment building up on the hard substratum required by larvae for settlement (Roberts *et al.* 2006). Under favourable environmental conditions, *Lophelia pertusa* colonies may form thickets, reefs and eventually giant carbonate mounds that can reach > 300 m in height and several kilometres in diameter (Wheeler *et al.* 2007). In Irish waters, these carbonate mounds are clustered in a number of provinces which occur in a relatively narrow depth range along the continental margin (Dorschel *et al.* 2011).

Davies & Guinotte (2011) produced a global HSM for *Lophelia pertusa,* which provides the most detailed and complete predicted map of its distribution. Their study used bathymetry data of 1 arc-sec (~1 km) resolution and a wide range of interpolated environmental data, significantly improving model reliability compared to a previous HSM at 1 degree (~100 km) resolution (Davies *et al.* 2008). The improved HSM successfully captures environmental drivers of coral distribution on a global scale (e.g. depth, temperature, aragonite saturation state and salinity) and predicts high probability of coral occurrence along the slopes of the Irish margin and the Rockall and Porcupine Banks (Figure 3-1). While these areas are known to support thriving cold-water coral reefs, the amount of predicted coral habitat is most likely an over estimate, due to the lack of high-resolution terrain parameters, substratum and current data (Davies & Guinotte 2011). This constrains the practical use of the global HSM to support marine management strategies.

Rengstorf *et al.* (2012) have stressed the need for high-resolution (< 250 m grid cell size) multibeam bathymetry data to ensure identification of the often relatively small carbonate mounds that support a significant proportion of living *Lophelia pertusa* habitat in Irish waters. This study addresses that deficiency for Irish waters by making use of Irish National Seabed Survey (INSS) multibeam data to produce the

first comprehensive *L. pertusa* reef HSM. We focus on living *L. pertusa* reef habitat and exclude occurrences of dead or isolated colonies for two reasons: 1) we want to develop a coherent model which predicts the presence of living coral reefs based on present-day environmental settings (Ross *et al.* 2012), and 2) inclusion of the more widespread isolated colonies would result in over estimation of suitable coral reef habitat (Howell *et al.* 2011). Following Roberts *et al.* (2006) we define *Lophelia pertusa* reefs as "biogenic structures formed by *L. pertusa* frameworks that alter sediment deposition, provide complex structural habitat and are subject to the processes of growth and (bio)erosion".

In this study, we provide a comprehensive environmental dataset that can be utilised for HSM of other benthic and demersal species in the region, and a methodology that can be easily modified for HSM of such species in other environments. We demonstrate how the high-resolution HSM can provide an objective assessment of the appropriateness of marine protected areas in conserving cold-water coral reef ecosystems to capture biogeographic shifts in associated fauna in the extensive Irish continental margin.

3.2. Materials and Methods

Study area

The Irish seabed stretches from the Rockall Bank in the North (58° 0' N) to the South-West Approaches in the South (46° 50' N), and reaches from the Irish Sea in the East (5° 16' W) to the margin of the Iceland Basin in the West (25° 46' W, Figure 3-1). The INSS and Integrated Mapping for the Sustainable Development of the Marine Resource (INFOMAR) projects have mapped an area of > 500 000 km^2 of the Irish seabed, revealing numerous submarine canyons, seamounts and mound features with great detail (Dorschel *et al.* 2011).

HSMs can be influenced by the spatial extent of the landscape used for the background sample (van der Wal *et al.* 2009) and wherever possible the area of prediction and projection should be limited to areas of plausibly suitable habitat. The HSM was therefore restricted to regions identified as suitable for scleractinian cold-water corals using the global model (Davies & Guinotte 2011). This excluded the

Rockall Trough area and resulted in an analysis area covering ~ 310 000 km^2 and ranging from ~ 100 - 4000 m water depth (Figure 3-1).

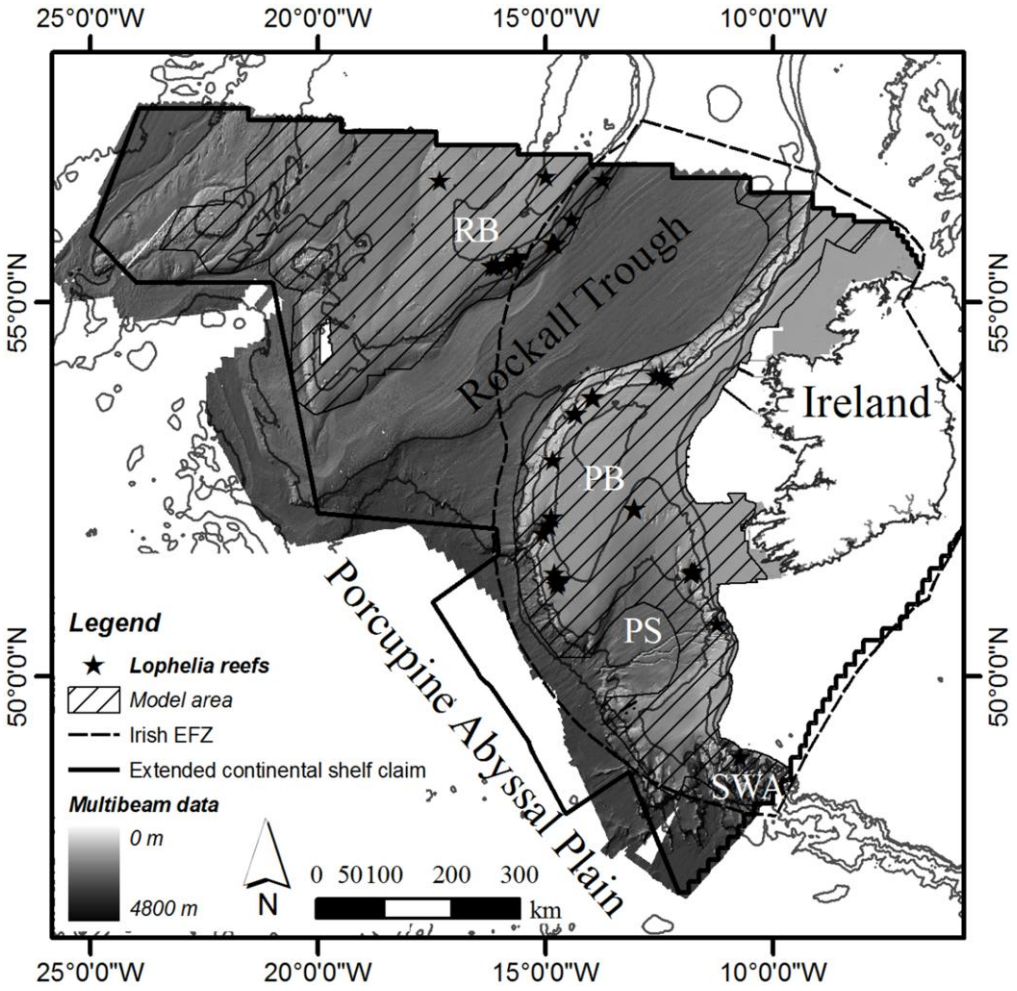

Figure 3-1: The extent of seafloor multibeam coverage undertaken by the Irish National Seabed Survey is shown together with the distribution of known living *Lophelia pertusa* reefs (black stars). The Irish Economic Fisheries Zone (EFZ, 200 nm limit) and the limit of the Irish extended continental shelf claim (cf. Symmons 2000, Long & Grehan 2002) are also shown. Hatching indicates the extent of the HSM study area, which encompasses the area of suitable coral habitat predicted by a global HSM (Davies & Guinotte 2011). RB = Rockall Bank, PB = Porcupine Bank, PS = Porcupine Seabight, SWA = South-West Approaches.

Species distribution data

Video data

A total of 20 video transects was acquired during two research cruises (CE0908 and CE10014) using the Irish Research Vessel *Celtic Explorer* and the remotely operated vehicle (ROV) *Holland I*: 2 transects on the Southern Porcupine Bank covering 800 m and 5200 m respectively (CE0908) and 18 transects, each of 2000 m length, covering areas on the Rockall Bank, Porcupine Bank and Porcupine Seabight (CE10014). The ROV was equipped with three low definition cameras (vertical, pilot and aft) as well as a forward facing oblique (45° to the seabed) High Definition video camera (all Kongsberg). Navigation data (accurate to ~ 1m) were provided by an Inertial Navigation System (PHINS, IXSEA) connected to an external ultra-short baseline sensor (GAPS, IXSEA). The HD video data was used for species identification and for differentiation between living and dead *L. pertusa* framework (based on coral branch colour and presence or not of polyp tissue). Video data were annotated in intervals of ~ 5 m and all observations of *L. pertusa* reef habitat were recorded and geo-referenced.

Lophelia pertusa distribution database

Lophelia pertusa occurrence records were assembled from databases, cruise reports and publications (Appendix S1). A total of 4423 records were integrated into a database including -where possible- their source, geographic position and information on the coral's life stage, occurrence type, sampling equipment and spatial precision of the record (Table 3-1). Quality control ensured that records used for analysis: 1) represented confirmed living *L. pertusa* reefs (so excluding 2900 records of dead and isolated coral colony records); 2) were derived from sampling equipment that allows for accurate (< 200 m) geo-referencing with sufficient accuracy to fall within the model's grid cell size (so excluding 620 records derived mainly from trawling and dredging activities); and 3) were not duplicated. A total of 245 occurrences were retained for the analysis.

Table 3-1: Sources of *Lophelia pertusa* distribution data. Available metadata are indicated by check marks. Total number of records and number of records retained after quality and spatial filtering are given.

Source	alive vs dead	colony vs. reef	sampling equipment	spatial precision	# records	# records retained
Cruise reports	✓	✓	✓	✓	145	8
HERMES[1]	✓	✓	✓	✓	322	6
OBIS[2]	✓	-	-	✓	375	0
OSPAR[3]	-	only reef	-	✓	176	0
Publications	✓	✓	✓	✓	251	3
Video data[4]	✓	✓	✓	✓	3154	36
Total:					**4423**	**53**

[1]De Mol (2009)
[2]Downloaded from iOBIS.org [25/07/2011, Databases: Cold Water Corals (354 records), Hexacorallians of the World (19 records), NMNH Invertebrate Zoology Collections (2 records)]
[3]OSPAR Threatened and/or Declining Habitats Database (2009). Maintained by the Joint Nature Conservation Committee
[4]Resulting from video analysis of two CoralFISH cruises (CE0908 and CE10014)

Table 3-2: Normally scaled environmental variables developed for this study. The abbreviations for the multi-scale terrain variables used in the text are given in brackets.

Variables	Native Resolution	Source & Software
Bathymetry variables		
Depth (m)	0.002°	INSS bathymetry (ArcGIS)[a]
Slope[1] (º) (slope-5, slope-25, slope-49)	0.002°	INSS bathymetry (Landserf)
SD of slope[1] (SD of slope-5, SD of slope-25, SD of slope-49)	0.002°	INSS bathymetry (Landserf, ArcGIS)
Bathymetric position index[2] (BPI-5, BPI-25, BPI-49)	0.002°	INSS bathymetry (BTM)
Rugosity[1] (rugosity-3, rugosity-25, rugosity-49)	0.002°	INSS bathymetry (BTM)
Chemical variables		
Alkalinity, total carbon dioxide (μmol kg^{-1})	1°	(Key *et al.* 2004)[c]
Aragonite (Ω), calcite (Ω), pH	1°	(derived from Key *et al*. 2004)
Nitrate, phosphate, silicate (μmol L^{-1})	1°	(Garcia *et al.* 2010a)[b]
Salinity (psu)	0.25°	(Antonov *et al.* 2010)[b]
Salinity (ROMS) (psu)	2.5 km	(Marine Institute 2012)[d]
Hydrodynamic variables		
Bottom stress (N m^{-2}), current speed (m sec^{-1}), vertical flow (m sec^{-1})	2.5 km	(Marine Institute 2012)[d]
Oxygen variable		
Percentage oxygen saturation (%) (oxygen)	1°	(Garcia *et al.* 2010b)[b]
Temperature variables		
Temperature (ROMS) (ºC)	2.5 km	(Marine Institute 2012)[d]
Temperature (ºC)	0.25°	(Locarnini *et al.* 2010)[b]

[1] three layers computed with neighbourhoods of 5 x 5, 25 x 25 and 49 x 49 grid cells
[2] three layers computed with an inner radius of 1 and an outer radius of 5, 25 and 49 grid cells
[a] Data download: http://jetstream.gsi.ie/iwdds/index.html
[b] Data download: http://www.nodc.noaa.gov/OC5/WOA09/pr_woa09.html
[c] Data download: http://cdiac.ornl.gov/oceans/glodap/Glodap_home.htm
[d] Model accessible at www.marine.ie/home/services/operational/oceanography/OceanForecast.htm

Environmental variables

We generated 29 environmental variables (Table 3-2) to determine which were most important for modelling coral distribution.

Terrain-based variables

The INSS multibeam bathymetry data of 0.002° spatial resolution were projected to the Universal Transverse Mercator coordinate system (UTM 28N) with a grid cell size of 200 m prior to terrain analysis. A multi-scale moving-window terrain analysis (Wilson *et al.* 2007) was conducted employing window sizes of 5^2, 25^2 and 49^2 grid cells (Table 3-2). Seabed slope, rugosity and bathymetric position index (BPI, Weiss 2001) were calculated following Wilson *et al*. (2007). The standard deviation (SD) of slope was generated by passing the same moving analysis windows as above over the fine-scale slope grid (slope-5, i.e. slope grid derived with the moving window size of 5^2 grid cells) and calculating the SD for the neighborhood (Dunn & Halpin 2009). From here on the suffixes behind the variables define the moving window size used for their generation.

Chemical variables

Chemical parameters were derived from the World Ocean Atlas (WOA 2009) and the Global Ocean Data Analysis Project (GLODAP, Key *et al*. 2004). The variables were extracted from global depth tiered grids and converted into a single layer benthic grid of 0.002° spatial resolution using the scaling process of Davies & Guinotte (2011). This process interpolates depth tiers into a higher resolution grid using inverse distance weighting and then selects the sea-bottom value directly from the depth tier suggested by the depth of the reference bathymetry grid. The aragonite saturation state has important implications for scleractinian corals as they can have difficulty maintaining their external calcium carbonate skeletons in under-saturated waters (Orr *et al.* 2005, Guinotte & Fabry 2008, Feely *et al.* 2009). The calcium carbonate saturation states (omega aragonite and omega calcite) were calculated from temperature, salinity, phosphate and silicate from the WOA along with alkalinity and total CO_2 from GLODAP using the methodology outlined in Orr *et al.* (2005) and implemented in the carb function of the "seacarb: seawater carbonate chemistry with R" package (http://CRAN.R-project.org/package=seacarb). Primary

productivity (chlorophyll a) was not included as it was only available as a sea surface layer which precludes its use for interpolating from depth-tiered grids.

Hydrodynamic variables

Hydrodynamic variables were derived from the Irish Marine Institute's Regional Ocean Modelling System (Marine Institute 2012), which simulates ocean circulation patterns over a large portion of the north-east Atlantic. The model has a spatial resolution of 2.5 km and 40 terrain-following vertical levels. Model output was computed at 6 hour intervals for the period between 15 April and 15 May 2010 (corresponding to the period of CE10014). We note that in spite seasonal differences in the strength of the hydrodynamic signals, their relative spatial distribution can be considered to be fairly stable, as near bottom tidal currents are relatively stable over long time periods (C. Mohn, personal communication). Grids were produced giving mean values for bottom (shear) stress, current speed, vertical flow, temperature and salinity at the near-bottom layer (thickness ~ 0.1% water depth) and were interpolated to 0.002° spatial resolution using bilinear interpolation in ArcGIS v. 9.3.

Selection of environmental variables

The choice of predictor variables for a particular species is crucial in HSM as the use of too many variables may result in over-fitting and co-linearity of environmental layers (Guisan & Zimmermann 2000). We followed the methods outlined in Yesson *et al.* (2012) for variable selection: environmental variables were clustered into ecologically meaningful groups: (i) "bathymetry"; (ii) "hydrodynamics"; (iii) "oxygen"; (iv) "temperature"; and (v) "chemistry" (Table 3-2); the variable with the highest predictive value within each cluster when used in isolation was selected as representative of each group for model building.

Maximum entropy modelling

Maximum entropy modelling was used to predict *Lophelia pertusa* reef distribution at a spatial resolution of 0.002°. Maximum entropy (Maxent, Phillips *et al.* 2006) is a commonly used algorithm for HSM with presence-only data. It has consistently been shown to perform well against other methods (Elith *et al.* 2006, Huang *et al.* 2011, Reiss *et al.* 2011) and has been successfully applied in previous cold-water coral HSMs (Davies & Guinotte 2011, Howell *et al.* 2011, Yesson *et al.* 2012). The

maximum entropy principle states that a probability distribution with maximum entropy (i.e. the closest to uniform), subject to known constraints (e.g. environmental constraints), is the best approximation of an unknown distribution (e.g. of a certain species or habitat), as it agrees with everything that is known, but avoids assuming anything that is unknown (Phillips *et al.* 2006). Maxent assigns log-scaled habitat suitability values to each grid cell within the study area, where values near 0 mean low and values near 1 mean high habitat suitability. We used Maxent version 3.3.3k with default settings. However, after visual inspection of results and extensive trials, prevalence was set to 0.7 to calibrate the model towards higher habitat suitability values in known coral-rich areas.

Model evaluation

Coral observations are highly clustered in regions targeted by research expeditions, which might lead to falsely inflated model evaluation measures (Veloz 2009). Therefore, we coarsened the distribution data by deleting all but one record within grid cells of 0.02° resolution (Davies & Guinotte 2011). The remaining 53 points were subject to a spatial cross-validation process: a random presence point was chosen, grouped with its 12 closest points based on Euclidean distance and withheld from model training. This process was repeated for all records resulting in 53 replicates of spatially non-overlapping sets of test (n=13) and training (n=40) data.

AUC and test gain

The area under the curve (AUC) of the receiver operating characteristic (ROC) is the dominant tool for the evaluation of presence-only models as it has the advantage of being threshold independent (Fielding & Bell 1997). AUC values range from 0 (worse-than-random model) to 1 (best model), with a random prediction scoring 0.5 (Phillips *et al.* 2006). AUC values have been criticized for being biased by the spatial extent of the study area (Lobo *et al.* 2007), so we applied test gain, a measure analogous to deviance used to assess performance of generalized linear and additive models (Phillips 2005).

Jackknife assessment

Maxent's jackknife test is a stepwise selection method which systematically drops variables one at a time and determines the respective variable's importance by

assessing predictive performances of a model using all variables except the dropped one and a model which is based on that variable only (Phillips 2005).

Threshold selection

A threshold is required for binary maps to indicate species presence and absences (Liu *et al.* 2005, Jiménez-Valverde & Lobo 2007). We used Maxent's 10th percentile (training presence value) threshold as cut-off for *L. pertusa* reef presence and absence.

3.3. Results

Environmental variable selection

Initial data exploration revealed significant degrees of correlation between clustered variables (Appendix S2a). Test AUC values for each of the 29 one-parameter models ranged from fair (0.59, pH) to high (0.92, SD of slope-5) (Appendix S2b). Besides SD of slope-5, BPI-5 (0.89) was retained as a bathymetric layer as there was no correlation between BPI and other bathymetry layers. The depth layer was excluded from final analyses, as all other environmental layers utilized bathymetry data at some point in their construction. Amongst the chemical variables, omega aragonite, omega calcite and silicate performed equally well (0.91) and omega aragonite was selected for analysis due to its immediate importance for calcifying corals. Temperature derived from the global dataset yielded a higher predictive value (0.83) than temperature derived from the regional ROMS model (0.72). Amongst the hydrodynamic variables, bottom stress had the highest predictive value (0.83). The full model used six selected variables: SD of slope-5, BPI-5, omega aragonite, bottom stress, percent oxygen saturation and temperature.

Distribution of Lophelia pertusa in Irish waters

Approximately 70% of all reef occurrence points were associated with mound features, 20% were found within canyons or channel systems, and the remaining were associated with steep slopes or the edges of escarpments. Figure 3-2 shows summary statistics of the selected environmental variables at reef locations compared to the overall environmental conditions in the study area. Summary statistics for the complete dataset are given in Appendix S3.

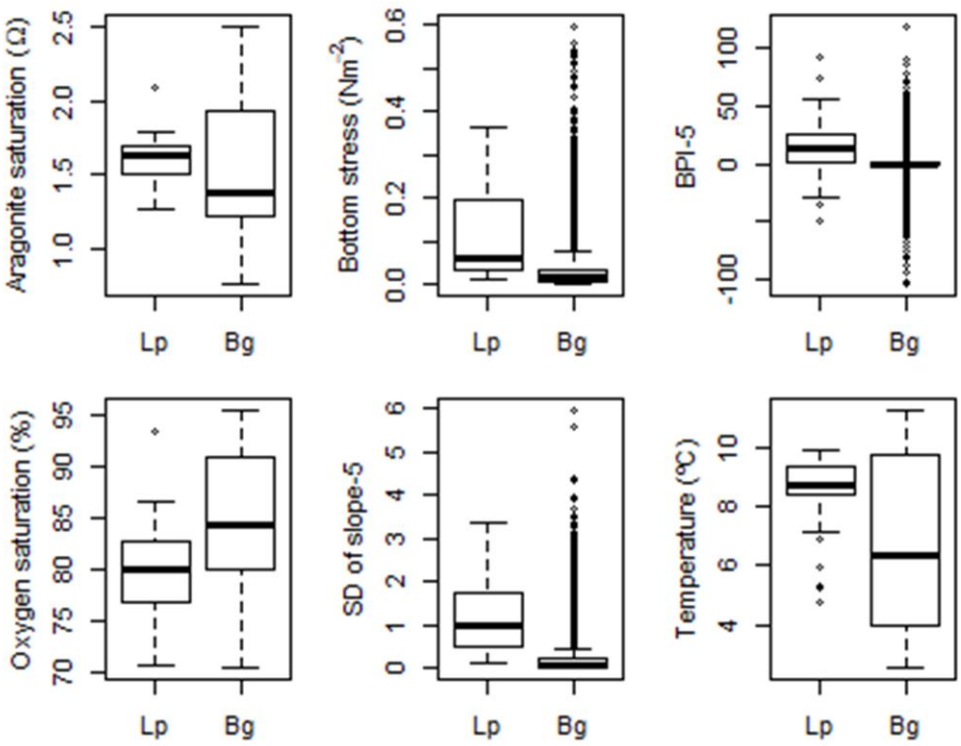

Figure 3-2: Boxplots showing range (dashed lines), median (thick black line), upper and lower percentiles (box) and outliers (points) for the environmental predictor variables at locations with *Lophelia pertusa* reefs (Lp) and for 10 000 random background points (Bg).

Approximately 95% of the existing reef records were located between 640 - 1440 m water depths. Reefs occurred in a relatively narrow salinity range of 35.0 -35.6 psu and at temperatures ranging from 4.8 - 9.9 ºC. All coral observations were located in areas supersaturated for aragonite ($\Omega > 1$). Oxygen saturation in the study area ranged from 70.3 to 95.5 % and reefs could be found throughout most of this range (70.5 - 93.4 %). Most reef records were located in areas of enhanced current speed and bottom stress and at locations of relatively high terrain variability compared to overall background values.

Model evaluation

Training and test AUC values were consistently high (> 0.97) indicating an accurate fit and successful prediction of the suitable habitat in test areas (Table 3-3). High AUC scores were supported by a high test gain (2.25). Jackknife tests revealed the high predictive importance of SD of slope-5 and temperature variables, together contributing 82 % to the model. Bottom stress and oxygen concentration were the

next important variables, followed by small contributions of BPI-5 and omega aragonite. The variable delivering highest AUC values when used in isolation was SD of slope-5, indicating that this variable had the most predictive information by itself. SD of slope-5 also decreased test and train AUC the most when omitted from the model build, indicating that it carries most information that is not present in the other variables.

Table 3-3: Summary statistics (average and SD of 53 replicate model runs) of evaluation measures, jackknife test of variable importance and 10th percentile threshold results.

Evaluation			
Training gain	Training AUC	Test gain	Test AUC
3.1 ± 0.2	0.98 ± 0.01	2.3 ± 0.7	0.97 ± 0.02
Jackknife test of variable importance			
	% variable contribution	Test AUC with-out variable	Test AUC with only variable
SD of slope-5	54	0.95	0.92
Temperature	28	0.97	0.83
Bottom stress	9	0.97	0.83
Oxygen	6	0.97	0.70
BPI-5	3	0.97	0.89
Aragonite	0	0.97	0.91
Threshold (10th percentile)			
Logistic value	Area suitable	Omission	
0.53	0.02	0.09	

Modelled distribution of Lophelia pertusa reef habitat

Analysis of response curves provided insight into how the variables shape the predicted environmental niche (Figure 3-3). Suitability scores rapidly increased with growing terrain variability (SD of slope-5) and hydrodynamic activity (bottom stress). Probability of reef presence was predicted to be highest in a temperature range from ~ 4 to 11 ºC. The one-parameter response for BPI-5 suggests high habitat suitability scores for low and high BPI values, reflecting reef occurrences on seabed features such as carbonate mounds as well as in canyon systems. However, the relative flatness of the solid BPI-5 curve demonstrates the variable's small contribution to the full model. High habitat suitability values were associated with aragonite saturation values > 1, however the contribution of aragonite to the full model was negligible (see discussion). Interestingly, probability of reef presence

seems negatively correlated with dissolved oxygen concentration, which is most likely a reflection of the limited oxygen range sampled.

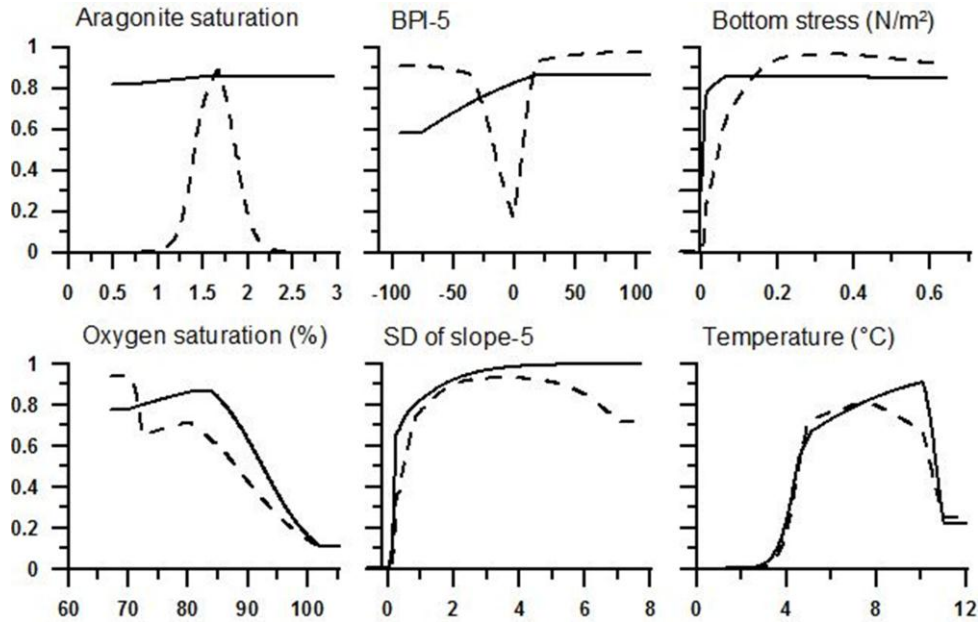

Figure 3-3: Response curves showing the relationships between predictor variables and habitat suitability scores. The solid curves show how Maxent's prediction changes as each environmental variable is varied, keeping all other environmental variables at their average sample value, whereas the dashed curves represent models built using only the corresponding variable (i.e. one-parameter models).

The final HSM was generated using all 53 occurrence records for model training. The 10th percentile training presence threshold (0.53) was applied to produce a presence/absence map of potential reef habitat (Figure 3-4). Generally, suitable habitat was predicted in areas of enhanced hydrodynamic regimes, mostly on mound features, along escarpments and in canyons systems along a narrow band following the slopes of the Irish continental margin, the Rockall Bank and the Porcupine Bank.

3.4. Discussion

Previous HSMs have been constructed at coarse resolution on a global scale (Davies & Guinotte 2011) or at high-resolutions over very small areas (Dolan *et al.* 2008, Guinan *et al.* 2009a, Rengstorf *et al.* 2012). Our model makes use of limited occurrence data to create a continuous coverage high-resolution predicted occurrence map for *L. pertusa* reefs, taking into account (i) effects of analysis scale on terrain

parameters (Wilson *et al.* 2007); (ii) reduction of co-variation between environmental variables (Yesson *et al.* 2012); (iii) quality control of coral occurrence records to avoid over estimation of reef habitat (Howell *et al.* 2011, Ross *et al.* 2012); (iv) minimization of spatial autocorrelation effects through data coarsening (Veloz 2009, Davies & Guinotte 2011) and spatial cross-validation; and (v) application of a habitat suitability threshold to produce a binary presence/absence map (Liu *et al.* 2005).

High-resolution HSM for cold-water corals

The lack of extensive high-resolution environmental data has been identified as a major limitation to the applicability of HSMs (Davies *et al.* 2008, Tittensor *et al.* 2009, Davies & Guinotte 2011). In a global cold-water coral HSM, for example, the coarse resolution of temperature data led to a mismatch between coral occurrences and temperature values beyond the species' thermal tolerance limit (Davies *et al.* 2008). Temperature is an important factor influencing the physiology (Dodds *et al.* 2007) and spatial distribution of cold-water corals (Freiwald *et al.* 2004). The suitable temperatures captured by our model (4.8 - 9.9 ºC) lie well within the limit of the species' reported temperature range (Freiwald *et al.* 2004).

Terrain parameters can indicate areas of enhanced current regimes (Genin *et al.* 1986) and hard bottom habitat (Dunn & Halpin 2009). Both factors are essential prerequisites for reef initiation and development (Freiwald *et al.* 2004). Depending on the analysis scale, corals have been associated with numerous seabed features ranging from continental slopes and large seamounts (Tittensor *et al.* 2009, Davies & Guinotte 2011) to carbonate mounds (Guinan *et al.* 2009a) and sediment waves (Dolan *et al.* 2008). Fine-scale terrain variability contributed >50% to the model in this study, highlighting the importance of high-resolution bathymetry data in resolving small topographic features likely to support corals (Rengstorf *et al.* 2012). Unsuitable terrain was identified in many open slope areas of known soft bottom habitat that had been considered suitable employing the global scale model (Davies & Guinotte 2011).

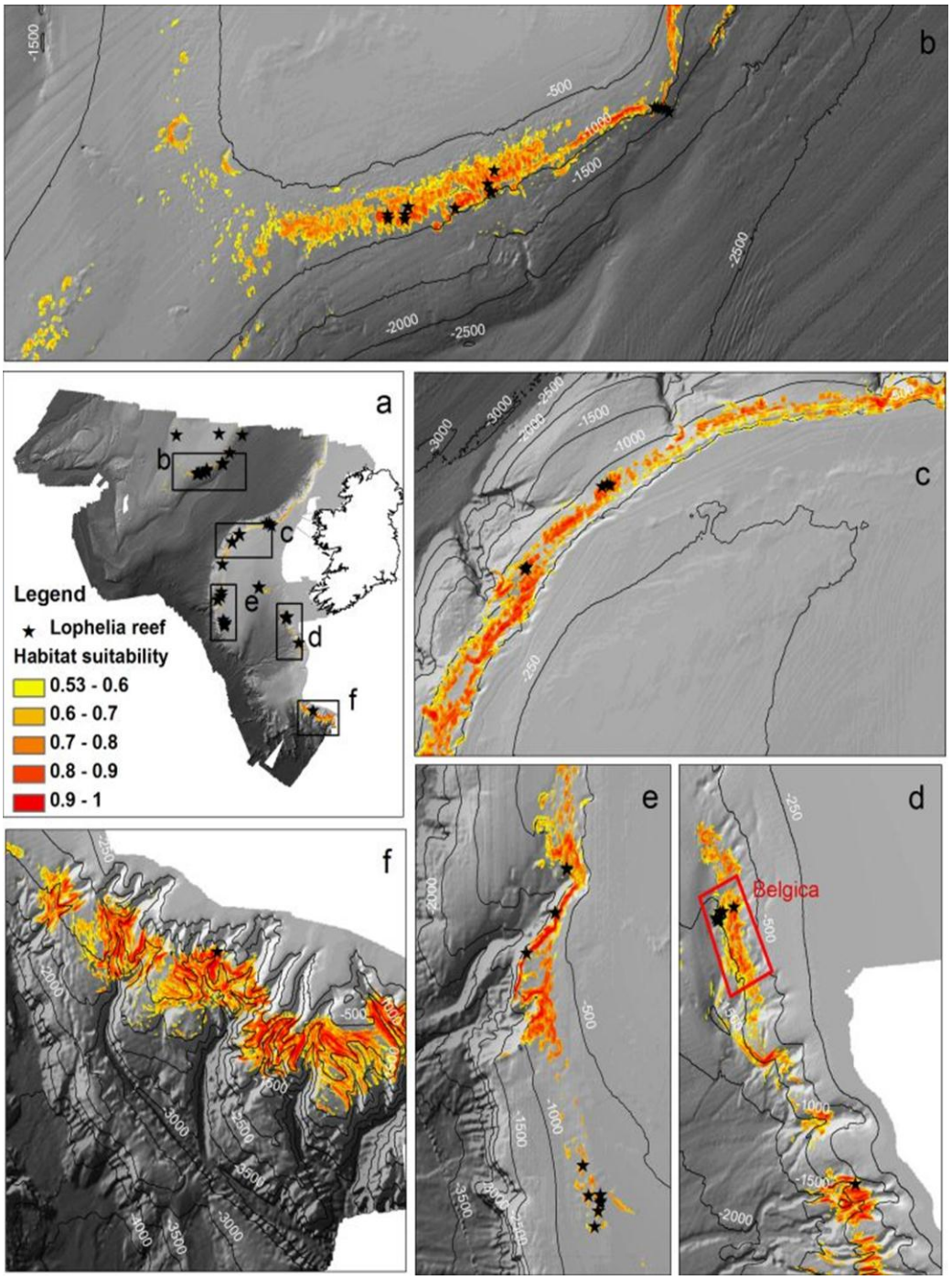

Figure 3-4: *Lophelia pertusa* habitat suitability map for the Irish continental margin (a). Black stars represent the 53 *L. pertusa* reef occurrence records used for HSM development. Insets show close-ups of the Southern Rockall Bank (b), the Northern Porcupine Bank (c), the Eastern Porcupine Seabight with the location of the Belgica mound province indicated (d), the Southern Porcupine Bank (e) and the South-West Approaches (f). Only areas identified as *L. pertusa* presence above the 10th percentile threshold (0.53-1) are colour-coded. Map projection is UTM 28N (WGS84).

None of the hydrodynamic variables were significantly correlated with any of the bathymetric variables. This may be due to differences in the variables' native resolution (Table 3-2), yet it indicates that the hydrodynamic model variables carried valuable information not reflected in terrain morphology. The Maxent model reveals a strong positive effect of bottom stress on suitable coral habitat, corroborating *L. pertusa* reefs' reliance on currents to provide food supply to the coral polyps and to reduce sediment deposition (Frederiksen *et al.* 1992, White *et al.* 2005, Thiem *et al.* 2006).

Aragonite is the calcium mineral form deposited by scleractinian corals to build their skeletons and its saturation state is an important driver of coral distribution on a global scale, with areas under-saturated for aragonite being difficult environments for scleractinian corals (Guinotte *et al.* 2006, Tittensor *et al.* 2010a, Rodolfo-Metalpa *et al.* 2011). This study area is uniformly supersaturated for aragonite, so this parameter had little effect on our model.

Global HSMs indicate that *L. pertusa* should not be found in oxygen limited environments (Tittensor *et al.* 2009, Davies & Guinotte 2011). Ecophysiological studies confirm that *L. pertusa* cannot maintain aerobic metabolism at oxygen concentrations below 3 mL L^{-1} (Dodds *et al.* 2007). The negative relationship suggested by the oxygen response curves is most likely a reflection of the limited oxygen range sampled.

Although *L. pertusa* reef occurrences in this study are derived from a large range of data sources, there are regions where no sample data are available. The area west of the Rockall Bank, for example, harbours numerous mounds and seamounts (Dorschel *et al.* 2011) but it is predicted to be unsuitable, mainly because water temperature values are outside the range captured by the available occurrence data. When using presence-only data, predictions in broad unsampled areas are affected by spatial sampling bias (i.e. some areas are sampled more intensively than others) and must be interpreted with caution (Phillips *et al.* 2009). Spatial sampling bias is thought to be less of an issue when using presence-absence algorithms, as both presence and absence records are affected and the bias effect is largely cancelled out (Elith *et al.* 2011). While not possible in the present study, Phillips *et al.* (2009)

propose a method to correct for sampling bias in presence-only models by choosing background data in a way that reflects the sampling effort.

Another limitation of presence-only modelling is that the prevalence of the species in the study area (i.e. proportion of occupied sites) cannot be exactly determined (see Elith *et al*. 2011 for details). While presence-absence models identify the probability of species occurrence, presence-only models estimate a "relative likelihood of occurrence" (Pearce & Boyce 2006). We note, however, that absence data do not always yield reliable estimates of prevalence, as they may be flawed due to varying sampling effort within grid cells and imperfect species detection (Elith *et al.* 2011). In the present study, absence data were not available from databases and could not be reliably inferred from video analysis due to the scale discrepancy between the camera's field of view (~ 2 m) and the model's grid cell size (~ 200 m). Presence-only modelling allowed us to use occurrence records derived from a wide range of sources and effectively ruled out the risk of confounding predictions due to false absence records.

Extensive suitable reef habitat is predicted in canyon systems (Figure 3-4f). These predictions are driven by the extreme terrain parameter values typical for these seabed features. Canyons are complex dynamic systems that are likely to be influenced by fine scale processes not captured by the environmental dataset used in this study. However, enhanced hydrodynamic activity and organic matter flux make some canyons hotspots of biodiversity and biomass (De Leo *et al.* 2010) and could provide favourable conditions for suspension-feeding corals. *Lophelia pertusa* reefs have been observed in many canyons along continental slopes of the north-east Atlantic (De Mol *et al.* 2010, Huvenne *et al.* 2011) and in the Mediterranean (Orejas *et al.* 2009). Extensive cold-water coral framework was found growing on walls and overhanging cliffs in canyons, reflecting not only favourable conditions for growth but also the possibility that these areas represent natural refuges protecting against adverse impacts from bottom trawling (Huvenne *et al.* 2011).

Preliminary models constructed using the species distribution data prior to quality control predicted a much wider range of suitable habitat. Shallow areas (< 400 m depth) were especially affected by the data cleaning process. Numerous observations

on top of the Rockall Bank lacked information about whether records represented living or dead coral reefs and were therefore omitted from analyses. Inclusion of these samples would have resulted in prediction of suitable habitat in shallower areas including the top of Rockall Bank. While *L. pertusa* colonies have been observed in water depths as shallow as 39 m in Norwegian fiords (Freiwald *et al.* 2004), most living reefs in Irish waters occur at depths below 600 m. One interesting aspect of our model is that living reef is predicted over all of the Belgica Mound Province (Eastern Porcupine Seabight, Figure 3-4d), whereas video data revealed the occurrence of mainly dead coral and coral rubble over some parts (Foubert *et al.* 2005). Further work is required to determine whether these corals are fossil reefs that were thriving in environmental conditions different from those encountered at present, or are dead due to the cumulative impact of trawling over the past 50 years. These findings also reinforce the need for databases incorporating as much sample information as possible (Ross *et al*., 2012).

Management implications

To demonstrate the utility of high-resolution HSMs in conservation planning, we take the example of current measures to protect coral reefs within the Irish Exclusive Fisheries Zone (200 nm limit, Figure 3-5). Four areas covering some 2500 km^2 of the seabed were designated as Special Areas of Conservation (SAC) under the European Union Habitats Directive in 2006 based on a partial knowledge at the time of the distribution of *Lophelia pertusa*. However, using a simple methodology where HSM outputs, based on our selected threshold, are gridded into 10 x 10 km squares, our results suggest that the existing SACs only occupy the central portion of the predicted reef distribution and fail to protect sufficient reefs to fully encompass the likely biogeographic variability of the associated fauna (Rogers 1999). Potential reef clusters to the north, south and west of the existing SACs (Figure 3-5) should be investigated to determine whether additional SACs are warranted to capture the biogeographical variability of Irish coral reefs.

A more representative network of protected areas might also ensure adequate gene flow between coral areas. This is particularly important as genetic analyses have revealed high levels of inbreeding and low gene flow among *Lophelia pertusa*

subpopulations (Le Goff-Vitry *et al.* 2004, Morrison *et al.* 2011); therefore the maximum distance between protected areas is an important consideration in planning MPA networks to protect cold-water corals. More research to better understand population connectivity and larval dispersal needs to be undertaken as a basis for more effective conservation planning (Morrison *et al.* 2011).

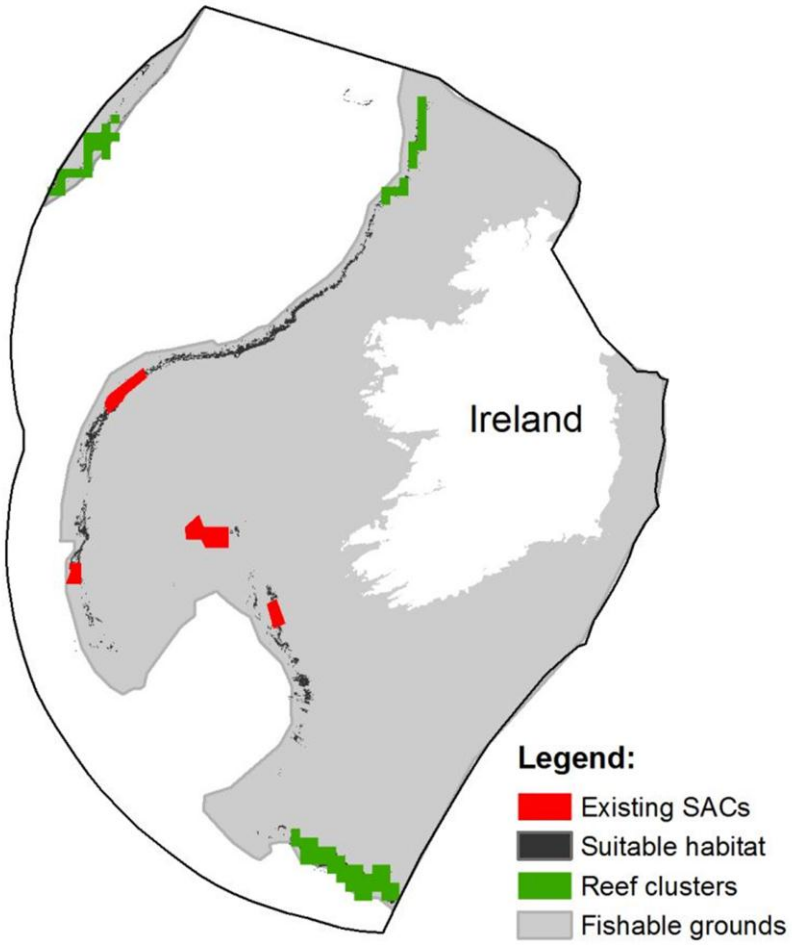

Figure 3-5: Map showing the distribution of suitable coral habitat and existing coral Special Areas of Conservation set against a backdrop showing the fishable grounds (down to a maximum depth of 1500 m) within the Irish Exclusive Fisheries Zone. Predicted reef clusters with the potential (upon further investigation) to improve the biogeographic representivity of the existing MPA network are highlighted in green.

In addition, our model can provide an estimate of the proportion by area of coral protected under existing conservation measures. In this example, based on the selected threshold, our model predicts 2 % (~ 7000 km^2) of the study area to be suitable *L. pertusa* reef habitat while existing SACs account for merely 10% of this

predicted distribution. The European Commission recommends that European Union member states conserve a minimum of 20% of prescribed habitat and species following an assessment of the proportion of the total regional resource contained within the designated SACs (JNCC 2009). This also suggests that further conservation measures are required.

Towards high-resolution multi-species habitat maps

This study is one example of a small number of studies (Huang *et al.* 2011, Tracey *et al.* 2011) that are using a wide range of environmental variables for regional habitat suitability modelling of benthic species. To the best of our knowledge, this study is the first to incorporate full coverage (> 500 000 km^2) high-resolution multibeam bathymetry over a wide variety of deep-sea (> 200 m depth) morphological features (seamounts, carbonate mounds, escarpments, canyons and channels, iceberg ploughmarks (Dorschel *et al.* 2011)). It can easily be adapted for an analysis of the distribution of other vulnerable benthic species that may require protection such as other scleractinian, antipatharian and gorgonian corals and deep-sea sponge aggregations known to be present in the region (Le Danois 1948). As habitat requirements vary between species, the selection of appropriate predictor variables constitutes a crucial step in analysis. The environmental data should be clustered into ecologically meaningful groups and predictor variables should be carefully chosen based on both their explanatory power and ecological relevance for the target species. As new data become available and as modelling techniques develop, so will the identification of biodiversity hotspots and priority areas for conservation management in the context of marine spatial planning.

Conclusions

Our model integrates ecologically meaningful environmental variables with high-resolution multibeam bathymetry data to predict the potential distribution of cold-water coral reef habitat. This significantly reduces over estimation demonstrated by global scale models and generates detailed prediction maps needed for conservation management. We provide a robust, coherent and transferrable methodology for benthic habitat suitability modelling in the deep sea. The comprehensive morphological and near-seabed environmental dataset for the Irish continental

margin can be applied to determine distribution of other species and, ultimately, biodiversity hotspots.

3.5. Supporting Information

Appendix S1: Sources for distribution data

	# records	**# retained after quality and spatial filtering**
Video data		
Johnson & Allcock & Shipboard Party (2010) Species at the margins –diversity cruise. CE10004. Cruise Report. School of Natural Sciences, NUI, Galway.	66	3
Grehan, A. & Shipboard Party (2009) A multidisciplinary investigation of ecosystem hotspots and their importance as fish habitat along the Irish and Biscay continental margins. CE0908 Cruise Report. Earth and Ocean Sciences, School of Natural Sciences, NUI, Galway.	301	5
Grehan, A. & Shipboard Party (2010) Deep water coral and fish interaction off the west coast of Ireland, CE10014 Cruise Report. Earth and Ocean Sciences, School of Natural Sciences, NUI, Galway.	612	13
Guinan, J. & Leahy, Y. (2010) Habitat Mapping of Geogenic Reef Offshore Ireland. Report prepared by the Marine Institute, Galway, Ireland and Geological Survey of Ireland to the Department of the Environment, Heritage and Local Government's National Parks and Wildlife Service.	2175	15
Total	**3154**	**36**
Publications		
Guinan, J., Brown, C., Dolan, M.F.J. & Grehan, A.J. (2009) Ecological niche modelling of the distribution of cold-water coral habitat using underwater remote sensing data. *Ecological Informatics*, **4**, 83-92	250	3
Mienis, F., De Stigter, H.C., De Haas, H. & Van Weering, T.C.E. (2009) Near-bed particle deposition and resuspension in a cold-water coral mound area at the Southwest Rockall Trough margin, NE Atlantic. *Deep Sea Research Part I: Oceanographic Research Papers*, **56**, 1026-1038	1	0
Total	**251**	**3**
Cruise Reports		
Duineveld G. & Shipboard Scientific Crew (2006) Cruise Report RV Pelagia, Cruise 64PE 249, Biodiversity, ecosystem functioning and food web complexity of cold-water coral reefs in the NE Atlantic (Rockall Bank). Royal Netherlands Institute for Sea Research, Texel, The Netherlands, 55 pp	14	0

Lavalaye M. & Shipboard Scientific Crew, Cruise Report RV Pelagia, Cruise 64PE 291-292, Biodiversity, ecosystem functioning and food web complexity of cold water coral reefs in the NE Atlantic, and the relation between fish and coldwater corals. & Testing the MOVE. Royal Netherlands Institute for Sea Research, Texel, The Netherlands, 90pp	1	0
Olu-Le Roy, K., Caprais, J.-C., Crassous, P., Dejonghe, E., Eardley, D., Freiwald, A., Galeron, J., Grehan, A., Henriet, J.P., Huvenne, V., Lorance, P., Noel, P., Opderbecke, J., Pitout, C., Sibuet, M., Unnithan, V., Vacelet, J., Van Weering, T., Wheeler, A. & Zibrowius, H. (2002) Caracole Cruise, N/O Atalante and ROV Victor, 1+2. In. Ifremer, Brest	43	6
Pfannkuche O. & Shipboard Party (2004b) Cruise Report RV Meteor, Cruise M61-1, Geo-Biological Investigations on Azooxanthellate Cold-Water Coral Reefs on the Carbonate Mounds Along the Celtic Continental Slope. IFM-Geomar, 67 pp	7	2
Van Duyl FC, Duineveld GCA. 2005. BIOSYS-HERMES 2005 cruise report with R.V. Pelagia. Cruise 64PE 238, Galway-Texel, 21 June-21 July 2005. Biodiversity, ecosystem functioning and food web complexity of deep water coral reefs in the NE Atlantic (Rockall Bank and Porcupine Bank)	80	0
Total	**145**	**8**
DATABASES		
De Mol, B. (2009) The HERMES cold-water coral database. In. PANGAEA. download: http://doi.pangaea.de/10.1594/PANGAEA.728313	322	6
Downloaded from iOBIS.org [25/07/2011, Databases: Cold Water Corals (354 records), Hexacorallians of the World (19 records), NMNH Invertebrate Zoology Collections (2 records)]	375	0
JNCC (2009) OSPAR Threatened and/or Declining Habitats Database. Maintained by the Joint Nature Conservation Committee	176	0
Total	**873**	**6**
TOTAL	**4423**	**53**

Appendix S2a: Pair-wise Pearson correlation coefficients (*r*) for environmental predictor variables developed for the study. Cells are colour-coded based on their *r*-value: red = high correlation (0.8 - 1); orange = moderate correlation (0.6 - 0.8); yellow = low correlation (0.4 - 0.6), white = no correlation (0 - 0.4).

	BATHYMETRY													CHEMISTRY										TEMPERATUR		HYDRODYNAMICS			OXYGEN
Variables	Depth	BPI-5	BPI-25	BPI-49	Rugosity-5	Rugosity-25	Rugosity-49	Slope-5	Slope-25	Slope-49	SD slope-5	SD slope-25	SD slope-49	Aragonite	Calcite	Alkalinity	Nitrate	Phosphate	Silicate	pH	tCO2	Salinity (ROMS)	Salinity	Temperature (ROMS)	Temperature	Bottom stress	Current speed	Vertical flow	Diss. Oxygen
Depth	1.00	0.05	0.14	0.22	-0.20	-0.23	-0.30	-0.38	-0.43	-0.47	-0.32	-0.40	-0.47	0.92	0.92	0.48	-0.84	-0.88	-0.93	0.74	-0.77	0.82	0.81	0.89	0.89	0.25	0.15	-0.06	0.56
BPI-5	0.05	1.00	0.65	0.47	-0.09	-0.03	-0.02	-0.02	0.00	0.00	-0.12	-0.05	-0.04	0.03	0.03	-0.03	-0.02	-0.03	-0.06	0.02	-0.03	-0.01	0.02	0.00	0.03	-0.01	-0.01	0.03	0.02
BPI-25	0.14	0.65	1.00	0.89	-0.16	-0.07	0.00	-0.11	-0.03	0.01	-0.19	-0.12	-0.10	0.09	0.09	-0.03	-0.08	-0.09	-0.17	0.07	-0.09	0.04	0.07	0.05	0.09	0.06	0.05	-0.08	0.06
BPI-49	0.22	0.47	0.89	1.00	-0.18	-0.12	-0.05	-0.13	-0.07	0.00	-0.19	-0.15	-0.13	0.14	0.14	-0.03	-0.12	-0.13	-0.26	0.10	-0.12	0.09	0.12	0.11	0.14	0.10	0.09	-0.13	0.07
Rugosity-5	-0.20	-0.09	-0.16	-0.18	1.00	0.86	0.72	0.86	0.70	0.55	0.65	0.67	0.66	-0.16	-0.16	-0.02	0.15	0.15	0.19	-0.15	0.15	-0.11	-0.09	-0.13	-0.13	0.08	0.07	-0.28	-0.16
Rugosity-25	-0.23	-0.03	-0.07	-0.12	0.86	1.00	0.86	0.81	0.82	0.66	0.58	0.70	0.71	-0.18	-0.18	-0.04	0.16	0.17	0.21	-0.16	0.16	-0.13	-0.12	-0.16	-0.15	0.08	0.07	-0.29	-0.16
Rugosity-49	-0.30	-0.02	0.00	-0.05	0.72	0.86	1.00	0.77	0.88	0.83	0.57	0.73	0.77	-0.24	-0.24	-0.06	0.21	0.22	0.27	-0.20	0.19	-0.18	-0.17	-0.22	-0.21	0.07	0.06	-0.30	-0.18
Slope-5	-0.38	-0.02	-0.11	-0.13	0.86	0.81	0.77	1.00	0.90	0.80	0.77	0.82	0.87	-0.33	-0.34	-0.10	0.31	0.32	0.34	-0.32	0.31	-0.23	-0.21	-0.28	-0.27	0.10	0.10	-0.36	-0.30
Slope-25	-0.43	0.00	-0.03	-0.07	0.70	0.82	0.88	0.90	1.00	0.95	0.67	0.82	0.92	-0.38	-0.38	-0.12	0.35	0.36	0.38	-0.36	0.34	-0.27	-0.25	-0.32	-0.31	0.11	0.11	-0.38	-0.33
Slope-49	-0.47	0.00	0.01	0.00	0.55	0.66	0.83	0.80	0.95	1.00	0.60	0.75	0.90	-0.41	-0.41	-0.13	0.38	0.39	0.42	-0.40	0.38	-0.29	-0.27	-0.34	-0.33	0.11	0.11	-0.38	-0.36
SD slope-5	-0.32	-0.12	-0.19	-0.19	0.65	0.58	0.57	0.77	0.67	0.60	1.00	0.82	0.73	-0.28	-0.28	-0.08	0.26	0.27	0.30	-0.26	0.26	-0.20	-0.18	-0.23	-0.23	0.07	0.09	-0.26	-0.24
SD slope-25	-0.40	-0.05	-0.12	-0.15	0.67	0.70	0.73	0.82	0.82	0.75	0.82	1.00	0.88	-0.34	-0.34	-0.10	0.31	0.32	0.37	-0.30	0.30	-0.26	-0.24	-0.30	-0.29	0.09	0.11	-0.32	-0.27
SD slope-49	-0.47	-0.04	-0.10	-0.13	0.66	0.71	0.77	0.87	0.92	0.90	0.73	0.88	1.00	-0.41	-0.41	-0.11	0.38	0.39	0.43	-0.39	0.38	-0.29	-0.26	-0.34	-0.33	0.10	0.11	-0.38	-0.36
Aragonite	0.92	0.03	0.09	0.14	-0.16	-0.18	-0.24	-0.33	-0.38	-0.41	-0.28	-0.34	-0.41	1.00	1.00	0.68	-0.96	-0.97	-0.80	0.88	-0.89	0.90	0.86	0.93	0.94	0.24	0.11	-0.04	0.69
Calcite	0.92	0.03	0.09	0.14	-0.16	-0.18	-0.24	-0.34	-0.38	-0.41	-0.28	-0.34	-0.41	1.00	1.00	0.68	-0.96	-0.97	-0.81	0.88	-0.89	0.90	0.86	0.93	0.94	0.24	0.11	-0.04	0.69
Alkalinity	0.48	-0.03	-0.03	-0.03	-0.02	-0.04	-0.06	-0.10	-0.12	-0.13	-0.08	-0.10	-0.11	0.68	0.68	1.00	-0.57	-0.59	-0.21	0.44	-0.38	0.81	0.82	0.76	0.77	0.18	0.07	-0.07	0.16
Nitrate	-0.84	-0.02	-0.08	-0.12	0.15	0.16	0.21	0.31	0.35	0.38	0.26	0.31	0.38	-0.96	-0.96	-0.57	1.00	0.99	0.79	-0.93	0.96	-0.83	-0.76	-0.85	-0.86	-0.22	-0.10	0.03	-0.84
Phosphate	-0.88	-0.03	-0.09	-0.13	0.15	0.17	0.22	0.32	0.36	0.39	0.27	0.32	0.39	-0.97	-0.97	-0.59	0.99	1.00	0.82	-0.91	0.94	-0.86	-0.80	-0.88	-0.89	-0.21	-0.09	0.03	-0.80
Silicate	-0.93	-0.06	-0.17	-0.26	0.19	0.21	0.27	0.34	0.38	0.42	0.30	0.37	0.43	-0.80	-0.81	-0.21	0.79	0.82	1.00	-0.69	0.77	-0.68	-0.67	-0.75	-0.75	-0.20	-0.12	0.06	-0.61
pH	0.74	0.02	0.07	0.10	-0.15	-0.16	-0.20	-0.32	-0.36	-0.40	-0.26	-0.30	-0.39	0.88	0.88	0.44	-0.93	-0.91	-0.69	1.00	-0.97	0.63	0.55	0.66	0.67	0.18	0.05	0.05	0.88
tCO2	-0.77	-0.03	-0.09	-0.12	0.15	0.16	0.19	0.31	0.34	0.38	0.26	0.30	0.38	-0.89	-0.89	-0.38	0.96	0.94	0.77	-0.97	1.00	-0.66	-0.58	-0.70	-0.71	-0.18	-0.07	-0.02	-0.92
Salinity (ROMS)	0.82	-0.01	0.04	0.09	-0.11	-0.13	-0.18	-0.23	-0.27	-0.29	-0.20	-0.26	-0.29	0.90	0.90	0.81	-0.83	-0.86	-0.68	0.63	-0.66	1.00	0.97	0.99	0.98	0.26	0.15	-0.12	0.43
Salinity	0.81	0.02	0.07	0.12	-0.09	-0.12	-0.17	-0.21	-0.25	-0.27	-0.18	-0.24	-0.26	0.86	0.86	0.82	-0.76	-0.80	-0.67	0.55	-0.58	0.97	1.00	0.96	0.97	0.24	0.13	-0.12	0.32
Temperature (ROMS)	0.89	0.00	0.05	0.11	-0.13	-0.16	-0.22	-0.28	-0.32	-0.34	-0.23	-0.30	-0.34	0.93	0.93	0.76	-0.85	-0.88	-0.75	0.66	-0.70	0.99	0.96	1.00	0.99	0.27	0.17	-0.12	0.47
Temperature	0.89	0.03	0.09	0.14	-0.13	-0.15	-0.21	-0.27	-0.31	-0.33	-0.23	-0.29	-0.33	0.94	0.94	0.77	-0.86	-0.89	-0.75	0.67	-0.71	0.98	0.97	0.99	1.00	0.26	0.15	-0.11	0.47
Bottom stress	0.25	-0.01	0.06	0.10	0.08	0.08	0.07	0.10	0.11	0.11	0.07	0.09	0.10	0.24	0.24	0.18	-0.22	-0.21	-0.20	0.18	-0.18	0.26	0.24	0.27	0.26	1.00	0.90	-0.66	0.12
Current speed	0.15	-0.01	0.05	0.09	0.07	0.07	0.06	0.10	0.11	0.11	0.09	0.11	0.11	0.11	0.11	0.07	-0.10	-0.09	-0.12	0.05	-0.07	0.15	0.13	0.17	0.15	0.90	1.00	-0.58	0.03
Vertical flow	-0.06	0.03	-0.08	-0.13	-0.28	-0.29	-0.30	-0.36	-0.38	-0.38	-0.26	-0.32	-0.38	-0.04	-0.04	-0.07	0.03	0.03	0.06	0.05	-0.02	-0.12	-0.12	-0.12	-0.11	-0.66	-0.58	1.00	0.06
Diss. Oxygen	0.56	0.02	0.06	0.07	-0.16	-0.16	-0.18	-0.30	-0.33	-0.36	-0.24	-0.27	-0.36	0.69	0.69	0.16	-0.84	-0.80	-0.61	0.88	-0.92	0.43	0.32	0.47	0.47	0.12	0.03	0.06	1.00

Appendix S2b: Best AUC scores for Maxent models of the distribution of Irish *L. pertusa* reefs based on a single parameter. From each group the variable with the highest score was selected for the final model build. BPI-5 was additionally retained, as no correlations were found between BPI and other bathymetric variables. The variables used for modelling are indicated with bold text.

Variable	Test AUC
BATHYMETRY	
Depth	0.906
BPI-5	**0.890**
BPI-25	0.782
BPI-49	0.712
Rugosity-5	0.843
Rugosity-25	0.724
Rugosity-49	0.759
Slope-5	0.811
Slope-25	0.748
Slope-49	0.764
SD slope-5	**0.916**
SD slope-25	0.826
SD slope-49	0.778

Variable	Test AUC
CHEMISTRY	
Aragonite	**0.907**
Calcite	0.907
Alkalinity	0.715
Nitrate	0.807
Phosphate	0.856
Silicate	0.907
pH	0.593
tCO2	0.675
Salinity (ROMS)	0.643
Salinity	0.756
TEMPERATURE	
Temperature (ROMS)	0.724
Temperature	**0.830**

Variable	Test AUC
HYDRODYNAMICS	
Bottom stress	**0.825**
Current speed	0.809
Vertical flow	0.767
OXYGEN	
Diss. Oxygen	**0.696**

Appendix S3: Box plots showing range (dashed lines), median (thick black line), upper and lower percentiles (box) and outliers (points) for all environmental variables at locations with *Lophelia pertusa* reefs (Lp) and for 10 000 random background points (Bg).

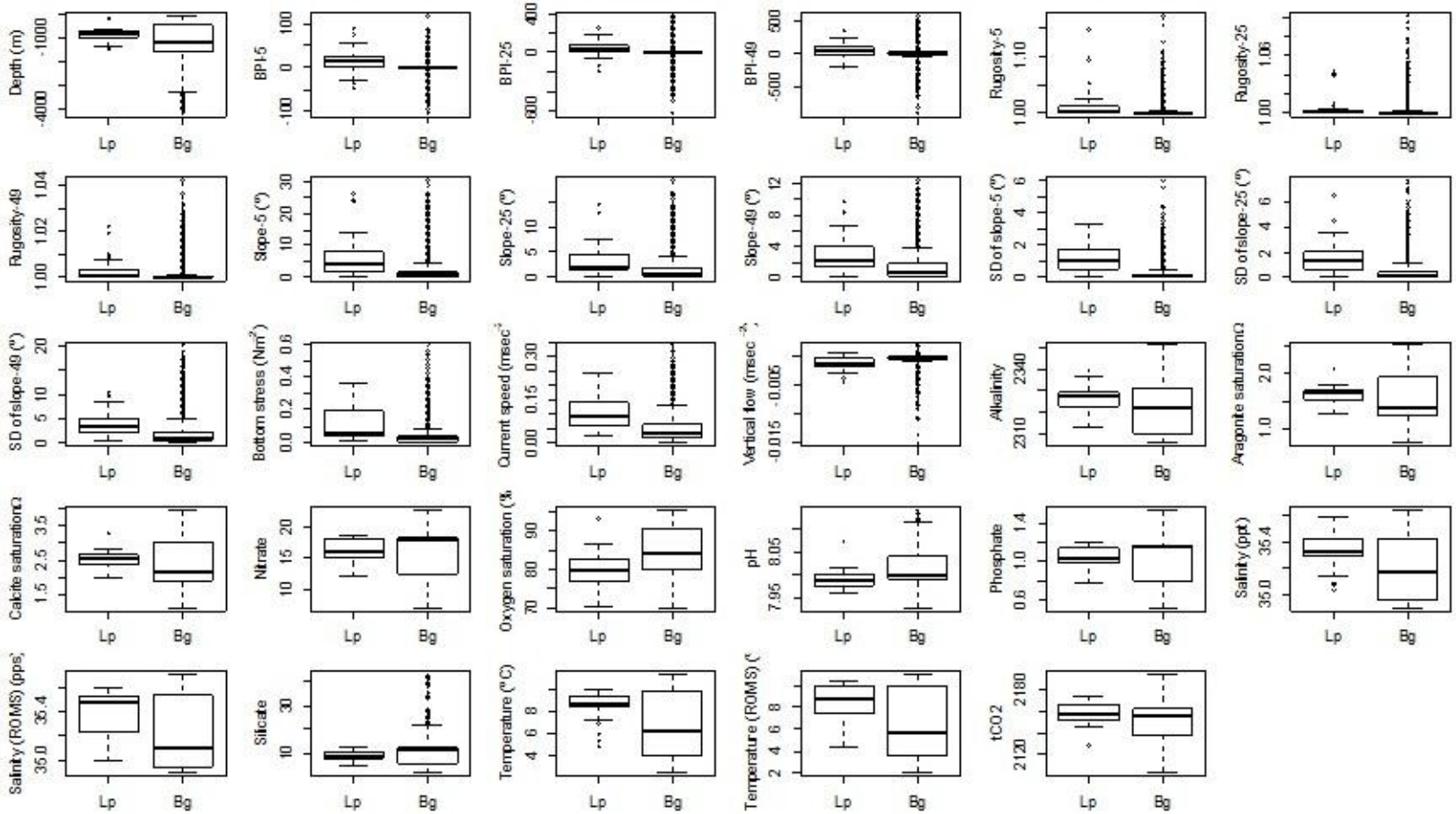

4. Linking benthic hydrodynamics and cold-water coral occurrences: A high-resolution model study at three cold-water coral provinces in the north-east Atlantic

Abstract

Linkages between key abiotic parameters and cold-water coral occurrences are investigated using a spatially explicit integrated modelling and observational approach. The 3D ocean circulation model ROMS-AGRIF was applied to describe oceanographic conditions at three cold-water coral provinces in the north-east Atlantic (Logachev Mounds, Arc Mounds and Belgica Mounds) adopting a nested model grid setup with a central model resolution of 250 m. Modelled fields of benthic currents, temperature and salinity were analysed at observed cold-water coral presence and absence locations within each province. Each respective model period covers one month (15th April – 15th May 2010) corresponding to the main cold-water coral survey period. Data from this survey were supplemented by additional data from other campaigns. The model bathymetry was taken from high-resolution INSS (Irish National Seabed Survey) seafloor mapping data. Modelled fields of benthic currents and temperature were validated against in-situ measurements and compared with main coral assemblage patterns from in-situ observations of the EU FP7 CoralFISH programme. The model results confirm the intensified benthic dynamics previously observed at individual coral sites, but also reveal substantial differences in hydrodynamic conditions both between and within cold-water coral provinces.

4.1. Introduction

The Porcupine Bank, Porcupine Seabight and Rockall Bank are areas of abundant occurrences of the scleractinian cold-water coral *Lophelia pertusa* (Linnaeus 1758) and associated faunal communities. Most of these occurrences are found in

connection with large cold-water coral mound structures or appear as individual coral colonies along the continental margin. The majority of coral mounds at the Irish continental margins occupy the depth range 500 – 1000 m (Kenyon *et al.* 2003, White & Dorschel 2010). Giant mounds can be up to 380 m high and several kilometres long and are in the north-east Atlantic exclusively found in the Porcupine Bank, Porcupine Seabight, Rockall Bank and Hatton Bank areas (De Mol *et al.* 2002, van Weering *et al.* 2003, Huvenne *et al.* 2005, Wheeler *et al.* 2007). Since cold-water corals in the north-east Atlantic appear most abundant on elevated topography, flow acceleration has been considered as an important condition for their growth (e.g. Genin *et al.* 1986). Stronger flow enhances delivery of particles such as larvae and food. Oceanographic influences at cold-water coral sites occur at a vast range of spatial and temporal scales. At the largest spatial scales, pelagic productivity and oceanic biogeochemical characteristics fundamentally control the global distribution of cold-water corals (Freiwald *et al.* 2004, Davies & Guinotte 2011). At intermediate scales of 10-100 km, a combination of suitable current flow conditions and supply of nutrients is required to sustain the local coral population. For example, along the Norwegian continental margin, the poleward along margin flow enhances a downwelling flux of organic material to benthic communities (Thiem *et al.* 2006). Clusters of carbonate mounds may be found where enhanced current dynamics are present, such as the permanent thermocline (Mienis *et al.* 2007, White & Dorschel 2010), or where there is a concentration of organic matter and a suitable delivery method (White *et al.* 2005, Mienis *et al.* 2007). Smaller scale "hotspots" of cold-water coral communities may be found where particular favourable dynamics are present, such as downwelling induced by hydraulic control processes (e.g. Davies *et al.* 2009), or the critical resonance of internal waves (e.g. Frederiksen *et al.* 1992).

Resolving key environmental factors for the distribution of cold-water corals in the deeper Atlantic, requires a rare combination of hydrodynamic modelli studies, in-situ measurements and data on the spatial distribution and food preferences of corals. In several locations, daily migrating zooplankton has been proposed as major food source for cold-water coral communities while elsewhere food is considered to mainly consist of suspended particles or a combination of both (Duineveld *et al.*

2004, Becker *et al.* 2009). Hydrography clearly has a different role and importance for food transport in these cases.

The EU-funded CoralFISH programme (http://www.eu-fp7-coralfish.net/) offered opportunity to conduct in-situ measurements at several principal Atlantic cold-water coral locations such as the Logachev and Belgica Mound Provinces. Within the framework of the CoralFISH programme, which was focused on interactions between deep-sea fish, fisheries and cold-water corals, long-term observations were made on fish abundance using baited cameras installed on benthic landers. Current meters attached to these landers yielded unique long-term data series in and outside coral reef framework. Likewise, during CoralFISH video surveys using a remotely operated vehicle (ROV), new data were collected on the distribution of corals in relation to topography.

Our focus is on a comparative description of oceanographic conditions at three north-east Atlantic cold-water coral provinces, based on a spatially explicit hydrodynamic modelling approach. These areas include the Logachev mounds (SE Rockall Bank), Arc mounds (Western Porcupine Bank) and Belgica mounds (Northern Porcupine Seabight), which were repeatedly surveyed as part of CoralFISH activities. This simulation study provides a spatially explicit picture of near-bottom flow conditions. Oceanographic key parameters are linked to cold-water coral distribution data (presence and absence locations) obtained from ROV-based observations carried out in April/May 2010 in each area, supplemented by additionally available survey data. Finally, we discuss the presence and relative importance of dynamical processes based on established scaling parameters, and implications for a better understanding of the main drivers shaping cold-water coral environments.

4.2. Materials and Methods

Study area

Three study areas were chosen, representing different cold-water coral carbonate mound provinces off the West of Ireland (Figure 4-1). The Logachev mound province (61 km x 103 km, Figure 4-2a) on the Southern margin of the Rockall Bank

is a belt of giant carbonate mounds with heights > 350 m and widths of several kilometres, that are predominantly arranged in down-slope oriented clusters (Kenyon *et al.* 2003, Mienis *et al.* 2006).

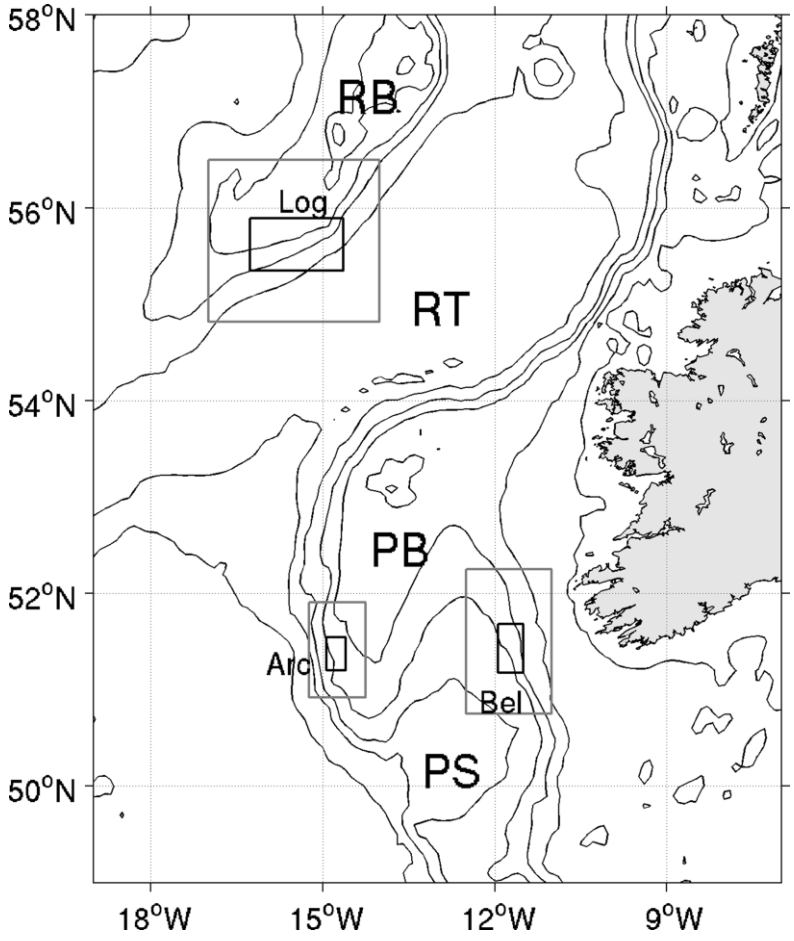

Figure 4-1: Study area and location of the three model domains used in this study covering the Logachev (Log), Arc (Arc) and Belgica (Bel) cold-water coral provinces. Grey rectangles indicate the large-scale domains (parent grids) and black rectangles represent the local high-resolution model domains (child grids). Major bathymetric features are the Rockall Bank (RB), Rockall Trough (RT), Porcupine Bank (PB) and Porcupine Seabight (PS).The 200 m, 500 m, 1000 m, 2000 m, 3000 m and 4000 m depth contours are shown.

The Arc mound province (23 km x 38 km, Figure 4-2b) on the south-western Porcupine Bank is comprised of much smaller, isolated mounds of ~50 - 100 m height with base lengths seldom exceeding 500 m (Rengstorf *et al.* 2012). The Belgica mound province (32 km x 56 km, Figure 4-2c) on the eastern Porcupine Seabight is comprised of partially buried conical mounds and some north-south trending elongated mound clusters. Mounds are up to 100 m high and may reach

base lengths up to 2000 m (Wheeler *et al.* 2007). Depressions, up to 50 m deep, often occur on the steep downslope side of mounds and are thought to be the result of strong bottom currents (Van Rooij *et al.* 2003). Video footage has revealed thriving *Lophelia pertusa* reefs on summits and terraced flanks of the Logachev mounds (Olu-Le Roy *et al.* 2002) and on the summits of the Arc mounds (Grehan *et al.* 2009). In the Belgica mound province, living corals can be found only on the deeper, north-western side, whereas the eastern mounds are characterized by asymmetric drift accumulations, sediment clogged dead corals and coral rubble (Foubert *et al.* 2005). In the northern Belgica province, White *et al.* (2007) described a predominantly cross-slope north-eastern alignment of mound clusters, consistent with the orientation of strong bottom-intensified diurnal tides.

The cold-water coral and carbonate mound provinces of the southern Rockall Trough and Porcupine Sea Bight region lie at the eastern margin of the north-east Atlantic between the two main north Atlantic gyre systems. The depth range of the cold-water coral presence spans water masses consisting of the upper layer Eastern North Atlantic Water (ENAW), and below 700-800 m, Mediterranean Outflow Water (MOW). MOW does not penetrate further north than the Porcupine Bank, hence its presence at the Logachev mound province on the south-east margin of Rockall Bank will likely be patchy (New & Smythe-Wright 2001, Ullgren & White 2010). Large-scale mean flows along the eastern Atlantic margin are dominated by the poleward flowing slope current, centred between 500-800 m, spanning the depth of the permanent thermocline (White & Dorschel 2010), and a time-mean anti-cyclonic recirculation around the Rockall Bank (Huthnance 1986). A variety of barotropic and baroclinic tidal period motions are present at the Rockall and Porcupine continental margins (Huthnance 1986). At the Belgica and Logachev mounds, near-seabed currents are characterised by bottom-trapped baroclinic motions of diurnal period (Mienis *et al.* 2007, White & Dorschel 2010), whilst along the western and northern Porcupine Bank margin, semi-diurnal tides dominate, again with a significant baroclinic component (Dickson & McCave 1986, Mienis *et al.* 2007).

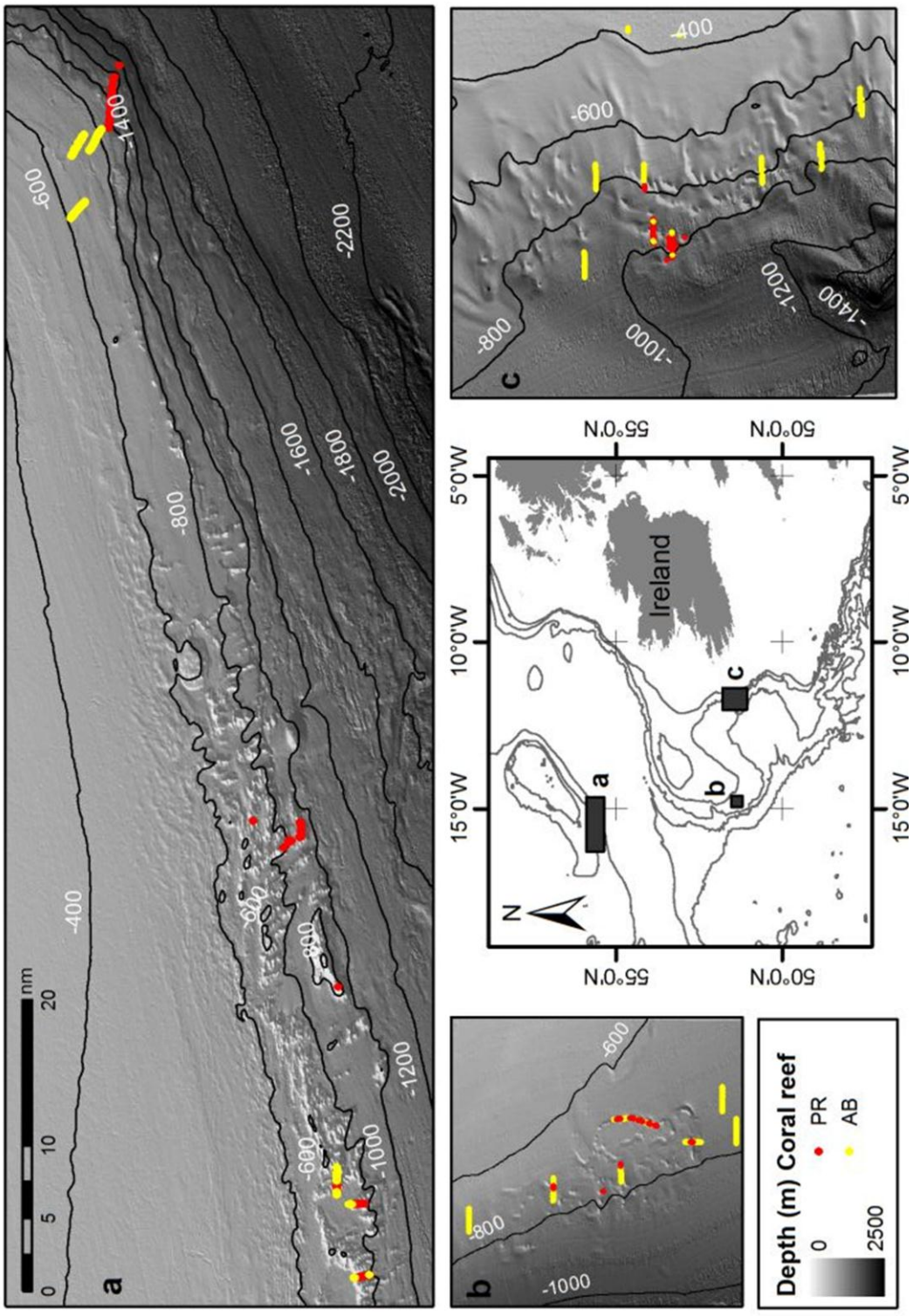

Figure 4-2: Local ROMS model domains and corresponding bathymetries (INSS data) of the Logachev (a), Arc (b) and Belgica (c) mound provinces. The horizontal resolution of each child grid is approximately 250 m x 250 m. ROV-based video observations of coral presences (PR) and absences (AB) are indicated in colour.

Field observations

Video data were acquired during a CoralFISH cruise (CE10014, Grehan *et al.* 2010) from 15th April to 15th May 2010 employing the Irish Marine Institute's 3000 m rated ROV *Holland I.* The vehicle was equipped with three Kongsberg low definition cameras (vertical, pilot and aft) as well as a forward-facing oblique (45° to the seabed) Kongsberg High Definition video camera. Lighting was provided by two forward facing HMI (hydrargyrum medium-arc iodide) lights (60° wideflood beam, 4,750 lumens) and 8 halogen lamps (250W, 120V). Navigation data (ROV positioning, speed, heading and attitude) was provided by an Inertial Navigation System (PHINS, IXSEA) connected to an external ultra-short baseline sensor (GAPS, IXSEA). ROV transects were conducted at an altitude between 1.5 – 2.5 m above seabed and at a constant speed of ~ 0.6 knots (~ 0.3 m/sec). Observations of living *Lophelia pertusa* framework were annotated in intervals of ~ 5 m and geo-referenced. The field of view of the ROV was roughly 2.5 m x 2.5 m depending on topography and visibility. Individual observations of coral presence and absence were imported into ArcGIS 9.3 (ESRI) and joined with existing *Lophelia pertusa* distribution data derived from previous video surveys (Olu-Le Roy *et al*. 2002, Grehan *et al.* 2009, Guinan & Leahy 2010). The data were matched with the spatial resolution of the hydrodynamic model by retaining only one observation per grid cell (250 m x 250 m). This record was coded 1, if coral had been observed and 0, if coral was absent. A total of 132 presence and 253 absence points remained. More detailed information on data source is given in Table 4-1.

Long-term time series of temperature and currents from an autonomous benthic lander deployment were used for model-data comparison (see Table 4-2 for lander location and deployment details). Current velocity and temperature data were recorded with a Nortek™ Aquadopp acoustic current meter and a Seabird SBE-37smp Conductivity-Temperature-Pressure (CTD) sensor. Both the current meter and CTD were mounted at 2 m above the seabed on a free-falling bottom lander (ALBEX, Duineveld *et al.* 2004) designed by NIOZ. The lander dataset used in this study was obtained from a deployment at Galway Mound (Belgica province) covering a total period of 324 days from October 2009 to September 2010. An

additional dataset from a mooring deployment at a carbonate mound in the Logachev province over a period of 45 days from August to September 2000 (White *et al.* 2007) was available to compare observed and modelled near-bottom currents (10 m above the seabed) with conditions higher up in the water column (150 m above the seabed).

Table 4-1: Coral records (presence-absence) obtained from ROV video data in the period March/April 2010 in the three study areas, supplemented by additionally available survey data. The depth ranges of sampled presence and absence locations are indicated.

Data source	Logachev	Arc	Belgica
Grehan *et al.* 2009		Presence: 12 Absence: 12	
Grehan *et al.* 2010	Presence: 27 Absence: 66	Presence: 8 Absence: 74	Presence: 34 Absence: 101
Guinan & Leahy 2010	Presence: 21		
Olu-Le Roy *et al.* 2002	Presence: 15		Presence: 15
TOTAL	Presence: 63 (500 – 1400 m) Absence: 66 (610 – 810 m)	Presence: 20 (604 – 740 m) Absence: 86 (630 – 790 m)	Presence: 49 (795 – 1035 m) Absence: 101 (370 – 1035 m)

Table 4-2: Description of measurements used for model and data comparison (corresponding model locations and depths are given in brackets).

Type	Deployment period	Deployment depth	Bottom depth (m)	Latitude (°)	Longitude (°)	Reference
Autonomous Lander	22-09-2010 to 08-07-2011	845 (843)	848 (857)	51.4511 (51.4527)	-11.7541 (-11.7515)	Lavalaye *et al.* 2010
Mooring	02-08-2000 to 15-09-2000	808 (809)	818 (816)	55.6067 (55.6047)	-15.4617 (-15.46)	White *et al.* (2007)
Mooring	02-08-2000 to 15-09-2000	668 (673)	818 (816)	55.6067 (55.6047)	-15.4617 (-15.46)	White *et al.* (2007)

Description and configuration of the ocean model

The 3D split-explicit, free-surface Regional Ocean Modelling System with grid refinement (ROMS-AGRIF) was applied to obtain local solutions of currents, temperature and salinity in all three areas for the observation period 15th March – 15th April 2010. ROMS solves the hydrostatic primitive equations using orthogonal curvilinear coordinates on a staggered Arakawa C-grid in the horizontal and stretched terrain-following coordinates (s levels) in the vertical (Shchepetkin & McWilliams 2005). ROMS incorporates a mode-splitting algorithm to separate the

time scales of barotropic and baroclinic processes in combination with an efficient temporal averaging of the barotropic mode with the benefit of avoiding aliasing of processes unresolved by the baroclinic mode and maintaining all important conservation properties at the same time (Shchepetkin & McWilliams 2005). Additional algorithms include a third-order, upstream-biased advection scheme and a non-local K-Profile Parameterization (KPP) of sub-grid scale vertical mixing processes (Durski *et al.* 2004). Explicit diffusion and viscosity was not imposed due to the capability of the horizontal advection scheme to effectively minimize numerical noise. Improved formulations of the horizontal pressure gradient force are an integrated component of ROMS to reduce systematic pressure gradient errors associated with abrupt topographic changes along s-coordinates (Shchepetkin & McWilliams 2003). Open boundary conditions are composed of mixed radiation and nudging terms for the baroclinic mode and the Flather condition to facilitate tidal forcing for the barotropic mode. ROMS has been successfully applied to study a wide range of processes associated with steep and abrupt topography from internal tidal dynamics at isolated topography (e.g. Robertson 2006) to larger scale shelf and slope dynamics (e.g. Otero *et al.* 2008). A setup of two structured model grids was applied for each sub-region consisting of a local high-resolution model domain (child grid) embedded in a coarser resolution model domain (parent grid). The ROMS version in this study makes use of the 1-way grid embedding capability using the AGRIF (Adaptive Grid Refinement in Fortran) Fortran 90 package (Penven *et al.* 2006). This procedure has two advantages. First, local processes associated with complex flow-topography interaction and larger scale processes driven by far-field dynamics are both represented in the local solution. Secondly, spatially coherent open boundary conditions are transferred from the parent to the child grid at each time step. The horizontal model resolution of the individual parent grids is set to 750 m. A spatial refinement factor of three was applied to generate the local child grids with a horizontal resolution of 250 m. This resolution and embedding ratio was found to be the best balance between topographic realism and affordable computational cost. Rengstorf *et al.* (2012) showed that a 250 m resolution is the minimum requirement to retain the major morphological features of individual mound provinces in Irish waters. The number of vertical s-levels is 32 everywhere,

with increased resolution at the surface and the bottom (θ_s = 3.4, θ_b = 1.0). The underlying bathymetry for the parent grid in all study regions was taken from the GEBCO08 data set (30 arc second resolution, GEBCO 2009). The multibeam bathymetry for the embedded model domains, processed to hydrographic standards (GOTECH, 2002), was extracted from the 100 m version of the Irish National Seabed Survey (INSS) bathymetry (data download: http://jetstream.gsi.ie/iwdds/index.html) and interpolated to each child grid. The model bathymetry in each local model domain is shown in Figure 4-2. Forcing and initialisation fields for temperature, salinity, sea surface elevation, wind stress and surface fluxes were obtained from monthly WOA05 (World Ocean Atlas 2005) and COADS (Comprehensive Ocean-Atmosphere Data Set) climatologies respectively. Climatologies were used to compensate for the lack of observational data and to provide spatially consistent boundary conditions to each parent grid. Open boundary conditions for tidal forcing with 10 constituents (M_2, S_2, N_2, K_2, K_1, O_1, P_1, Q_1, M_m, M_f) were taken from the OSU (Oregon State University) global inverse tidal solution TPXO7 (Egbert & Erofeeva 2002) starting from the 1st January 2010. The total simulation time was 1 year for all nested model domains.

4.3. Results

Model-data comparison

Model output was compared with time series of observed currents at two locations in the Belgica and Logachev provinces respectively (Table 4-2). At the location of the Belgica deployment, the model simulations covered the full period of the observed data, whereas August 2000 observations were compared with August 2010 model results at the Logachev deployment, due to the lack of corresponding direct current measurements in 2010. Time series of two-hourly instantaneous currents were extracted from the model at the locations and depths closest to the lander deployments (Table 4-2). Figure 4-3 shows the 31 day time series for each east (u) and north (v) velocity component and the corresponding scatter plots. At Logachev, the change in flow orientation from predominantly cross-slope currents near the seabed to mainly along-slope south-westward currents higher up in the water column is visible in both observations and model results (Figure 4-3g-h).

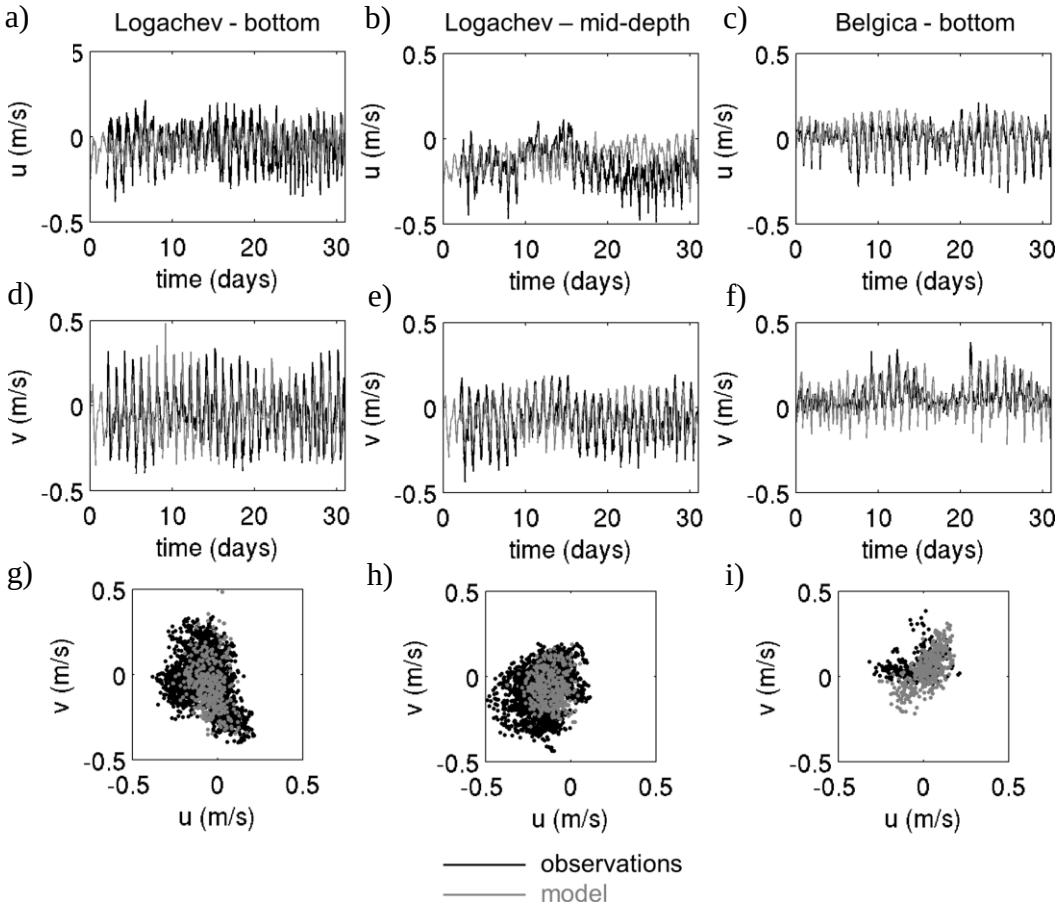

Figure 4-3: Time series of observed and modelled currents at two mound locations. At Logachev, the time series covers the period of 1st - 31st August 2000 (observed) and 2010 (modelled). At Belgica, observed and modelled time series start at the 15th April 2010. Depth and locations are shown in Table 4-2.

At Belgica, the model results also well reproduce the observed cross-slope orientation of the near seabed-flow (Figure 4-3i). The principal variability, both in the current records and the model results, is at a diurnal period with a pronounced spring-neap tidal cycle. Observations and model results generally show a good agreement in magnitude and timing of the observed flow variability, but the model is occasionally misrepresenting observed currents in the along-slope direction. This mismatch is most pronounced at the Logachev mid-depth (Figure 4-3b) and Belgica near-seabed (Figure 4-3f) locations. The differences can be partly explained by remaining deficits of the present model resolution to resolve fine-scale seabed characteristics and, as a consequence, the full spectrum of observed near-seabed dynamics. Another bias might be introduced by the barotropic tidal forcing at the model boundaries. Deviations from the real situation may result in inaccurate

estimates of the barotropic to baroclinic energy conversion along and across the continental slopes. Despite these uncertainties, the good qualitative and, to large extent, quantitative agreement provides reasonable confidence in the model skill to capture the principle patterns and phenomena associated with topography induced benthic dynamics at the different mound locations.

Benthic currents

Modelled time-mean horizontal currents averaged over the full 31 day simulation period (15^{th} April – 15^{th} May 2010) in the bottom-most model layer are shown for each cold-water coral province in Figure 4-4. The overall tendency of the time-mean flow in the Logachev region is along-slope to the southwest (Figure 4-4a). Strong currents with maximum speeds of 0.5 m s^{-1} without a characteristic preference of flow direction are present near major coral mound structures at bottom depths ranging from 600 – 1200 m. The most prominent pattern is the asymmetric flow amplification with the strongest currents occurring downslope of the major mound axis. In the deeper downslope and shallower upslope regions of the southeastern Rockall Bank currents are considerably weaker with typical speeds $\leq$ 0.1 m s^{-1}. Modelled time-mean currents in the Arc province are generally along-slope to the northwest and appear almost unaffected by the presence of the mound structures. Current speeds are moderately elevated in the central Arc mound region (depth range 600 – 800 m) compared to its surroundings, but do not exceed 0.2 m s^{-1} (Figure 4-4b). Similar conditions are found in the Belgica region in the north-eastern Porcupine Seabight (Figure 4-4c). The model simulations predict domain-wide maximum speeds of up to 0.3 m s^{-1} within a band of time-mean along-slope flow centred at the 700 m isobath in the northern model area where the accumulation of mound structures is less dense. This constitutes a three-fold amplification relative to the shallower and deeper areas along the north-eastern Porcupine Seabight margin. However, this relative amplification seems rather associated with the presence of numerous channels and gullies than with the dynamical feedback of flow interacting with individual mounds. Locally enhanced near-seabed residual currents over sloping bottom often indicate the presence of resonantly amplified diurnal tidal currents. The eastern and south-eastern Rockall Bank slopes and the Irish continental

margin (NE Porcupine Seabight including the northern Belgica province) have been previously identified as areas of strongly amplified diurnal tidal currents in excess of 10 cm s^{-1} and an associated tidally rectified mean flow (Huthnance 1974, White *et al.* 2007). Tidal amplification along the SW Porcupine slopes (including the Arc mound province) is comparatively weak (White *et al.* 2007) and associated near-seabed mean flows can be expected to be small. This is confirmed by our model results, although direct measurements of near-seabed currents were not available to validate modelled currents.

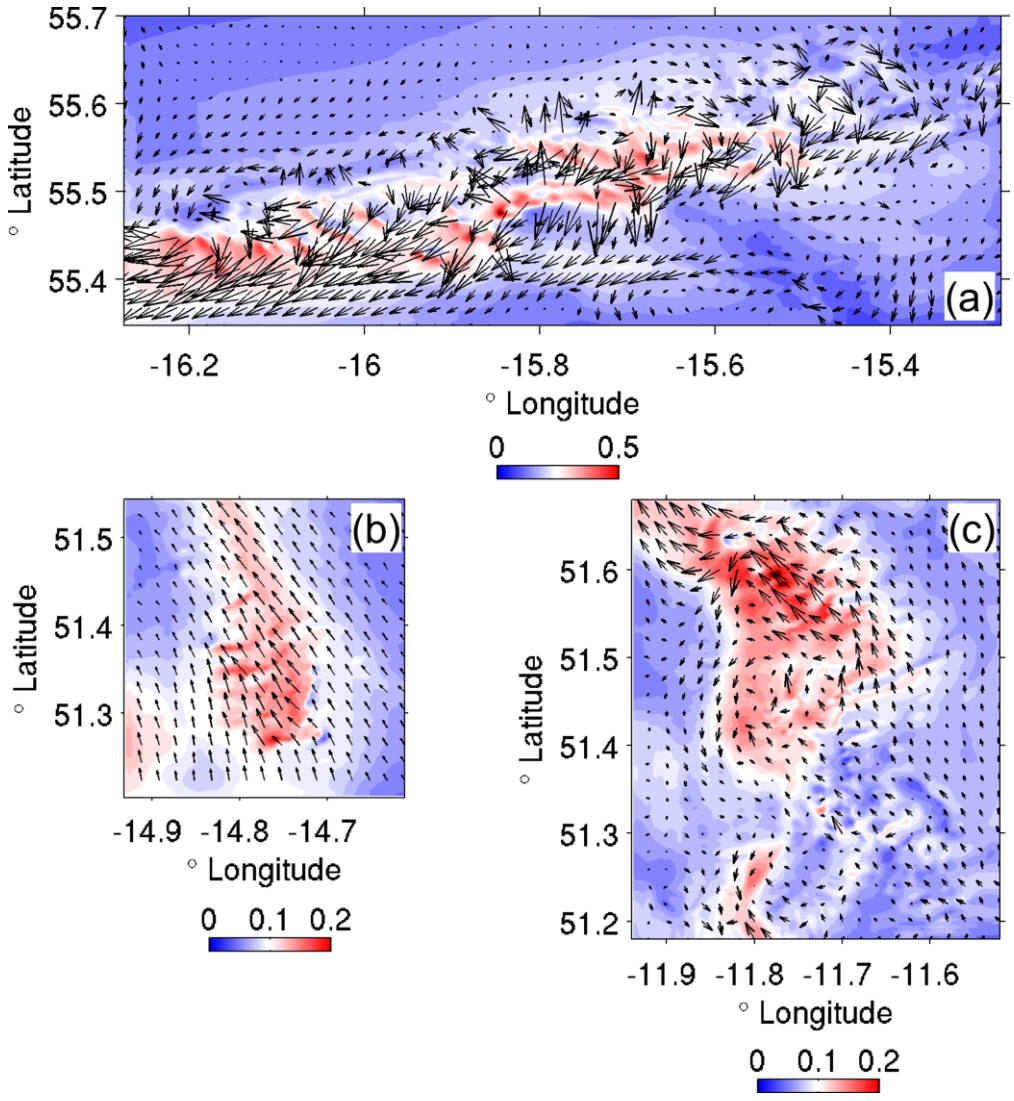

Figure 4-4: 31 day time-mean currents (arrows) and current speed (coloured contours) in the Logachev (a), Arc (b) and Belgica (c) mound provinces. For better visibility only part of the Logachev model domain is shown.

Figure 4-5 shows variability patterns of the time-mean near-seabed circulation over the full simulation period in each model domain. It is expressed by the Neumann flow stability B as a measure of the flow variability (time-averaged vector velocity) relative to the mean flow (time-averaged current speed). B was calculated from daily averaged model velocities to eliminate the effect of tidal oscillations.

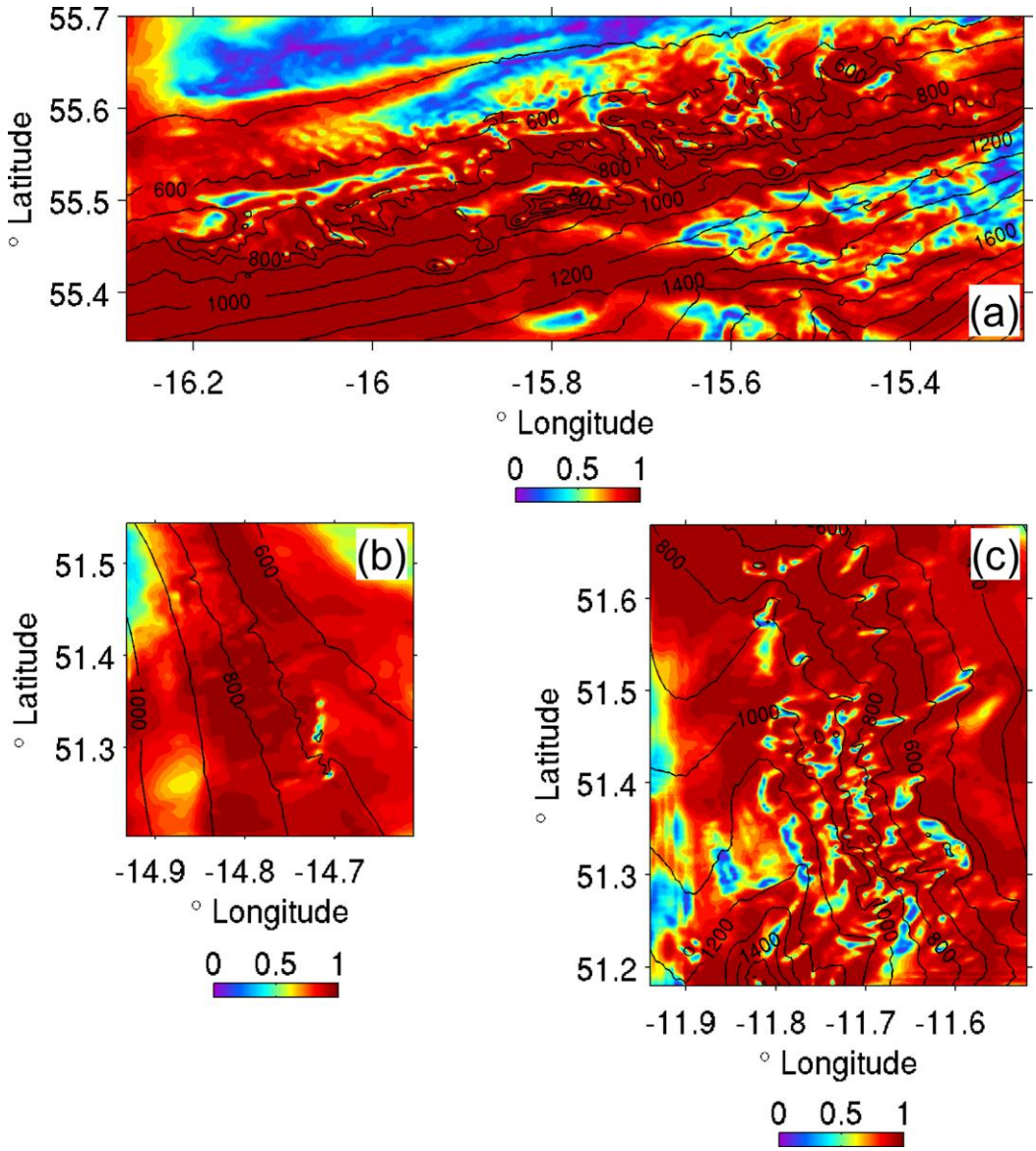

Figure 4-5: Normalized flow stability of benthic currents in the Logachev (a), Arc (b) and Belgica (c) mound provinces. The depth contour interval is 100 m. For clarity only part of the Logachev model domain is shown.

In general, high mean flow stability B is connected to strong mean currents and is most pronounced along slope regions where mound clusters and aggregations of individual mound structures are present. In the Logachev region flow stability is highest at bottom depths between 600 m and 1000 m, where the strongest currents are associated with the main giant mound corridor (Figure 4-5a). In the Arc province both mound clusters and individual mound structures are less pronounced and patterns of mean flow variability near individual mound structures cannot be clearly separated from surrounding areas (Figure 4-5b). However, high current stability is again mainly associated with bottom depths where the majority of mound structures are found (600 m – 900 m). Stable currents in combination with strong residual flow in the Belgica province occur in the northern region, often pervaded by small cross-slope channels and gullies. Further south, flow conditions are generally more variable with the exception of individual mound locations, but without a noticeable impact on the off-mound larger scale far field flow (Figure 4-5c). This is consistent with observations of steady and relatively strong (11 cm s^{-1}) poleward near-bottom (1000 m) residual currents at the north-easterrn Porcupine Seabight slope associated with strong diurnal internal tides (Pingree & LeCann 1990). In the same study, weaker (2-5 cm s^{-1}) and less steady near-bottom residual currents were observed in the southern Porcupine Seabight (Pingree & LeCann, 1990).

Oceanographic conditions and coral occurrences

Near-seabed physical attributes (mean current speed U_{mean}, mean upward velocity W_{mean}, mean temperature T_{mean}, mean salinity S_{mean}) were compared at observed cold-water coral presence and absence locations and 1000 random background points inside bottom depths between 600 and 1200 m (Figure 4-6). Random background points were used to give an overview of the "available" oceanographic conditions in each study area. The analysis represents conditions for a specific hydrodynamic situation (April/May 2010), based on 6 hourly averages obtained from a 31 day simulation period. Pronounced discrepancies between physical attributes at cold-water coral locations were found for current speed and upward velocity. Mean current speeds at coral presence locations generally exceed mean values in other areas. The largest differences occur in the Logachev region where mean current

speeds at coral presence locations can be a factor of two higher than typical values at absence and background locations (Figure 4-6).

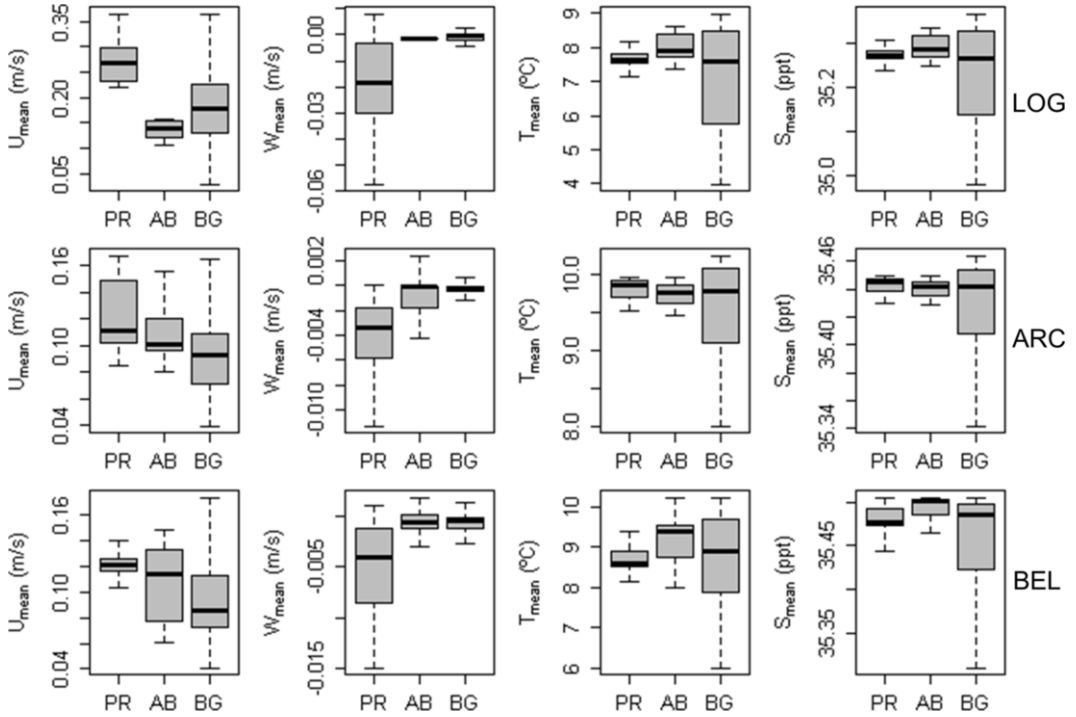

Figure 4-6: Box plots of 31 day mean near-bottom oceanographic attributes current speed (U_{mean}), upward velocity (W_{mean}), temperature (T_{mean}) and salinity (S_{mean}) at coral presence (PR), absence (AB) and background locations (BG). Region acronyms refer to the Logachev (LOG), Arc (ARC) and Belgica (BEL) provinces.

The secondary circulation at cold-water coral presence locations at the level of topography is dominated by time-mean downwelling almost everywhere. The highest mean downward velocities (up to 6 cm s^{-1} at individual locations) can again be found in the Logachev region (Figure 4-6). Corresponding values at coral presence locations in the Arc and Belgica regions do not exceed 1.5 cm s^{-1}, but are yet one order of magnitude higher than vertical velocities at non-coral locations. The box plots do not show significant differences between coral and non-coral locations with regard to temperature. The analysis indicates lower temperatures and salinities at Logachev and Belgica coral presence locations when compared to absence and random background locations. This tendency of lower temperatures and salinities at coral presence locations may develop as a consequence of enhanced vertical mixing. It is important to note that the wide spatial scattering of coral presence, absence and

background locations complicates a statistically robust comparison and leads to the suggestion that differences in temperature and salinity are more likely caused by bottom depth-related variations of local regimes at individual coral locations.

Dynamical considerations

We now further examine the probability and spatial distribution of physical processes developing as a consequence of complex flow-topography interactions and with particular relevance for cold-water coral development. This analysis is based on a spatially explicit assessment of important dynamical scaling parameters in the Logachev province by using the simulated model fields (see Table 4-3 and Figure 4-7).

Table 4-3: Description of dynamical scaling parameters and major references.

Dynamical scaling parameter	Description	Main references
$N \sin(\alpha)$	Resonantly amplified tidal and tidally rectified flow may be strongest in areas where $N \sin(\alpha)$ = maximum.	Huthnance (1981), White & Dorschel (2010)
α/c	Dynamic slope parameter representing the angle of semi-diurnal tide internal wave propagation c in relation to the topographic slope α. Slope conditions can be critical ($\alpha/c \approx 1$), sub-critical ($\alpha/c < 1$) or super-critical ($\alpha/c > 1$).	Cacchione *et al.* (2002), St Laurent & Garrett (2002), Kunze & Smith (2004)
Fr^{-1}	Vertical tidal excursion inverse Froude number indicating linear internal wave regimes ($Fr^{-1} < 3$) or non-linear wave regimes where internal hydraulic jumps can occur ($Fr^{-1} \geq 3$).	Legg & Klymak (2008)
U/N	Vertical tidal excursion distance. Large U/N is a second requirement for high amplitude hydraulic jumps.	Legg & Klymak (2008)

Many parts of the European continental margin exhibit an energetic conversion from barotropic to baroclinic tidal energy modulated by the presence and shape of topographic irregularities. This tidal energy conversion creates two distinct baroclinic motions, bottom-trapped topographic waves and freely propagating internal tides (Baines 1974). Freely propagating internal tides exist in the frequency band $f < \omega < N$ (f = local inertial frequency, ω = tidal forcing frequency $2\pi/T$, N =

buoyancy frequency). The predominant barotropic tidal forcing at mid-latitudes originates from the main semi-diurnal M_2 tide. Internal tide characteristics are modified by the bottom slope and are defined by the slope parameter α/c (Cacchione *et al.* 2002, Kunze & Smith 2004). It describes the ratio of the topographic slope $\alpha = \nabla h$ to the angle of the internal wave propagation β, defined as:

$$c = \tan(\beta) = \sqrt{\frac{\omega^2 - f^2}{N^2 - \omega^2}} \quad (1)$$

Internal wave reflection conditions can be separated into three regimes: subcritical reflection of the internal tide at gentle topographic slopes and transmission towards shallow water (α/c < 1), supercritical reflection towards deep water at steep slopes (α/c > 1) and critical reflection where highly energetic internal tides and associated turbulent mixing are generated locally (α/c ≈ 1). Figure 4-7b shows the spatial distribution of α/c in the Logachev area. The buoyancy frequency

$$N^2 = -\frac{g}{\rho_0}\frac{d\rho}{dz} \quad (2)$$

was calculated from modelled density fields (g = 9.81 m s^{-2} is the gravitational acceleration, dρ is the difference between surface and bottom density at each grid point, dz is the corresponding difference of water depths at each grid point, ρ_0 is a typical mean density). Most of the upper southern Rockall Bank (water depths < 600 m) exhibit gentle subcritical slopes (α/c < 1) where local internal tide generation is highly unlikely. Similar conditions are also found in single areas further downslope. The bulk of the slope associated with the presence of coral mounds show mostly critical slopes (α/c ≈ 1) with the potential to contribute significantly to local internal tide generation and tidal dissipation. Supercritical slopes (α/c > 1) are confined to the steep flanks of larger mound structures within the depth range 600 - 1100 m. Supercritical slopes of ridge systems have been previously found to support the formation of non-linear transient internal hydraulic jumps, an energetic process by which tidal flow over isolated topography generates large-amplitude vertical mixing

(Klymak *et al.* 2008; Legg & Klymak 2008). Two dimensionless parameters are of particular importance in this context, the tidal excursion inverse Froude number

$$Fr^{-1} = \frac{dh}{dx}\frac{N}{\omega} \quad (3)$$

(dh/dx is the horizontal bottom depth variation), and the tidal excursion distance

$$D = \frac{U}{N} \quad (4)$$

(U is the maximum barotropic current speed over the full simulation period at each grid point to include effects of the spring-neap tidal cycle). According to Legg & Klymak (2008), nonlinear internal jumps occur at maximum offslope flow and sufficiently steep topography, so that $Fr^{-1} > 3$ and the vertical displacement scale U/N is much larger than the frictional bottom boundary layer. These conditions require large flow velocities and weak stratification. Figure 4-7c and d show the distribution of these scaling parameters in the Logachev region. Both conditions for large amplitude hydraulic control are satisfied at a number of locations mainly associated with larger mound structures. However, this number is significantly less than the predicted number of locations with steep, supercritical slopes (Figure 4-7b).

In contrast to freely propagating internal waves, wave motions are trapped to the topography, if their period exceeds the local inertial period $2\pi/f$. In this case, diurnal tidal currents may be resonantly amplified and an associated tidally rectified residual flow will form under certain conditions of vertical stratification N and bottom slope α (Huthnance 1981, White 2007, White & Dorschel 2010). Trapped subinertial tidal motions, if present, will be located at the sea-floor maximum of $N \sin(\alpha)$, i.e. the maximum resonance frequency:

$$N \sin(\alpha) = max \quad (5)$$

Accordingly, the response of the local stratification to the tidal forcing determines the order of amplification and can be expressed as the minimum resonance period of the density oscillation $2\pi / N \sin(\alpha) \sin(\gamma)$ (White & Dorschel 2010). The term $\sin(\gamma)$

represents the angle of the baroclinic wave motion to the orientation of the continental slope, with $\sin(\gamma) = 1$ (waves directed across-slope) in the Logachev area (White & Dorschel, 2010). Relative maxima of $N \sin(\alpha)$ are typically found in the bottom depth range 600 – 1000 m (Figure 4-7a). Corresponding minimum resonance periods in the same depth range would reach relative minima smaller than the principal diurnal forcing period, thus permitting high amplitude resonant amplification. This agrees well with the presence of the strongest mean near-bottom currents in this depth range (Figure 4-4a).

4.4. Discussion and conclusions

In this study, we have carried out hydrodynamic model simulations exploring oceanographic conditions in three north-east Atlantic CWC provinces and linkages between observed CWC occurrences and properties of oceanographic key attributes in the bottom-most layers. Despite the fact that our model results represent a specific hydrodynamic situation within a limited period, previously described oceanographic settings of CWC occurrences in the Belgica and Logachev provinces are largely confirmed by this study. Coral presence locations can be linked to dynamic oceanographic regimes consisting of strong tidal and time-mean currents, and a secondary circulation of mean downwelling in connection with enhanced vertical mixing. In the Arc province, this relationship is less definite, perhaps as a consequence of insufficient spatial model resolution to account for the finer-scale and less abundant mound features in this particular region.

Flow-topography interaction covers a wide spectrum of processes acting on different temporal and spatial scales, and some of them have been identified as potential mechanisms of food supply to cold-water coral communities. It is present consensus that the development of cold-water corals is largely controlled by the presence of strong currents supporting a continuous or periodic flux of organic material to coral and other suspension feeding mound communities and preventing smothering through sediment deposition (Dorschel *et al.* 2005, White 2007). Important processes from more complex interactions between currents and topography include trapped wave dynamics and local tidal amplification.

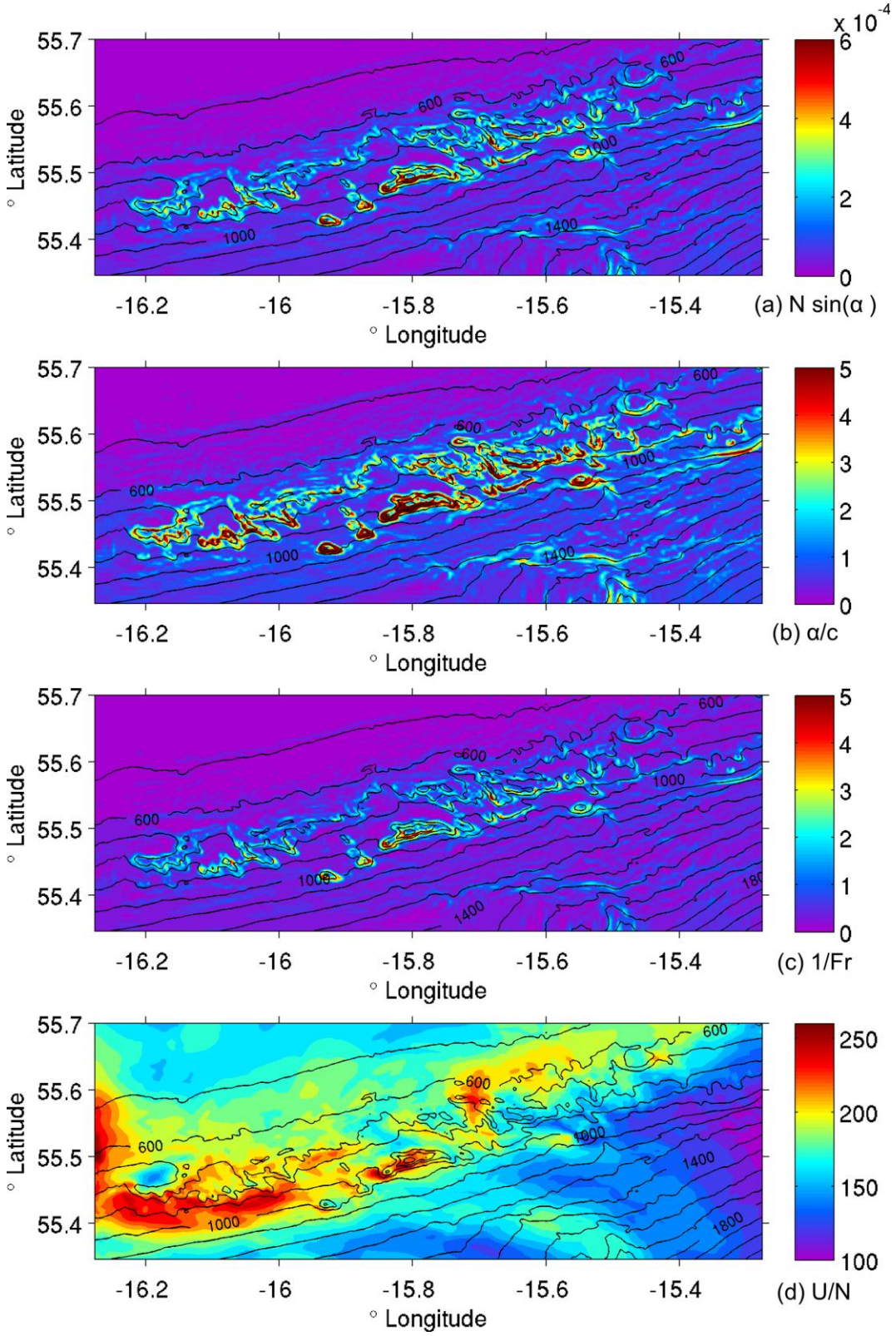

Figure 4-7: Dynamic scaling parameters: (a) Tidal amplification parameter N sin(α), (b) M_2 internal tide slope parameter α/c, (c) vertical tidal excursion inverse Froude number Fr^{-1}, (d) vertical tidal excursion distance U/N (m).

Topographic trapping and resonant amplification of diurnal tidal oscillations have been frequently described at isolated seamounts (Brink 1995, Beckmann & Haidvogel 1997, Lavelle & Mohn 2010) and submarine banks (Huthnance 1974, Mohn & Beckmann 2002, White *et al.* 2007). Recent studies highlight the potential importance of trapped wave dynamics for local mixing and organic matter fluxes at carbonate mound systems in the north-east Atlantic (White *et al.* 2007, White & Dorschel 2010). Another dynamical characteristic at continental slopes are freely propagating internal tides and related turbulent mixing (Frederiksen *et al.* 1992, Cacchione *et al.* 2002). Rapid downwelling events (vertical velocities of up to 10 cm s^{-1}) associated with internal hydraulic jumps have recently been discussed as a fast and effective mechanism to provide shallow (125 – 160 m) cold-water coral reefs off Scotland with fresh organic matter from surface production (Davies *et al.* 2009, Duineveld *et al.* 2012). The Logachev province model simulations also indicate the presence of such overturning events, but there is no observational evidence of internal jumps to date in deeper living coral assemblages. In a detailed modelling study, Legg & Klymak (2008) investigated the conditions at which internal hydraulic jumps are formed. Tidal flow over topography in a hydraulically controlled regime consists of two phases. Initially, the downslope barotropic tidal flow moves stratified waters over the topography disrupting the density and temperature field in the form of a lee-side depression. At the turn of the tide, this depression propagates up the slope and beyond in the form of an internal wave of substantial amplitude in connection with overturning and strong energy dissipation. This sequence of different tidal regimes is also present in our model results at individual locations in the Logachev region (Figure 4-8a-b). Our results also indicate that the same process is developing in the opposite direction in the case of isolated topography such as mounds (Figure 4-8c).

The relative importance and presence of trapped wave and freely propagating internal wave dynamics is mainly controlled by the local topographic slope, stratification and flow magnitude. Figure 4-9 summarizes characteristic values of the scaling parameters introduced above within each study area and for all coral

locations. Bottom trapped diurnal waves and associated tidal amplification, i.e. relative maxima of N sin(α), are generally confined to coral presence locations.

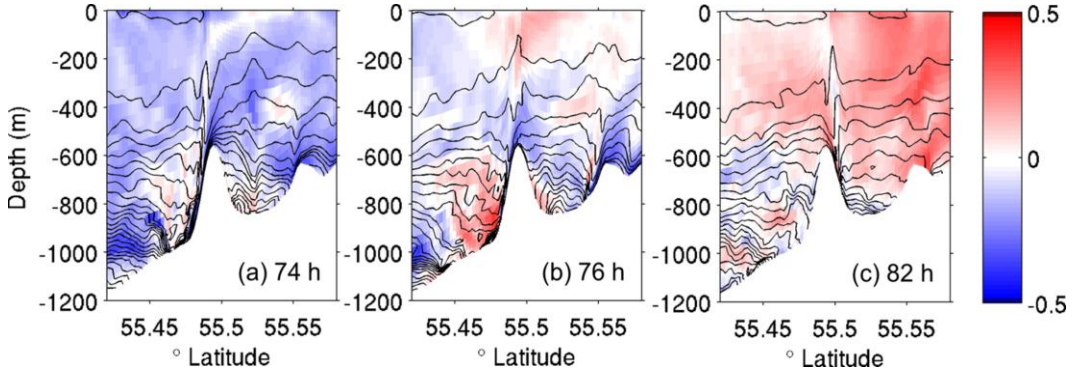

Figure 4-8: Snapshots of the cross-slope velocity v (m/s, in colour) and isotherms (black lines, contour interval is 0.2 °C). Negative velocities indicate down-slope flow. Hours refer to timing after the 15th April 2010. The transect is taken at -15.808° Longitude.

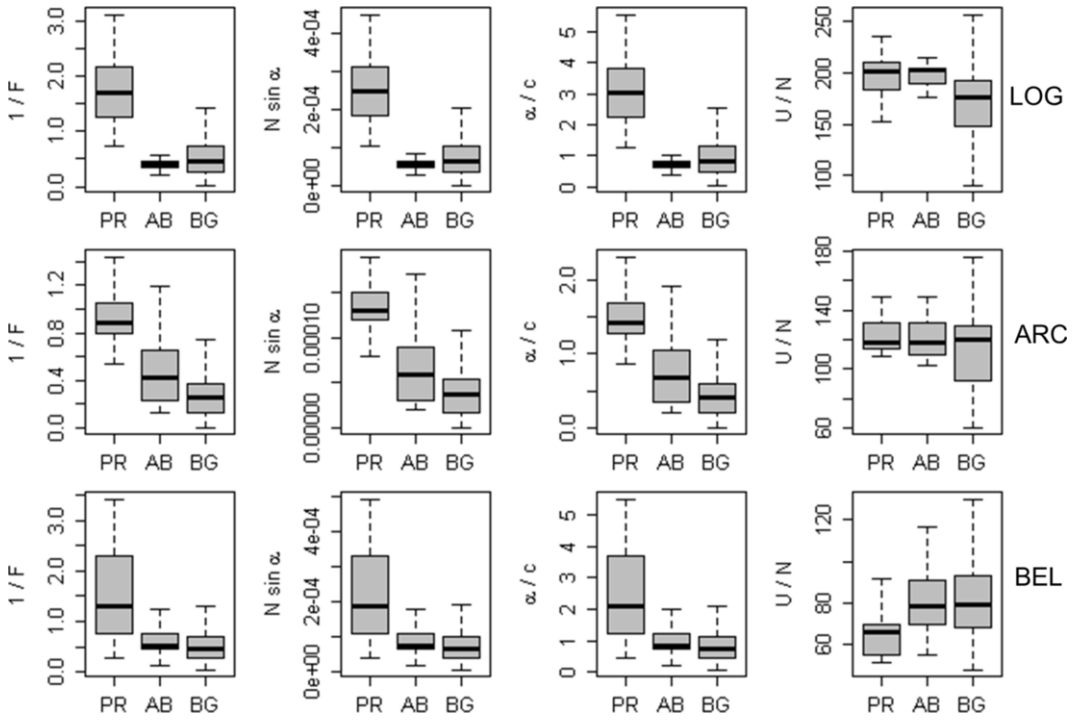

Figure 4-9: Box plots of dynamical scaling parameter distributions at cold-water coral presence (PR), absence (AB) and background locations (BG) in the Logachev (LOG), Arc (ARC) and Belgica (BEL) provinces (see Table 4-3 for a description of scaling parameters).

The distribution of slope criticality α/c indicates mostly supercritical conditions at coral presence locations in contrast to near-critical and sub-critical slopes at non-coral locations. A notable exception is the Arc province where the slope criticality is also near-critical at coral presence locations. We did not find a consistent relationship between slope criticality α/c and possible formation areas of internal hydraulic jumps defined by combinations of $Fr^{-1} > 3$ and large U/N. Supercritical slopes are a basic requirement for hydraulic jumps to occur, but other factors such as flow magnitude and stratification conditions are equally important (Legg & Klymak 2008). Therefore internal hydraulic jumps can be mainly expected to form at or near the giant mound structures of the Logachev province. The vigorous mixing resulting from such internal jumps may explain the development of extensive dense coral framework not hampered by baffling effects as occur in the linear CWC mounds that develop under unidirectional currents. In these linear or teardrop-shaped mounds, e.g. Traena, Cape Lookout, living coral is only found on the current facing slope while most parts of the mound consist of coral rubble with sediment.

Intra-annual variability of stratification and flow magnitude is an important constraint for the local occurrence and extent of the processes presented above. Large magnitude flow as a major physical control of tidally driven internal hydraulic jumps of sufficient amplitude in parts of the Logachev area varies with the period of the spring-neap tidal cycle. The role of changing stratification is twofold: Strong stratification increases the probability of internal jump formation, but reducing the vertical displacement scale at the same time (Legg & Klymak 2008). The opposite effect can be expected in periods of weaker stratification. The near-bottom flow along the deeper Porcupine Seabight continental margin (600 – 1000 m) is mainly controlled by diurnal tide-topography interaction and a steady poleward along-slope residual flow (Pingree & LeCann 1990, Pingree *et al.* 1999). Seasonality is less important in slope areas where resonant diurnal tidal amplification and associated rectified mean flow generation is strong, e.g. along the northern Porcupine Seabight slope (Pingree & LeCann 1990; White 2007). In slope areas further south, diurnal tidal resonance is less likely and the near-bottom flow is more prone to seasonality (Pingree & LeCann, 1990, White, 2007).

This study also highlights the benefit of hydrodynamic models for developing a better understanding of benthic dynamics at CWC locations, especially in regions where direct measurements of benthic hydrography and currents are missing. The model skill critically depends on the accuracy of open boundary conditions and the underlying bathymetry, and the adequacy of the model grid to resolve fine-scale topographic details associated with the presence of mound clusters and individual mounds. Thus, integrating hydrodynamic model data and video-based coral presence and absence data at a 250 m scale must be considered as a first step, given the presently limited data availability. Future studies will offer the opportunity to combine hydrodynamic model output with quantitative observations of cold-water coral coverage (%) at higher spatial resolution. Using predictive modelling techniques (Elith & Leathwick 2009), these relationships can then be used to estimate the actual distribution of cold-water corals over the full extent of each coral province.

5. Important considerations on the methodology for predicting deep-sea benthic species distributions using high-resolution environmental variables

Abstract

Little is known about species distribution patterns in deep-sea environments, primarily because sampling surveys in the high seas are expensive and time-consuming. The increasing need to manage and protect deep-sea marine resources has motivated the use of predictive modelling tools which produce continuous maps of potential species or habitat distribution from limited point observations and full coverage environmental data. Rapid advances in acoustic remote sensing, oceanographic modelling and sampling technology now provide high quality datasets, facilitating model development with high spatial detail. This paper provides a short overview of existing data and methodologies for deep-sea benthic habitat suitability modelling. It illustrates emerging issues related to spatial and thematic data resolution and the use of transect-derived species occurrence data. Aiming towards enhancement of ecological relevance and reliability of habitat suitability maps, novel techniques are proposed and presented based on the predictions of the cold-water coral *Lophelia pertusa* in three selected carbonate mound provinces in Irish waters. Specifically, the study applies generalised linear models to explore 1) the explanatory power of newly developed high-resolution (250 m grid cell size) hydrodynamic variables, 2) the potential of quantitative species occurrence proportion data, 3) mixed effect modelling as a method to deal with spatially grouped transect data, and 4) the ability to transfer models in space. The paper concludes with a discussion of how habitat suitability models can be used to inform marine spatial planning and conservation measures and to improve our understanding of ecosystem functioning and processes.

5.1. Introduction

This paper is concerned with habitat suitability models (HSMs) to predict the distribution of species and habitats in regions of the deep sea where direct observations are logistically difficult, time consuming and expensive. The premise is that spatially-extensive and relatively easily-available remotely sensed or modelled data (e.g. seabed bathymetry and water column physical properties) can be used as the basis to make statistical predictions of species or habitat distributions that are consistent with direct observations of the species based on small quantities of occurrence records. The paper starts with a summary of deep-sea species occurrence and environmental datasets that are now readily available or collected routinely. It discusses the ecological framework that underpins HSM and summarises some of the common algorithms used to realise the predictions. Using a case study for the prediction of *Lophelia pertusa* (Linnaeus 1758) in the north-east Atlantic, it assesses some emerging methodological issues, such as 1) the usefulness of high-resolution hydrodynamic variables to improve model predictions, 2) advantages or otherwise of species occurrence proportion data compared to presence-absence data to improve model fit, 3) the use of mixed effect models as an approach to deal with spatially pseudo-replicated distribution data and 4) the ability to transfer local scale HSMs generated in one region in order to predict species occurrence in another region.

Deep Sea Datasets

Distribution data for deep-sea benthic species originate from a variety of sources such as fisheries bycatch, trawling and dredging surveys, boxcores and grab samples, video and photographic surveys, amongst others. The Ocean Biogeographic Information System (OBIS, www.iobis.org) collates, integrates and disseminates global geo-referenced marine species distribution data from museum collections, libraries and databanks. These multi-source data vary significantly in quality, with common issues including poor spatial precision, taxonomic errors and lack of important metadata (e.g. information on the organism's life stage). Quality control of readily available distribution data is therefore essential to ensure realistic representation of the target species or taxon (Ross *et al.* 2012, Rengstorf *et al.* in press).

Over the last decade, video and photographic surveys have evolved to be the standard method for benthic habitat mapping and modelling (Brown *et al.* 2011), as they are non-destructive, provide information on seabed substrata and biological assemblages (e.g. Howell *et al.* 2010), provide quantitative benthic diversity data (e.g. Schoening *et al.* 2012), and allow for precise spatial matching with very high-resolution environmental data (e.g. Dolan *et al.* 2008). Considerable effort is now directed towards the development of image libraries to standardize the identification of deep-sea species (Howell & Davies 2010) and towards the development of automated image recognition and analysis (Purser *et al.* 2009, Schoening *et al.* 2012).

Ecologically relevant environmental variables for estimating deep-sea benthic species distribution include primary productivity in the photic zone, near-seabed water chemistry and hydrodynamics as well as terrain morphology and seabed substratum. Full-coverage environmental data can be derived from ship- or satellite-borne remote sensing, point-interpolations from in-situ measurements, ocean circulation models, and hybrids of these. Gridded data layers are readily available on a global scale (Table 5-1), and have been applied in several modelling studies for deep-sea benthic species (O'Hara & Tittensor 2010, Tittensor *et al.* 2010a, Tittensor *et al.* 2010b, Davies & Guinotte 2011, Yesson *et al.* 2012).

Rapid advances in seabed mapping techniques using single-beam, multi-beam and side-scan sonars can now provide full-coverage data on terrain morphology and seabed substrata at high spatial resolutions (Anderson *et al.* 2008, Brown *et al.* 2011). Bathymetry-derived parameters such as seabed slope, aspect, rugosity and bathymetric position index (Weiss 2001) may act as proxy variables for seabed substratum (Dunn & Halpin 2009) and current flow (e.g. Genin *et al.* 1986). Significant relationships between local terrain morphology and distribution patterns have been observed for many benthic biota (Kostylev *et al.* 2001, Lundblad *et al.* 2006, Holmes *et al.* 2008), including deep-sea corals (e.g. Dolan *et al.* 2008, Guinan *et al.* 2009a, Woodby *et al.* 2009), crustaceans (Wilson *et al.* 2007, Hovey *et al.* 2012) and sponges (Huang *et al.* 2011). A recently developed depth-based interpolation technique (Davies & Guinotte 2011) now enables the integration of

coarse scale environmental data with high-resolution bathymetry data; it constitutes a promising approach for developing detailed regional habitat suitability maps relevant for marine spatial planning (Rengstorf *et al.* in press).

Table 5-1: Examples of environmental data grids available on a global scale. Datasets with multiple depth levels can be up-scaled to higher resolutions using a novel depth-based interpolation method (Davies & Guinotte 2011).

Variables	Spatial Resolution	Multiple depth levels	Source
Bathymetry variables			
Depth	0.083°	no (seabed)	SRTM30_PLUS (Becker *et al.* 2009)
Slope, bathymetric position index, rugosity	0.083°	no (seabed)	Derived from bathymetry (Wilson *et al.* 2007)
Biological variables			
Primary productivity	0.04°	no (surface)	MODIS L3 Annual SMI
Primary productivity export	0.05°	no (surface)	Derived from MODIS (Behrenfeld & Falkowski 1997)
Chemical variables			
Alkalinity, total CO_2	1°	yes	GLODAP (Key *et al.* 2004)
Aragonite and calcite saturation	1°	yes	Derived from GLODAP (Key *et al.* 2004)
Nutrients	1°	yes	WOA (Garcia *et al.* 2010a)
Oxygen	1°	yes	WOA (Garcia *et al.* 2010b)
Salinity	0.25°	yes	WOA (Antonov *et al.* 2010)
Temperature	0.25°	yes	WOA (Locarnini *et al.* 2010)
Hydrodynamic variables			
Regional current flow, vertical flow	0.5°	yes	SODA (Carton *et al.* 2005)

Ecological Framework and high-resolution HSM

Habitat suitability models (HSMs, also known as species distribution models, environmental niche models or resource selection functions) relate species occurrence data with environmental predictor variables to give statistical estimates of a full-coverage potential species distribution in geographic space (Guisan & Zimmermann 2000, Elith & Leathwick 2009b). The conceptual framework is based on the *habitat* and *niche* concepts in ecology. The term *habitat* simply describes the nature of a place where an organism lives, which can be defined and mapped as spatial area where the physical, chemical and biological conditions are distinctively different from the surrounding areas (Kostylev *et al.* 2001). The *niche* of an organism was defined by Hutchinson (1957) as a multidimensional space whose axes comprise the conditions that limit the organism's fitness (i.e. survival and

reproduction). Hutchinson (1957) further distinguished between the "fundamental niche", which describes the environmental conditions permitting a population's long term survival, and the realized niche, which is the subset of the fundamental niche in which the species normally exists. In this sense, an HSM using purely environmental predictors estimates a species' fundamental or potential distribution, whereas the realized distribution is further affected by biotic interactions, dispersal constrains, anthropogenic effects and stochastic events, amongst others (Jiménez-Valverde *et al.* 2008).

Common HSM algorithms are well described in, for example, Franklin (2009). The appropriateness of an algorithm depends on the amount and type of data available, as well as the objective of the investigation. They vary substantially in complexity and in the type of response variable they use (Guisan & Zimmermann 2000, Elith *et al.* 2006). Environmental envelopes such as BIOCLIM (Busby 1991) were amongst the first and most intuitive methods developed and are based on a simple description (e.g. range or mean) of environmental variable values at locations of species presence. Environmental niche factor analysis (Hirzel *et al.* 2002) uses a multivariate analysis technique based on principal component analysis to describe the environmental space at species occurrence locations; it accounts effectively for correlations between predictor variables. Regression-based methods such as generalized linear and additive models (Guisan *et al.* 2002) and classification and regression tree based methods (De'Ath & Fabricius 2000) use binary presence-absence data to identify the probability of species occurrence. In the common case of unavailable (e.g. museum collections or databases) or unreliable (e.g. when a species is difficult to detect) absence data, pseudo-absence data can be generated by either random or environmentally weighted sampling of locations from the study area background from which species observations are missing. Similar to presence-only models, presence-absence models, using pseudo-absence data, estimate a species' relative likelihood of occurrence (Pearce & Boyce 2006). Increasing computer power has given rise to machine learning algorithms (Elith *et al.* 2006), such as Maxent, which employs a maximum entropy algorithm to model habitat suitability (Phillips *et al.* 2006), GARP, which uses genetic algorithms (Stockwell & Peters 1999) and

Artificial Neural Networks (Lek & Guègan 1999). These algorithms can fit a variety of complex responses and provide useful tools when modelling with large datasets where complex relationships amongst variables occur. It has been argued that complex non-parametric models based on presence-absence data are more likely to reflect a species' realized distribution, whereas simple models using presence-only data are more likely to predict a species' potential distribution (Jiménez-Valverde *et al.* 2008).

HSMs have been developed for terrestrial, freshwater and marine species and used for a wide range of applications including the prediction of the potential distribution of invasive species (Peterson 2003, Tyberghein *et al.* 2012), the estimation of impact of a changing climate on future distributions (Thomas *et al.* 2004, Lima *et al.* 2007, Tittensor *et al.* 2010a), and to aid conservation planning (Carroll 2010), amongst others (Elith & Leathwick 2009b). Marine HSMs are becoming increasingly important because of the drive to exploit marine biological and physical resources, and the establishment of legislative and regulatory frameworks for conservation and management of these resources (Robinson *et al.* 2011, Tyberghein *et al.* 2012). Effort to develop HSM in deep-sea environments has largely focused on cold-water corals, driven by national and international obligations to develop appropriate conservation measures for these vulnerable marine ecosystems (Davies *et al.* 2008, Guinan *et al.* 2009a, Woodby *et al.* 2009, Tittensor *et al.* 2010a, Davies & Guinotte 2011, Howell *et al.* 2011, Marshall 2012, Yesson *et al.* 2012, Rengstorf *et al.* in press). Sessile species constitute a convenient HSM target, as their detection and habitat characterisation is relatively simple compared to mobile marine species (e.g. fish or migrating mammals) that intermittently use patchily distributed resources for feeding, reproducing and nursing (Elith & Leathwick 2009b). An important consideration for HSMs of locally mobile or sessile benthic species is, however, that all habitat requirements must coincide at exactly the same spatial location (Guisan & Thuiller 2005). Reliable HSMs therefore require high-resolution data that ensure precise spatial matching between distribution records and corresponding environmental conditions, and also amongst the different environmental conditions themselves.

Theoretical motivations for the use of detailed high-resolution data to estimate distributions of sessile species are confirmed by recent deep-sea benthic HSMs. Davies *et al.* (2008) showed that a 1º by 1º temperature grid was too coarse to resolve changes in water temperature, leading to a mismatch between cold-water coral occurrences and temperature values beyond the species' thermal tolerance limit. Rengstorf *et al.* (2012) found that bathymetric data of 1 km resolution are too coarse to resolve local morphological features supporting cold-water coral growth and they stressed the need for high-resolution multibeam bathymetry data to avoid an over-estimation of the spatial extent of suitable coral habitat. Several authors (e.g. Frederiksen *et al.* 1992, White *et al.* 2005) have demonstrated, using in-situ current measurements, the preference of benthic suspension feeders for enhanced current flows, but spatially explicit correlative models have not always been able to quantify this relationship (Table 5-2). The poor performance of the global SODA grid (Carton *et al.* 2005) in predicting cold-water coral distribution was attributed to its coarse resolution and the lack of information on topographically influenced and locally varying factors (Davies & Guinotte 2011, Yesson *et al.* 2012). Ocean circulation models at higher resolutions can simulate ecologically relevant processes, such as internal wave dynamics (Nycander 2005) and resonant tidal amplification (Goldner & Chapman 1997), and constitute important predictors for scleractinian and gorgonian cold-water corals at regional scales (Bryan & Metaxas 2007, Rengstorf *et al.* in press).

Emerging considerations for high-resolution HSM in the deep sea

The summary above sets the scene for a consideration of four key issues that are encountered when integrating high-resolution environmental and species occurrence data into a modelling framework.

High-resolution hydrodynamic variables

Hydrodynamic conditions and processes are critical in driving spatial patterns of benthic biota, as they regulate larval dispersal and sediment settlement rates and, most importantly, determine food supply to the benthic boundary layer. Yet, most local and some regional benthic HSMs rely on seabed characteristics only to predict species distributions (Wilson *et al.* 2007, Dolan *et al.* 2008, Holmes *et al.* 2008,

Woodby *et al.* 2009, Howell *et al.* 2011, Hovey *et al.* 2012, Rengstorf *et al.* 2012, Tong *et al.* 2012). To date only one local study has used hydrodynamic variables (Guinan *et al.* 2009a) and these were of too low resolution (4 km) to contribute to model predictions in that particular study (Table 5-2). This paper uses generalised linear models (GLMs) to assess the use of hydrodynamic parameters derived from a high-resolution (250 m) simulation study using the Regional Ocean Modelling System (ROMS) to explain and predict the spatial distribution of the cold-water coral *Lophelia pertusa* in three carbonate mound provinces along the Irish continental shelf.

Table 5-2: A summary of HSMs using hydrodynamic variables for predicting the distribution of scleractinian and gorgonian cold-water corals. Asterisks represent low (*****), moderate (******) and high (*******) predictive power (PP) of hydrodynamic variables in the respective study.

Model scale	Taxon[1]	Hydrographic variables	Cell size	Data source	PP	Authors
global	S	Regional current flow	50 km	Carton *et al.* (2005)	*	Tittensor *et al.* (2010a)
global	O	Regional current flow, vertical flow	50 km	Carton *et al.* (2005)	*	Yesson *et al.* (2012)
global	S	Regional current flow, vertical flow	50 km	Carton *et al.* (2005)	*	Davies & Guinotte (2011)
regional	O	Current speed	25 km	Bleck (2002)	**	Davies *et al.* (2008)
regional	S	Tidal current speed	?	Walters *et al.* (2001)	**	Tracey *et al.* (2011)
regional	O	Current speed	2 km	Hannah *et al.* (2001)	***	Bryan & Metaxas (2007)
regional	S	Current speed,bottom stress, vertical flow	2.5 km	Marine Institute (2012)	***	Rengstorf *et al.* (in press)
local	S	Current speed and direction	4 km	Mohn & Beckmann (2002)	*	Guinan *et al.* (2009a)

[1] S = Scleractinia, O = Octocorallia

Species occurrence proportion data

Recent deep-sea benthic HSMs using video transects have generated both presence and absence data of the target species (Woodby *et al.* 2009, Howell *et al.* 2011, Marshall 2012). Grid cells containing at least one occurrence observation are generally coded as "present" (1), whereas grid cells where the species was not observed are coded as "absent" (0), assuming that the limited area surveyed by the camera's footprint is representative of the entire area encompassed by the grid cell. Figure 5-1 illustrates two main shortcomings of this data simplification; it eliminates information on the species' prevalence (i.e. abundance or coverage) within the grid

cell, and it eliminates information on how much of the grid cell has been actually surveyed (i.e. sampling effort). In this paper we explore the effectiveness of a simple modification of the GLM's response variable to proportion data (as opposed to presence-absence data), which retains information on both prevalence *(n presences / n absences)* and sampling effort *(n presences + n absences)* within each grid cell.

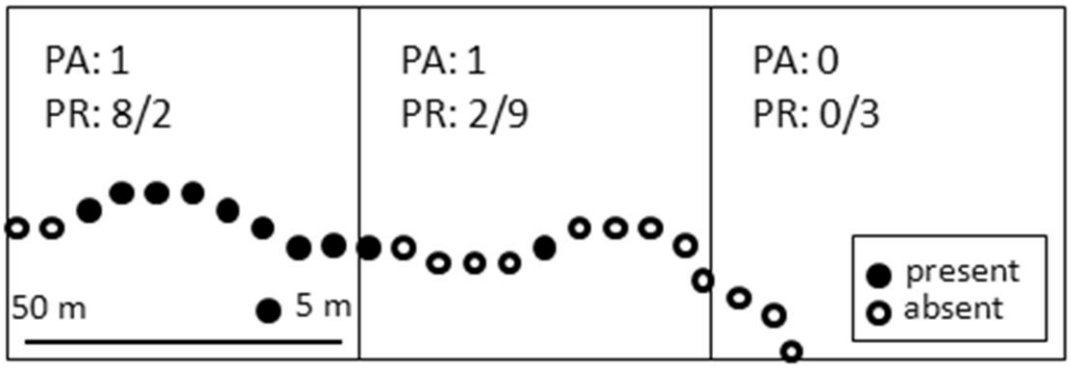

Figure 5-1: Scheme showing observations of species presence (filled circle) and species absence (open circle) along a video transect in context with the environmental data grid cells (large squares). The corresponding response codes specified for a presence-absence model (PA) and a proportion model (PR) are given for each cell.

Generalised linear mixed models (GLMMs)

Most statistical models rely on strong assumptions about the data such as their need to be random and spatially independent from each other (Hirzel *et al.* 2002). As is the case in the present study, individual observations are often derived from continuous transects, which in turn are nested within study areas of scientific interest. Data originating from the same data blocks or groups are spatially pseudo-replicated and ignoring their correlation may lead to biased parameter estimates and invalid model results (Bolker *et al.* 2009). Generalised linear mixed models (GLMMs) are an extension to GLMs in which a linear predictor may contain random effects (groups) and within-group errors may be correlated (Dormann *et al.* 2007, Bolker *et al.* 2009). As an alternative to the traditional GLM, we therefore assess the use of GLMMs, specifying *study area* and *transect station* as nested random effects.

Model transferability

Transferability is an important attribute of HSM, as it is often required to use a model trained in one context to make useful predictions in a different context, i.e. a different environmental space from the one in which the model was calibrated

(Phillips 2008). HSMs transferred in either space (Pittman *et al.* 2007) or time (Tittensor *et al.* 2010a) have many applications in marine research including guiding future survey effort, identifying areas vulnerable to invasive species and investigating how populations might respond to climate change (Marshall 2012). Recent investigations in the deep sea suggest that an increase in a model's spatial resolution might lead to a loss of its transferability (Marshall 2012). In addition to the full model, we therefore assess the transferability of locally trained HSMs from one study area to another.

5.2. Case study

The framework building cold-water coral *Lophelia pertusa* was selected as target species, as it is a well-studied deep-sea benthic organism whose habitat requirements are now largely understood (Roberts *et al.* 2009). Transect-based distribution data was collected in a standardized manner, which enabled the generation of quantitative proportion data and justified the use of GLMMs. Three study areas were chosen to assess species-habitat relationships in different environmental settings and to allow for investigations of model transferability.

Study areas

Three study areas comprising cold-water coral carbonate mounds off the West of Ireland were chosen (Figure 5-2). The Logachev mound province (Figure 5-2a) on the Southern margin of the Rockall Bank is a belt of giant carbonate mounds with heights > 300 m and widths of several kilometres, that are predominantly arranged in down-slope oriented clusters (Kenyon *et al.* 2003, Mienis *et al.* 2006). The Arc mound province (Figure 5-2b) on the south-western Porcupine Bank is made of much smaller mound features ~50 -100 m high and base lengths seldom exceeding 500 m (Rengstorf *et al.* 2012). The Belgica province (Figure 5-2c) on the eastern Porcupine Seabight is roughly arranged in north-south trending ridges. Mounds are up to 100 m high and may reach base lengths up to 2000 m (Wheeler *et al.* 2007). Video footage has revealed thriving *Lophelia pertusa* reefs on summits and terraced flanks of the Logachev mounds (Olu-Le Roy *et al.* 2002) and on the summits of the Arc mounds (Grehan *et al.* 2009).

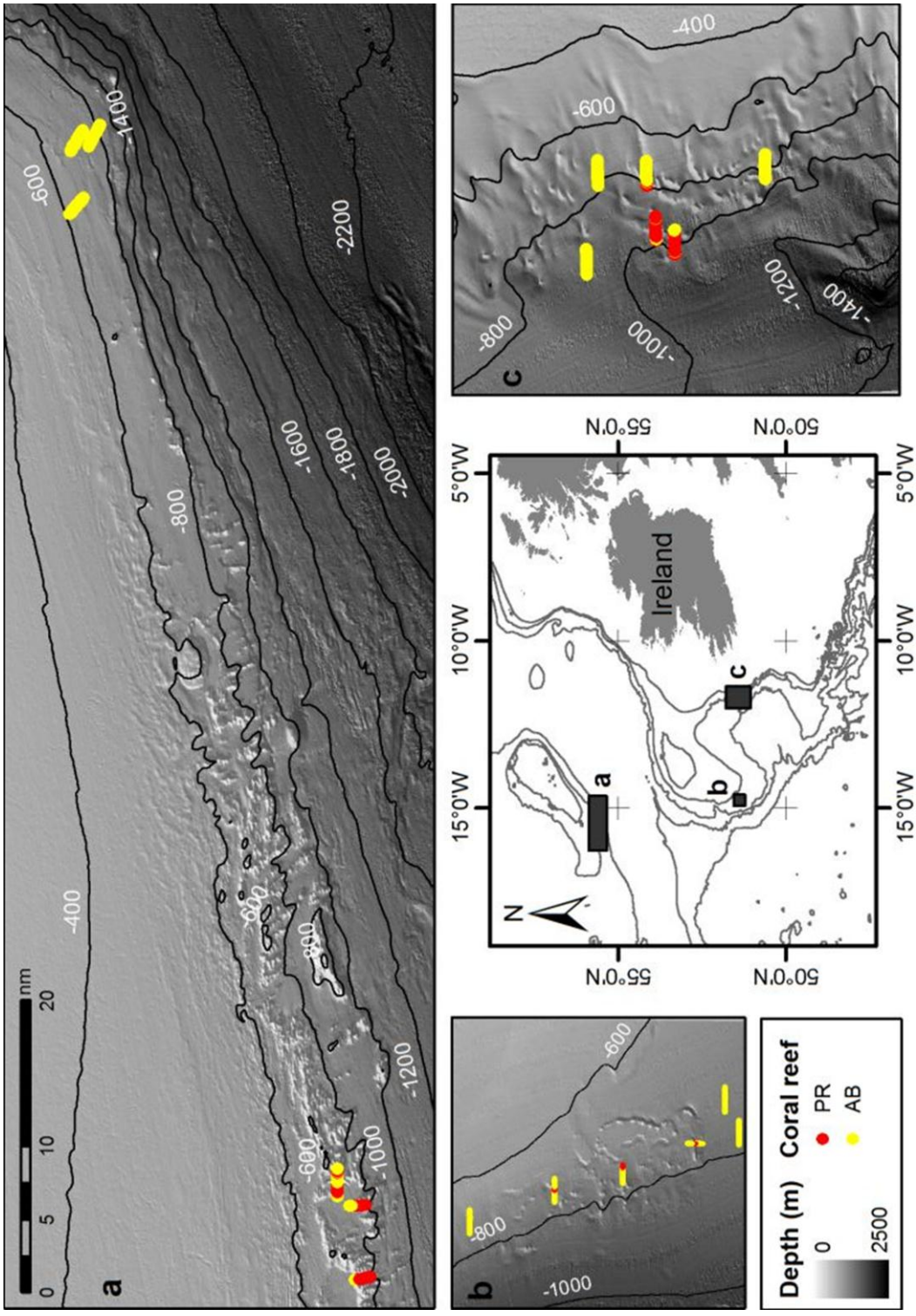

Figure 5-2: Maps showing the locations and high-resolution multibeam bathymetry (INSS data) of the study areas: Logachev (a, 61 km x 103 km), Arc (b, 23 km x 38 km) and Belgica (c, 32 km x 56 km) mound provinces. ROV-based video observations of coral presences (PR) and absences (AB) are indicated in colour.

In the Belgica mound province corals can be found only on the deeper, western alignment of the mounds, whereas the eastern mounds are characterized by asymmetric drift accumulations, sediment clogged dead corals and coral rubble (Foubert *et al.* 2005).

Coral distribution data

Video transects were conducted during the *RV Celtic Explorer* cruise CE10014 in April/May 2010, employing the Irish remotely-operated vehicle (ROV) *Holland I*. In each study area, six transects of ~ 2 km length were conducted, with three transects crossing the summits of carbonate mounds (i.e. likely coral reef areas) and three transects following the general depth-gradient on the open slope (i.e. likely non-coral areas) (Figure 5-2). The ROV was equipped with a forward facing oblique (45° to the seabed) Kongsberg High Definition video camera. Lighting was provided by two forward facing HMI (hydrargyrum medium-arc iodide) lights (60° wideflood beam, 4,750 lumens) and 8 halogen lamps (250W, 120V). Navigation data (ROV positioning, speed, heading and attitude) was provided by an Inertial Navigation System (PHINS, IXSEA) connected to an external ultra-short baseline sensor (GAPS, IXSEA). ROV transects were conducted at an altitude between 1.5 – 2.5 m above seabed and at a constant speed of ~ 0.6 knots (~ 0.3 m/sec). The camera's field of view was roughly 2.5 x 2.5 m depending on seabed topography. The presence and absence of *Lophelia pertusa* framework was annotated in intervals of ~ 5 m and records were geo-referenced using the ROV navigation data.

Environmental variables

A large range of terrain (*n*=6) and hydrodynamic (*n*=17) variables were generated and tested for their importance in predicting coral distribution (Table 5-3).

Bathymetry variables

Multibeam data covering the study areas were acquired as part of the Irish National Seabed Survey (INSS). The clean *.xyz ASCII data were acquired from the Geological Survey of Ireland by the authors and Fledermaus v.7 gridding software was used to produce a digital elevation model (DEM) with a resolution of 0.0005º x 0.0005º (WGS84). The DEM was imported into ArcGIS v.9.3 and projected in UTM

Zone 28N (Logachev and Arc mounds) and UTM Zone 29 N (Belgica mounds) with a resolution of 50 m x 50 m. Terrain variables were derived following Wilson *et al.* (2007) and included seabed slope, small-scale bathymetric position index (BPI3: inner radius = 1, outer radius = 3), large-scale bathymetric position index (BPI25: inner radius = 1, outer radius = 25), aspect (converted to eastness and northness) and rugosity (using the Benthic Terrain Modeller extension to ArcGIS).

Table 5-3: Environmental variables developed for this study, clustered into ecologically meaningful groups.

Variables	Native Resolution	Source & Software used
Bathymetry variables		
Aspect (°)[1], slope (°), BPI3[2], BPI25[3], rugosity	0.0005°	INSS bathymetry, ArcGIS, BTM
Horizontal flow variables		
Bottom stress (N m^{-2})[4], current speed (m s^{-1})[4], mean current direction (°)[1]	0.002°	ROMS[a], ArcGIS
Vertical flow variables		
Vertical flow (m s^{-1})[4]	0.002°	ROMS[a], ArcGIS
Chemistry variables		
Salinity (ppt)[4]	0.002°	ROMS[a], ArcGIS
Temperature (°C)[4]	0.002°	ROMS[a], ArcGIS

[1] Converted to eastness and northness following Wilson *et al*. (2007)
[2] Bathymetric position index computed with an inner radius of 1 and an outer radius of 3 pixels
[3] Bathymetric position index computed with an inner radius of 1 and an outer radius of 25 pixels
[4] 3 near-bottom layers computed for maximum, mean and minimum values over a 30 day time period (15 April – 15 May 2010)
[a] Mohn *et al*., in prep.

Hydrodynamic variables

Hydrodynamic variables were obtained from simulations with the Regional Ocean Modelling System (ROMS, http://roms.mpl.ird.fr/) described in Mohn *et al.* (in prep.). The model has a spatial resolution of 0.002° (~ 250 m) and 32 terrain-following vertical levels from sea surface to bottom layer (thickness ~ 0.01% of water depth). ROMS model output was generated in the form of averages at 6 hour intervals for the time period between the 15th of April and the 15th of May 2010 (corresponding to the period of the CE10014 survey). Variables included current speed (m sec^{-1}), mean current direction (converted to eastward and northward flow), bottom (shear) stress (N m^{-1}), vertical flow (m sec^{-1}), temperature (°C) and salinity (psu) at the near-bottom layer of the three-dimensional model. For each variable (except current direction) we generated grids giving mean, maximum and minimum

values over the one month time period. The resulting grids were projected and interpolated to match the respective 50 m x 50 m bathymetry grids.

A priori variable selection

The choice of predictor variables for a particular species is crucial in HSM as the use of too many variables may result in over-fitting and multi-collinearity (Guisan & Zimmermann 2000). Our variable selection process involved several steps: 1) we clustered environmental variables into ecologically meaningful groups (Table 5-3) and calculated pair-wise Pearson correlation coefficients; 2) the variable with highest explanatory power, measured in % deviance explained based on uni-variate GLMs, was retained from each cluster. Current direction (direast, dirnorth) were not correlated with other variables, but explained < 0.03% deviance and where therefore omitted from further analyses. Besides slope, BPI3 and BPI25 were retained as bathymetric variables because of their only moderate correlations and relatively high predictive power in previous coral HSMs (e.g. Howell *et al.* 2011). The three hydrographic variables selected were maximum bottom stress (botstrmax), maximum vertical flow (wmax) and mean temperature (tmpmean) (see Appendix S1).

Statistical Modelling

All statistical analyses were conducted using the R software package version 2.14.1 for Windows (R Development Core Team 2006). We chose generalised linear models (GLMs) as they are flexible and descriptive modelling tools (Guisan *et al.* 2002), that can be easily manipulated and extensively customized in R. The software's built-in *glm* function was used with binomial error distribution and logit link, which is appropriate for modelling both presence-absence and proportion data (Crawley 2007). Response variables were created as in Figure 5-1. For the proportion models, R uses the *number of presences* and the *number of absences* per grid cell bound together as response variable and then carries out a weighted regression based on the total *number of observations* per grid cell. We did not use simple percentage data because: 1) the errors are not normally distributed; 2) the variance is not constant; and 3) by calculating the percentage, information on

sampling effort per grid cell is lost and all observations are equally weighted (Crawley 2007).

Distribution data used in this study are spatially pseudo-replicated: individual observations within a mound transect are more likely to be "presences", whereas observations in an off-mound transect are more likely to be "absences". Generalized linear mixed models (GLMMs) provide a flexible approach for analysing data when such random effects are present (Crawley 2007, Dormann *et al.* 2007, Bolker *et al.* 2009). GLMMs group individual observations into data blocks (random effects) and model the covariance structure introduced by the grouping of the data (Crawley 2007). We used the "lme4: Linear mixed-effects models using S4 classes" package (http://CRAN.R-project.org/package=lme4) to generate GLMMs using the same specifications as the GLMs, but additionally to the environmental variables (i.e. fixed effects), we specified "study area" and "transect station" as nested random effects.

Stepwise predictor selection is commonly used in regression-based models. However we found that stepwise selection resulted in minimally adequate models which fitted the data only slightly better than combinations of other predictor variables. An alternative method, which can effectively account for this model uncertainty, is the information-theoretic approach for model selection and inference (Burnham & Anderson 1998). The Akaike information criterion (AIC) quantifies the relative performances between alternative models by comparing their goodness of fit (deviance) and by penalising more complex models based on the number of parameters they use (Burnham & Anderson 1998). The AIC thereby provides a basis for model averaging, which can deliver better parameter estimates and confidence intervals that account for model uncertainty (O'Hara & Tittensor 2010).

We followed the methodology in O'Hara & Tittensor (2010) and ran multiple GLMs covering the entire subspace of all first-order additive combinations of the six a priori environmental variables ($2^6 = 64$ models). We used the "Model selection and multimodel inference based on (Q)AIC(c)" package (http://www.CRAN.R-project.org/package=AICcmodavg) to rank models based on their AICc (a variant of AIC corrected for small sample sizes), to calculate model-averaged parameter

estimates and standard errors, and to estimate relative predictor variable importance (Burnham & Anderson 1998). Distribution data pooled from the three study areas (*n*=900) were used for generating GLMs and GLMMs using presence-absence and proportion data. Habitat suitability maps were generated using the parameter coefficients of the highest ranked models when using 1) terrain and hydrodynamic parameters together, 2) hydrodynamic parameters only, and 3) terrain parameters only.

Model transferability was tested using the parameter combination of the overall highest ranked GLM model using presence-absence data (GLM_{PA}). Parameter coefficients were determined using locally trained GLMs (i.e. using data from one study area only) and were then projected onto the other two study areas.

5.3. Results

Parameter responses

The results of our study suggest that all terrain and hydrodynamic (especially vertical flow and bottom stress) variables are important parameters in explaining coral distribution. Figure 5-3 shows the uni-variate response curves for the 6 parameters remaining after the a priori selection, using presence-absence and proportion data. In accordance to previous studies, habitat suitability rapidly increased with terrain complexity (slope, BPI3 and BPI25), reflecting the corals' association with the cold-water carbonate mounds. The strong positive response curves of the horizontal and vertical flow parameters (botstrmax and wmax) confirm the corals' preference for areas of enhanced benthic currents, as well as for downwelling areas with enhanced vertical mixing. The slightly negative relationship with temperature (tmpmean) is likely to reflect the temperature range sampled, as all study areas lie well within the temperature range thought to be suitable for the species (~ 4 – 13°C).

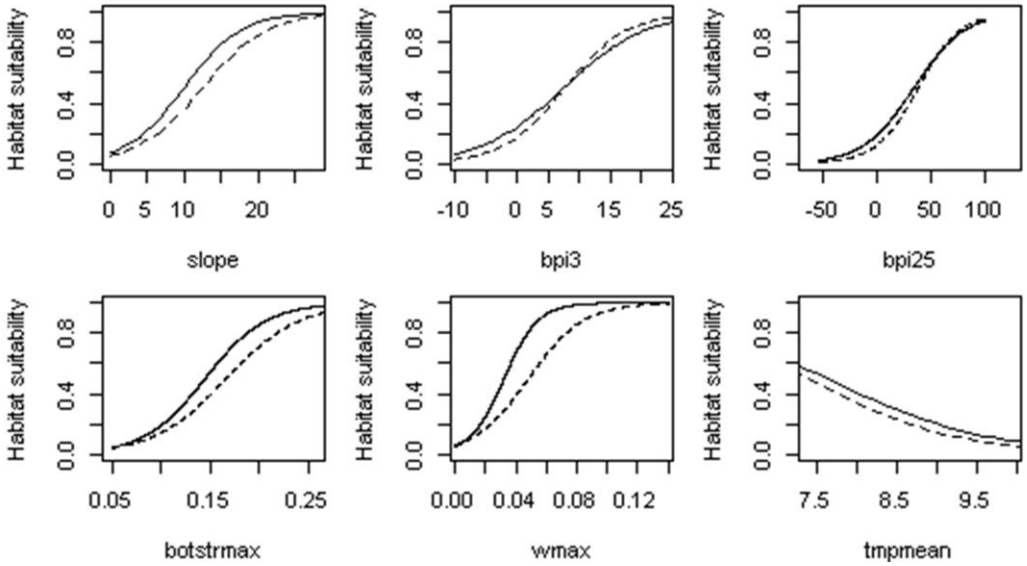

Figure 5-3: Uni-variate GLM response curves for the selected environmental predictor variables using data pooled from all study areas (n=900). The solid line shows the presence-absence responses, the dashed line shows the proportion responses. bpi3 = small-scale BPI (bathymetric position index), bpi25 = large-scale BPI, botstrmax = maximum bottom (shear) stress (N m^{-2}), wmax = maximum vertical flow (m s^{-1}), tmpmean = mean temperature (°C).

Table 5-4: A selection of the 64 GLMs generated based on presence-absence data and ranked by their AICc value. The first 42 models use a combination of terrain and hydrodynamic parameters. The best model using only terrain parameters combines slope and BPI3 and was ranked # 49.

		TERRAIN PARAMETERS			HYDRODYNAMIC PARAMETERS		
Model rank	AICc	slope (°)	bpi3	bpi25	wmax ($msec^{-1}$)	botstrmax (N $m^{-2)}$	tmpmean. (°C)
1	**571**	●		●	●	●	
2	572	●	●	●	●	●	
3	573	●		●	●	●	●
4	574	●	●	●	●	●	●
5	577	●	●	●		●	
…	…	…	…	…	…	…	…
43	**640**				●		
...	…	…	…	…	…	…	…
49	**677**	●	●				
…	…	…	…	…	…	…	…
64	1045	(null model)					

The importance of hydrodynamic parameters for HSM

High-resolution hydrodynamic parameters significantly improved model fit of GLMs and GLMMs and using both presence-absence and proportion data (GLM_{PA}, GLM_{PR}, $GLMM_{PA}$, $GLMM_{PR}$). Table 5-4 shows the top 5 ranked AICc scores and parameter combinations derived from the GLM_{PA}, as well as the highest ranked models that used only hydrodynamic (rank 43) and terrain (rank 49) variables. Thus, the best 48 out of 64 parameter combinations included at least one of the three hydrodynamic variables available, highlighting their importance in explaining local scale coral distribution. Similar results were found for GLM_{PR}, $GLMM_{PA}$, $GLMM_{PR}$ (not shown).

Table 5-5 summarizes parameter estimates, standard errors and relative parameter importance averaged over the 64 model runs conducted for the GLM_{PA}, GLM_{PR}, $GLMM_{PA}$, $GLMM_{PR}$ trials, as well as the percentages of deviance explained by the highest ranked models when using terrain-only (*Terrain*), hydrodynamic-only (*Hydro*) or combined (*Both*) environmental predictor variables. The percentage of deviance explained was consistently higher for the *Both* models (mean ± standard deviation: 0.49 ± 0.04), than for the *Terrain* (0.39 ± 0.04) and *Hydro* (0.37 ± 0.03) models. The model averaged relative variable importance revealed high predictive power for slope, BPI25, wmax and botstrmax (≥ 0.94), while BPI3 and tmpmean were less important (≤ 0.54). Figure 5-4 shows habitat suitability maps for *Lophelia pertusa* generated by the highest ranked GLM_{PA}: *Both* (slope, BPI25, wmax and botstrmax), *Hydro* (wmax) and *Terrain* (slope and BPI3). The best *Hydro* model generated almost identical results to the *Both* model, revealing the strong dependency of coral distribution on areas of local downwelling, as well as the interplay between local current regimes and morphological features. Maps including hydrodynamic variables showed generally higher habitat suitability values in the Logachev mound province compared to the Arc and Belgica mound provinces (Figure 5-4).

Inspection of summary statistics of the hydrodynamic variables revealed significantly stronger current flows in the Logachev mound province compared to the other two areas (see Mohn *et al.* in prep.). As data pooled from all study areas

were used for model calibration, the lower flow speeds in the Arc and Belgica mound provinces resulted in lower habitat suitability scores in these areas.

Table 5-5: Model-averaged parameter estimates, standard errors (SE) and relative parameter importances for GLMs and GLMMs using presence-absence and proportion data. The parameters used by the best *Both* (B), *Hydro* (H) and *Terrain* (T) models are indicated as superscripts beside the variables, and their respective percentage deviance explained is given.

	PRESENCE-ABSENCE DATA				PROPORTION DATA			
	Variable	*Variable importance*	*Estimate*	*Standard Error*	*Variable*	*Variable importance*	*Estimate*	*Standard Error*
GLM	Intercept	1.00	-4.66	1.51	Intercept	1.00	-4.65	0.75
	slope $^{B, T}$	0.97	0.10	0.03	slope $^{B, T}$	1.00	0.06	0.01
	bpi3 ^{T}	0.43	0.05	0.04	bpi3 $^{B, T}$	0.54	-0.02	0.01
	bpi25 ^{B}	0.98	0.03	0.01	bpi25 $^{B, T}$	1.00	0.05	0.00
	wmax $^{B, H}$	0.94	29.67	11.83	wmax $^{B, H}$	1.00	13.28	3.46
	botstrmax ^{B}	0.99	19.11	5.81	botstrmax $^{B, H}$	1.00	20.37	2.23
	tmpmean	0.29	0.04	0.24	tmpmean ^{H}	0.39	-0.09	0.08
		Both	*Hydro*	*Terrain*		*Both*	*Hydro*	*Terrain*
	% dev. expl.	0.46	0.39	0.36	% dev. expl.	0.53	0.34	0.43
GLMM	Intercept	1.00	5.73	13.78	Intercept		13.17	5.46
	slope $^{B, T}$	0.68	0.09	0.05	slope $^{B, T}$	1.00	0.08	0.01
	bpi3 $^{B, T}$	0.66	0.12	0.07	bpi3 $^{B, T}$	1.00	0.09	0.02
	bpi25 $^{B, T}$	0.85	0.04	0.02	bpi25 $^{B, T}$	1.00	0.03	0.00
	wmax $^{B, H}$	1.00	83.81	23.16	wmax $^{B, H}$	1.00	47.81	5.44
	botstrmax ^{H}	0.44	-27.75	26.97	botstrmax ^{H}	0.37	-7.15	7.37
	tmpmean	0.58	-2.02	1.31	tmpmean $^{B, H}$	1.00	-2.32	0.59
		Both	*Hydro*	*Terrain*		*Both*	*Hydro*	*Terrain*
	% dev. expl.	0.44	0.39	0.36	% dev. expl.	0.52	0.34	0.43

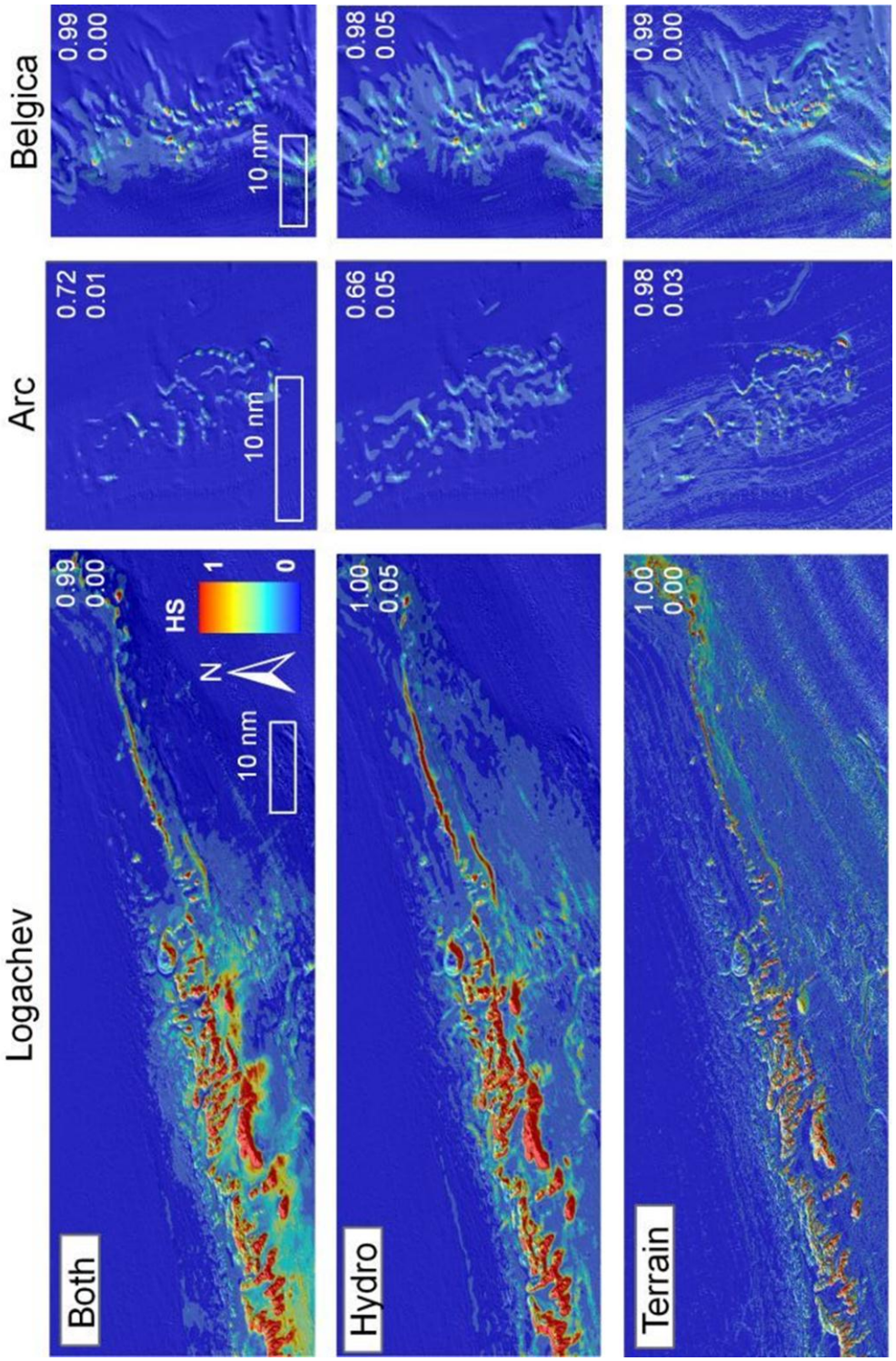

Figure 5-4: Maps showing habitat suitability for *Lophelia pertusa* reefs in the three study areas (Logachev, Arc and Belgica mound provinces from left to right) as generated by the highest ranked models using presence-absence data: *Both* (slope, BPI25, wmax and botstrmax), *Hydro* (wmax) and *Terrain* (slope and BPI3). Habitat suitability ranges from low (0, blue) to high (1, red). Maximum and minimum habitat suitability values are indicated in each map. The north-east oriented line features visible in the lower right corner of the Logachev Mound Province (Terrain model) are due to artefacts in the multibeam bathymetry data.

Proportion data

Based on the percentage of deviance explained, GLMs and GLMMs using proportion data performed on average slightly better (0.43 ± 0.08) than models using presence-absence data (0.40 ± 0.04). Consistently lower standard errors (SE) suggest an increase in model precision. Model averaged parameter estimates (Table 5-5) and uni-variate response curves (Figure 5-3) were comparable between response variables, however presence-absence curves were slightly steeper than the equivalent proportion curves. This was to be expected, as even small proportions (e.g. 1 presence record out of 10 observations: 10 %) would be coded as 1 (100 %) in the presence-absence response. Preliminary analyses using more complex, data driven modelling techniques (generalized additive models, GAMs) resulted in more pronounced discrepancies between the two response curves.

Generalised linear mixed models

Uni-variate response curves created with the GLMMs (not shown) were significantly flatter and skewed towards the x axis. Model averaged parameter coefficients considerably differed from the ones generated by GLM (Table 5-5). GLMMs essentially compute individual responses for each within-group dataset (e.g. 6 response curves for 6 individual transects), and then generate a model explaining the maximum variance between these individual response curves. Therefore, while GLMs use individual observations (n=900) as independent records, the sample size in GLMMs is based on the number of groups (e.g. transects). In the present study, a relatively small number of groups were available. Model specifications using more than 3 or 4 environmental predictors frequently resulted in numerical problems and models failed to converge. Further, three out of six transects were conducted in off-mound areas and hence included little or no coral presence records. These within-group response curves resembled straight horizontal lines of zero habitat suitability, severely skewing the averaged GLMM curves towards lower values. Preliminary GLMMs, including only mound-transects, produced responses more comparable to the GLMs, but here calculations were hampered due to data reduction by 50 %.

Model transferability

Figure 5-5 shows habitat suitability maps of the GLM_{PA} calibrated within one study area only and then projected onto the other two study areas. Predictions of the GLM_{PR} (not shown) were similar but with slightly lower habitat suitability scores. Model transferability was limited by the fact that hydrodynamic conditions varied considerably between study areas (Mohn *et al.* in prep). Models performed well in areas where they had been calibrated, but poorly to moderately well in the other study areas. For example, when training the HSMs in the Arc mound area, where current flow speeds are relatively low, projection onto the Logachev area, where current speeds are generally higher, resulted in severe over prediction of suitable habitat; when training the model in the Logachev area, severe under prediction occurred in the Arc and Belgica mound provinces. The severe reduction in model calibration data probably further decreased model performance.

5.4. Discussion

The present study is the first to assess the use of high-resolution (250 m) hydrodynamic variables for estimating a deep-sea benthic species distribution. While the use of depth-related proxy variables is common practice in benthic HSM, more proximal and functionally relevant predictors (e.g. bottom stress and vertical current flow) are desirable for ecological explanation and insight (Elith & Leathwick 2009b). It is noteworthy that the present study, generating static predictions of present-day conditions, does not yet exploit the full potential of these 3D hydrodynamic models. Coupled with virtual particle tracer studies, hydrodynamic models can provide valuable information on deep-sea dynamic processes that influence spawning patterns and larval dispersal (Levin 2006). Once the relationships between hydrodynamic processes and species distributions are sufficiently established, hind-casts of hydrodynamic settings can be linked to fossil species records (e.g. dated remains of corals, bivalves or brachiopods) to estimate past species distributions and to assess niche stability over geological time-scales (Stigall 2009). Model forecasts can provide insight into the effects of regional climate change and possibly identify new recruitment areas for vulnerable marine species (Tittensor *et al.* 2010a).

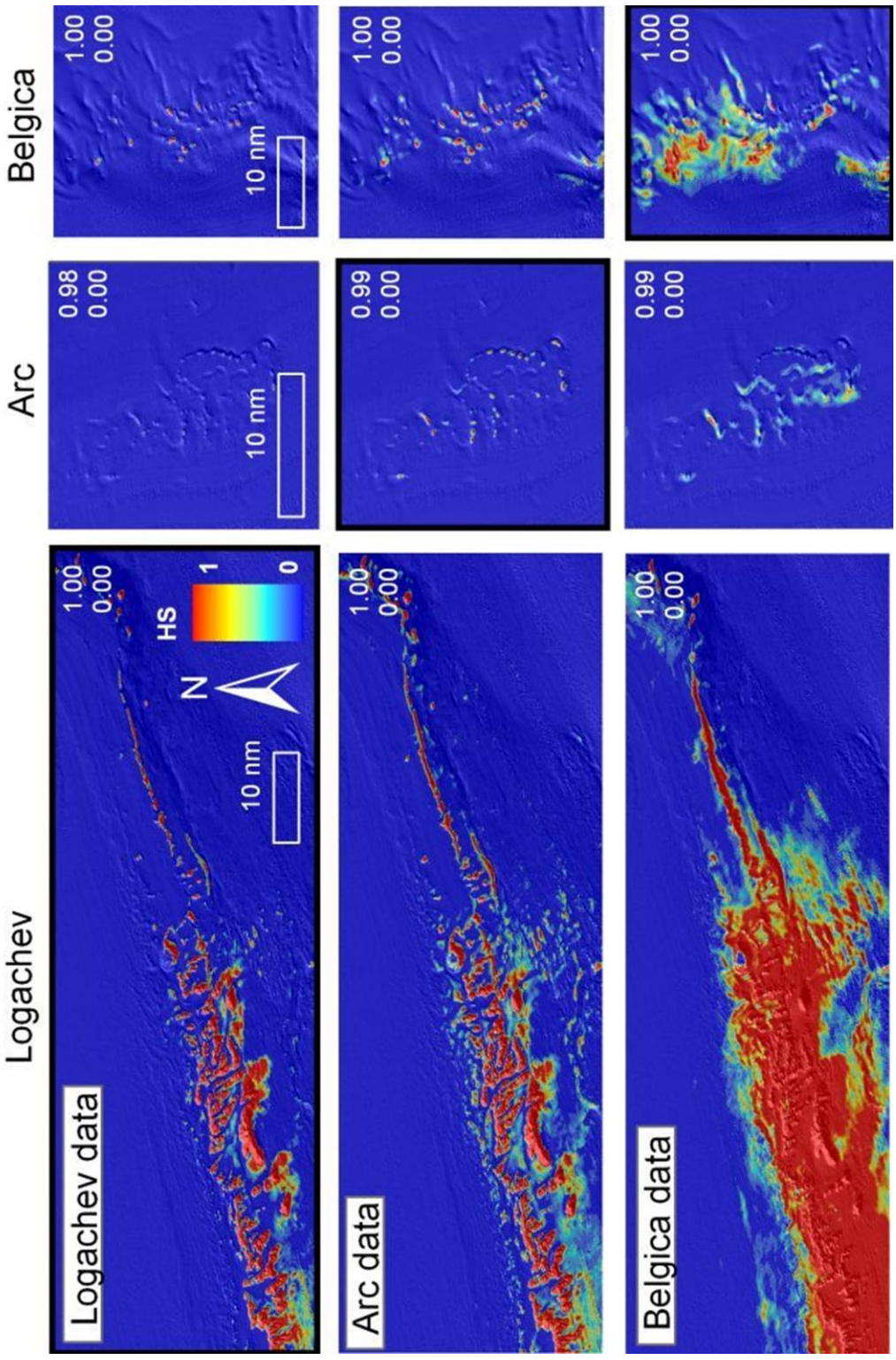

Figure 5-5: Maps showing habitat suitability for *Lophelia pertusa* reefs in the three study areas based on the best Both model (slope, BPI25, vertical flow and bottom stress) as analysed by the GLM model using presence-absence data. Models were trained using data from only one study area and then projected onto the other study areas. Highlighted boxes show maps where models were trained and applied in the same area. The other maps display transferability of models from one study area to another. Habitat suitability ranges from low (0, blue) to high (1, red). Maximum and minimum habitat suitability values are indicated in each map.

Future efforts will also concentrate on the development of more process-based models combining spatial predictions from HSMs with 3D physical and biological mechanisms to resolve the dynamical controls of bentho-pelagic coupling (Soetart *et al.* in prep.).

Several deep-sea benthic investigations relate environmental variables to quantitative video-based species data, for example in the form of abundance (Dolan *et al.* 2008, Howell *et al.* 2010), density (Orejas *et al.* 2009) or percentage coverage (Guinan *et al.* 2009b, Vertino *et al.* 2010). The latter is derived during time-consuming post-processing, which involves calibrating images and overlaying sampling quadrats (Vertino *et al.* 2010) or random sampling points (Guinan *et al.* 2009b). While proportion data are commonly used in, for example, medical studies (Crawley 2007), the approach has not yet been applied in HSM. The preliminary results in this paper suggest that the use of proportion models increases model fit and precision. By taking into account sampling effort per grid cell, the effect of false absences, generated by extrapolating video-based observations onto entire grid cells, is greatly reduced. With converging trends in autonomous surveying (Williams *et al.* 2010), automated image recognition techniques (Purser *et al.* 2009, Schoening *et al.* 2012), and increasingly available high definition video data, proportion modelling as described in this paper suggests a fruitful avenue of research for analysing large quantities of video data in a detailed, time-efficient manner.

HSMs are highly dependent on data quality and quantity. In the deep sea, commonly applied survey strategies such as random or random-stratified sampling (Hirzel *et al.* 2002) are currently difficult to implement. Continuous transect and spatially clustered data require the use of statistical methods that take into account spatial pseudoreplication and autocorrelation. These methods include mixed effect models, generalised estimation equations, autocovariate models or spatial eigenvector mapping, amongst others (Dormann *et al.* 2007). The GLMM approach tested in this study was probably hampered by the small number of transects. Woodby *et al.* (2009) compared traditional GLMs to generalised estimation equations (GEEs) in order to extrapolate deep-sea coral distribution from 27 transects distributed among 9 study sites. Even with a dataset larger than in the present study, the authors found

that not enough data clusters (i.e. transects) were available to generate reliable GEEs. The compromise between the demands of statistical sampling and the logistics of continuous data acquisition suggests that the most effective sampling will be achieved with a large number of short, randomly distributed transects. Future mapping activities will probably use a combination of AUVs, ROVs and drop-frame cameras in order to maximise the data's information content (standardized visual data) and spatial coverage. ROVs are particularly useful for the in situ sampling of voucher specimen, often required for identification and genetic bar-coding of poorly known deep-sea species.

Multibeam backscatter data, commonly used for the discrimination of seabed substratum and habitat mapping in shallow waters (Brown *et al.* 2011), would significantly improve deep-sea HSMs (Woodby *et al.* 2009, Davies & Guinotte 2011). In the high seas, ship-borne multibeam echosounder systems (MBES) result in large seafloor footprints and a reduced ability to discriminate small-scale features, especially in poor weather conditions (Anderson *et al.* 2008). While some studies have suggested the possibility of using shipborne MBES for distinguishing substratum in water depths > 200 m (e.g. Howell *et al*. 2011), issues of spatial resolution and data quality mean that MBES backscatter data will be acquired increasingly using ROVs or AUVs that fly closer to the seabed.

With technological and hydrodynamic modelling developments, process-driven habitat characterisation, pioneered for shallow waters, will become increasingly feasible in the deep sea. For example, Kostylev & Hannah (2007) computed characteristic friction velocities and critical shear stress to develop habitat maps based on ecologically relevant variables such as seafloor disturbance and scope for growth. Models quantifying disturbance of deep-sea benthic habitats will be valuable to assess habitat resilience and vulnerability to anthropogenic adverse impacts such as sediment smothering due to deep-sea bottom trawling (Althaus *et al.* 2009).

Conclusions and future perspectives

The spatial prediction of sessile benthic deep-sea species requires high-resolution data to ensure precise spatial matching between model components and reliable model outcomes. The addition of high-resolution hydrodynamic variables,

particularly horizontal and vertical flow parameters, significantly improve model fit compared to purely terrain-based models. However, model transferability is severely compromised if hydrodynamic parameters in the projected regions are outside the range sampled within the calibration area. Quantitative species proportion data can be easily generated, increase model precision and enhance the model's ecological relevance. Issues related to spatial pseudoreplication should be considered when using transect-based distribution data. A large number of short transects rather than a small number of long transects should be conducted for efficient survey design. Future developments in deep-sea benthic HSM are likely to be more process-driven, to include the organisms' larval stages, and to integrate the spatio-temporal aspects of complex 3D hydrodynamic processes.

5.5. Supporting Information

Appendix S1: Pair-wise Pearson correlation coefficients (*r*) for environmental predictor variables developed for the study. Cells are colour-coded based on their *r*-value: red = high correlation (0.8 - 1); orange = moderate correlation (0.6 - 0.8); yellow = low correlation (0.4 - 0.6), white = no correlation (0 - 0.4). The % deviance explained based on uni-variate GLMs using presence-absence data and proportion data are given. The 6 variables retained for habitat suitability modelling are highlighted.

	BATHYMETRY						HORIZONTAL FLOW						VERTICAL FLOW			CURRENT DIRECTION		CHEMISTRY						% DEVIANCE EXPLAINED		
Variable	slope	BPI3	BPI25	rugosity	east	north	spdmax	spdmean	spdmin	botstrmax	botstrmean	botstrmin	wmax	wmean	wmin	direast	dirnorth	tmpmax	tmpmean	tmpmin	salmax	salmean	salmin	Variable	Presence Absence data	Proportion Data
slope	1.00	0.20	0.53	0.95	-0.09	0.27	0.54	0.55	0.13	0.53	0.55	0.37	0.74	0.70	0.42	-0.01	0.25	-0.25	-0.29	-0.30	-0.15	-0.19	-0.21	**slope**	**0.33**	**0.36**
BPI3	0.20	1.00	0.70	0.28	0.04	0.10	0.04	0.10	0.05	0.06	0.11	0.12	0.11	0.11	0.26	-0.01	0.03	-0.04	-0.05	-0.05	-0.05	-0.05	-0.05	**BPI3**	**0.06**	**0.12**
BPI25	0.53	0.70	1.00	0.56	0.09	0.20	0.12	0.19	0.20	0.13	0.19	0.18	0.31	0.32	0.52	0.02	0.16	-0.10	-0.10	-0.10	-0.07	-0.08	-0.08	**BPI25**	**0.17**	**0.27**
rugosity	0.95	0.28	0.56	1.00	-0.13	0.22	0.51	0.53	0.15	0.50	0.54	0.37	0.69	0.66	0.40	-0.07	0.21	-0.24	-0.28	-0.29	-0.18	-0.21	-0.23	rug3	0.30	0.31
east	-0.09	0.04	0.09	-0.13	1.00	-0.19	0.11	0.06	-0.06	0.09	0.04	-0.21	-0.08	-0.10	-0.04	0.31	-0.36	-0.46	-0.44	-0.42	-0.44	-0.44	-0.43	east	0.00	0.00
north	0.27	0.10	0.20	0.22	-0.19	1.00	0.06	0.04	0.06	0.07	0.07	0.19	0.19	0.17	0.11	0.09	0.30	0.19	0.17	0.17	0.24	0.23	0.22	north	0.05	0.04
spdmax	0.54	0.04	0.12	0.51	0.11	0.06	1.00	0.92	0.13	0.99	0.93	0.41	0.83	0.80	0.28	-0.14	0.11	-0.67	-0.75	-0.78	-0.52	-0.59	-0.65	spdmax	0.27	0.25
spdmean	0.55	0.10	0.19	0.53	0.06	0.04	0.92	1.00	0.36	0.92	0.99	0.62	0.82	0.83	0.36	-0.34	0.26	-0.57	-0.66	-0.70	-0.60	-0.65	-0.70	spdmean	0.21	0.22
spdmin	0.13	0.05	0.20	0.15	-0.06	0.06	0.13	0.36	1.00	0.14	0.34	0.59	0.21	0.25	0.29	-0.39	0.43	0.04	0.03	0.00	-0.16	-0.15	-0.14	spdmin	0.00	0.01
botstrmax	0.53	0.06	0.13	0.50	0.09	0.07	0.99	0.92	0.14	1.00	0.94	0.42	0.82	0.79	0.28	-0.17	0.12	-0.66	-0.74	-0.77	-0.52	-0.59	-0.65	**botstrmax**	**0.27**	**0.26**
botstrmean	0.55	0.11	0.19	0.54	0.04	0.07	0.93	0.99	0.34	0.94	1.00	0.62	0.82	0.83	0.34	-0.33	0.26	-0.56	-0.65	-0.69	-0.56	-0.62	-0.66	botstrmean	0.23	0.23
botstrmin	0.37	0.12	0.18	0.37	-0.21	0.19	0.41	0.62	0.59	0.42	0.62	1.00	0.53	0.58	0.43	-0.48	0.52	0.07	0.00	-0.05	-0.07	-0.10	-0.12	botstrmin	0.07	0.09
wmax	0.74	0.11	0.31	0.69	-0.08	0.19	0.83	0.82	0.21	0.82	0.82	0.53	1.00	0.98	0.53	-0.14	0.25	-0.40	-0.46	-0.49	-0.34	-0.39	-0.43	**wmax**	**0.39**	**0.33**
wmean	0.70	0.11	0.32	0.66	-0.10	0.17	0.80	0.83	0.25	0.79	0.83	0.58	0.98	1.00	0.59	-0.19	0.27	-0.38	-0.44	-0.47	-0.36	-0.40	-0.43	wmean	0.25	0.29
wmin	0.42	0.26	0.52	0.40	-0.04	0.11	0.28	0.36	0.29	0.28	0.34	0.43	0.53	0.59	1.00	-0.02	0.20	-0.10	-0.11	-0.10	-0.09	-0.09	-0.09	wmin	0.17	0.18
direast	-0.01	-0.01	0.02	-0.07	0.31	0.09	-0.14	-0.34	-0.39	-0.17	-0.33	-0.48	-0.14	-0.19	-0.02	1.00	-0.50	-0.03	0.02	0.06	0.30	0.30	0.29	direast	0.01	0.00
dirnorth	0.25	0.03	0.16	0.21	-0.36	0.30	0.11	0.26	0.43	0.12	0.26	0.52	0.25	0.27	0.20	-0.50	1.00	0.35	0.30	0.26	0.13	0.13	0.12	dirnorth	0.03	0.03
tmpmax	-0.25	-0.04	-0.10	-0.24	-0.46	0.19	-0.67	-0.57	0.04	-0.66	-0.56	0.07	-0.40	-0.38	-0.10	-0.03	0.35	1.00	0.99	0.96	0.77	0.80	0.84	tmpmax	0.08	0.11
tmpmean	-0.29	-0.05	-0.10	-0.28	-0.44	0.17	-0.75	-0.66	0.03	-0.74	-0.65	0.00	-0.46	-0.44	-0.11	0.02	0.30	0.99	1.00	0.99	0.78	0.82	0.87	**tmpmean**	**0.11**	**0.13**
tmpmin	-0.30	-0.05	-0.10	-0.29	-0.42	0.17	-0.78	-0.70	0.00	-0.77	-0.69	-0.05	-0.49	-0.47	-0.10	0.06	0.26	0.96	0.99	1.00	0.78	0.82	0.88	tmpmin	0.10	0.13
salmax	-0.15	-0.05	-0.07	-0.18	-0.44	0.24	-0.52	-0.60	-0.16	-0.52	-0.56	-0.07	-0.34	-0.36	-0.09	0.30	0.13	0.77	0.78	0.78	1.00	0.99	0.98	salmax	0.01	0.02
salmean	-0.19	-0.05	-0.08	-0.21	-0.44	0.23	-0.59	-0.65	-0.15	-0.59	-0.62	-0.10	-0.39	-0.40	-0.09	0.30	0.13	0.80	0.82	0.82	0.99	1.00	0.99	salmean	0.01	0.03
salmin	-0.21	-0.05	-0.08	-0.23	-0.43	0.22	-0.65	-0.70	-0.14	-0.65	-0.66	-0.12	-0.43	-0.43	-0.09	0.29	0.12	0.84	0.87	0.88	0.98	0.99	1.00	salmin	0.03	0.05

6. Conclusion

6.1. Summary of achievements

This thesis assesses current concepts and practices regarding the use of benthic habitat suitability modelling (HSM) in the deep sea. Robust and transferrable methods have been developed to generate habitat suitability maps with enhanced spatial resolution, ecological relevance and applicability, hence addressing all of the thesis objectives (Section 1.2). **Paper 1** investigates the effect of initial bathymetric grid resolution on terrain parameters and demonstrates that multibeam bathymetry data finer than 250 m resolution are necessary to detect many of the carbonate mound features found in Irish waters that are associated with coral (Objective 1). The paper suggests that in order to generate reliable estimates of coral coverage, a hierarchical HSM framework should be used which integrates available oceanographic data with derivates of high-resolution multibeam bathymetry (where available). Building on these recommendations, **Paper 2** combines a wide range of interpolated chemical and hydrodynamic variables with full coverage (> 500 000 km^2) multibeam bathymetry data to predict *Lophelia pertusa* reef distribution within the limits of the Irish extended continental shelf claim. The standard deviation of the seabed slope, water temperature and bottom shear stress were found to be the most important parameters in determining coral distribution (Objective 2). The resulting map shows significantly reduced suitable habitat compared to global scale analyses, and provides a potentially valuable tool for ecosystem-based management in Irish waters (Objective 3). **Paper 3** describes the local scale 3D hydrodynamic regimes simulated by a regional ocean modelling system (ROMS) for three selected cold-water coral carbonate mound provinces in Irish waters. By relating oceanographic key parameters with ROV-based video data, the study confirms previously measured intensified benthic dynamics at individual coral sites (Objective 4). **Paper 4** specifically quantifies and models these relationships, and demonstrates that the addition of high-resolution hydrodynamic variables significantly improves model fit compared to models using terrain parameters only (Objective 5). However,

transferability of such high-resolution HSMs may be limited if hydrodynamic conditions vary considerably between study areas. Water temperature was found to be less important in determining coral distribution at the local scale, given it is unlikely to change significantly over short distances; here the combination of bathymetric position index, seabed slope, bottom shear stress and vertical flow achieved best model fit (Objective 2). The investigation of novel approaches within this study (Objective 6) suggests that models using proportion distribution data (derived from video analysis) perform slightly better than models constructed using presence-absence species data, and better represent sampling effort per grid cell. Proportion data provide a fruitful avenue of research for analysing large amounts of video data in a quantitative and time-efficient manner. Mixed modelling is considered as an approach to build statistically robust HSMs using transect-based (i.e. spatially grouped) distribution data. However, a relatively large number of independent transects is required to achieve robust results with this technique.

6.2. Limitations

The limitations encountered throughout the course of this PhD project were mostly related to data issues quite typical for (applied) deep-sea research. The relatively limited data availability, varying data quality, and a suboptimal (or lack of) survey design had to be addressed (e.g. rigorous data filtering, data coarsening and spatial cross-validation) and also affected the choice of HSM algorithms.

Coral distribution data used for the regional scale HSM originate from a large number of sources using a range of sampling equipment. Such datasets impede the use of presence-absence models, as absences cannot be reliably inferred. Presence-only methods can "model the same quantity as presence-absence models", with the difference that they cannot identify the species' prevalence within the study area (Elith *et al.* 2011). While this might have implications for model interpretation (i.e. presence-absence models identify the probability of species occurrence, presence-only models estimate a relative likelihood of occurrence), it does not hamper the models' value for marine spatial planning (see Paper 2). Presence-only data give no quantitative information on species occurrence or coverage, therefore a solitary coral

occurrence record is given the same weight as a record representing a dense coral garden or reef. This issue might be solved by classifying available distribution data prior to modelling (e.g. based on % coral coverage) and developing distinct models for sparse, medium and dense coral coverage. This approach however is only possible if quantitative species distribution data are available in the first place. The rigorous data filtering adopted in this study to model the distribution of *Lophelia pertusa* reef habitat also resulted in a severe reduction of species occurrence points. Maxent (Phillips *et al.* 2006) was chosen for this particular study as it is amongst the most effective HSM presence-only algorithms (Elith *et al.* 2006), is relatively insensitive to sample size (Wisz *et al.* 2008), and has performed well in previous studies targeting *Lophelia pertusa* (Tittensor *et al.* 2009, Davies & Guinotte 2011, Howell *et al.* 2011). The option to use presence-absence models in conjunction with pseudo-absence data was dismissed, as the (subjective) selection of pseudo-absences significantly biases model results, therefore adding to model uncertainty (Chefaoui & Lobo 2008). A promising future approach to reduce effects of spatial sampling bias might be to draw pseudo-absences from sampling stations of research cruises carried out within the respective study area, but where no corals were recorded (Tracey *et al.* 2011).

Coral distribution data used for the local-scale models were collected in a standardised manner during cruise CE10014 (Grehan *et al*. 2010). The survey was originally designed so that video transects would follow the tracks of a long-line fisheries survey, in order to facilitate a comparative fish study within the CoralFISH project. This resulted in a relatively small number of independent video transects (only 6 per study area), which certainly is not ideal for HSM analyses which require a large amount of independent occurrence records. Generalised linear models (GLMs) were chosen for this study, as they are flexible and descriptive modelling tools that can be easily manipulated and extensively customized in R. However, GLMs can only fit relatively simple response curves compared to machine learning algorithms. Once more distribution data becomes available, it would be interesting to compare GLM results to other presence-absence models such as Boosted Regression

Trees (BRTs), which enable sophisticated regression analyses of more complex responses while optimizing the model's predictive performance (Elith *et al.* 2008).

Finally, due to the longevity of cold-water coral reefs, it might have been ecologically more relevant to integrate hydrodynamic data derived from ROMS model runs over multiple years or decades, rather than using the 6-hourly intervals during a month-long sampling cruise. While global hydrodynamic data are available over longer time periods (e.g. Carton *et al.* 2005), long term simulations of high-resolution ROMS models are limited by computing time and computer power. While seasonal differences certainly affect the strength of the signals found within the oceanographic key variables, their relative spatial distribution is likely to be maintained, as near bottom tidal currents are relatively stable over long time periods (Christian Mohn, personal communication).

6.3. Applications and outlook

The HSMs developed within this PhD project provide valuable insight into species-habitat relationships at local and regional scales and can contribute to the scientific knowledge requirements of international legislations and initiatives summarized in Table 1-1. Continuous or binary habitat suitability maps can be used as information layers in decision support tools such as Marxan (Wilson *et al.* 2005, Leathwick *et al.* 2008). Integration of coral maps with spatial information of deep-water bottom fishing effort (e.g. derived from vessel monitoring systems), for example, helps to identify areas of potential adverse impact and facilitates informed risk assessment (Clark & Tittensor 2010). Maps of coral distribution can further serve as predictor variables in studies investigating environmental drivers of other marine species distributions, for example ophiuroids (O'Hara & Tittensor 2010).

In the context of the CoralFISH project, the produced habitat suitability maps contribute to an inter-regional comparison between cold-water coral provinces on a European level (the "Coral Atlas"). Combining HSM outputs with fish distribution data derived from long-line and echo sounder surveys helps to determine spatial relationships and linkages between deep-sea fish and coral habitat. Multi-disciplinary efforts are also concentrating on the combination of the local scale HSMs with 3D

physical and biological mechanisms to resolve the dynamical controls of bentho-pelagic coupling (Soetart et al., in prep.).

This thesis demonstrates that ocean circulation models can provide a valuable resource for full coverage oceanographic predictor variables, provided they are of sufficient spatial resolution to resolve ecologically relevant processes (e.g. internal waves). The combination of HSM and 3D ROMS models is a significant advancement in deep-sea analyses, as it facilitates the integration of the third dimension (i.e. the water column) as well as temporal aspects (e.g. seasonal variations or changes over geological timescales) in future modelling efforts. Model projections into the past, for example, can help to assess niche stability over geological time-scales (Stigall 2009). Model forecasts can provide insight into the effects of climate change and identify new recruitment areas, which might have important implications for marine protected area network design. Tittensor *et al.* (2010a), for example, suggested that global protection measures for cold-water corals should focus on future suitable habitat located in elevated, shallower areas (e.g. continental slopes and seamounts) rather than in surrounding deeper areas, due to the predicted shoaling of the aragonite saturation horizon. HSM could also help to predict the impacts of climate change related habitat fragmentation on a species' dispersal capabilities. For example, potentially suitable and potentially colonisable coral habitat distribution is likely to differ due to dispersal restrictions imposed by dominant water currents and geographic barriers. Methods combining HSMs and dispersal models have recently been developed for terrestrial plants (Engler & Guisan 2009) and could be easily adopted for the use in the marine realm (Robinson *et al.* 2011). Linking both the benthic and the pelagic realm in a holistic, 3D modelling framework will ultimately allow us to better understand, predict and protect the spatial distribution of marine species and habitats.

6.4. Recommendations

Based on the finding of this PhD thesis, the following actions are recommended for future deep-sea HSM analyses:

- ➔ Bathymetry data should be sufficient to resolve the deep-sea morphological features that drive benthic species distribution. Terrain parameters should be generated at multiple spatial scales.
- ➔ Hydrodynamic data should be sufficient to resolve processes such as internal waves, resonant tidal amplification, and other phenomena likely to affect benthic species distribution.
- ➔ Environmental predictor variables should be clustered into ecologically meaningful groups and carefully chosen based on their explanatory power and ecological relevance for the target species.
- ➔ Readily available distribution data should be revised in detail and filtered to ensure representativeness of modelling target. Data submissions to public databases should include important metadata such as the sampling equipment and effort, and the organism's life stage.
- ➔ Sampling design should aim for a large number of short and independent transects. It should be spatially unbiased, randomly-stratified, and cover the main gradients of the study area's geographic and environmental space.
- ➔ Predictions of presence-only models in broad un-sampled regions must be interpreted with caution. If possible, pseudo-absence data could be generated that reflects the sampling effort within the study region.
- ➔ If using presence-absence data, the absence observations should be weighted based on their certainty (e.g. measured by the sampling effort/coverage within the respective grid cell).
- ➔ Commonly used modelling software such as OpenModeller (Sutton *et al.* 2007) or BIOMOD (Thuiller *et al.* 2009) should implement the option to use species distribution proportion data for model calibration.

List of references

Albani, M., Klinkenberg, B., Andison, D.W. & Kimmins, J.P. (2004) The choice of window size in approximating topographic surfaces from Digital Elevation Models. International Journal of Geographical Information Science, 18, 577-593

Althaus, F., Williams, A., Schlacher, T., Kloser, R., Green, M.A., Barker, B.A., Bax, N.J., Brodie, P. & Schlacher-Hoenlinger, M.A. (2009) Impacts of bottom trawling on deep-coral ecosystems of seamounts are long-lasting. Marine Ecology Progress Series, 397, 279-294

Anderson, J.T., Van Holliday, D., Kloser, R., Reid, D.G. & Simard, Y. (2008) Acoustic seabed classification: current practice and future directions. ICES Journal of Marine Science, 65, 1004-1011

Antonov, J.I., Seidov, D., Boyer, T.P., Locarnini, R.A., Mishonov, A.V., Garcia, H.E., Baranova, O.K., Zweng, M.M. & Johnson, D.R. (2010) World Ocean Atlas 2009, Volume 2: Salinity (ed. by S. Levitus). NOAA Atlas NESDIS 69, U.S. Government Printing Office, Washington, D.C., 184 pp.

Ardron, J., Gjerde, K., Pullen, S. & Tilot, V. (2008) Marine spatial planning in the high seas. Marine Policy, 32, 832-839

Armstrong, C.W., Foley, N.S., Tinch, R. & van den Hove, S. (2012) Services from the deep: Steps towards valuation of deep sea goods and services. Ecosystem Services, 2, 2-13

Auster, P., Gjerde, K.M., Heupel, E., Watling, L., Grehan, A. & Rogers, A.D. (2011) Definition and detection of vulnerable marine ecosystems on the high seas: problems with the "move-on" rule. ICES Journal of Marine Science, 68, 254-264

Baines, P.G. (1974) The generation of internal tides over steep continental slopes. Philosophical Transactions of the Royal Society of London. Series A, Mathematical and Physical Sciences, 277, 27-58

Ball, I.R. & Possingham, H.P. (2000) Marxan (v. 1.8.6): Marine Reserve Design Using Spatially Explicit Annealing. User Manual: http://www.uq.edu.au/marxan.

Becker, J.J., Sandwell, D.T., Smith, W.H.F., Braud, J., Binder, B., Depner, J., Fabre, D., Factor, J., Ingalls, S., Kim, S.-H., Ladner, R., Marks, K., Nelson, S., Pharaoh, A., Trimmer, R., Von Rosenberg, J., Wallace, G. & Weatherall (2009) Global Bathymetry and Elevation Data at 30 Arc Seconds Resolution: SRTM30_PLUS. Marine Geodesy, 32, 355-371

Beckmann, A. & Haidvogel, D.B. (1997) A numerical simulation of flow at Fieberling Guyot. Journal of Geophysical Research, 102, 5595-5613

Behrenfeld, M.J. & Falkowski, P.G. (1997) Photosynthetic rates derived from satellite-based chlorophyll concentration. Limnology and Oceanography, 42, 1-20

Benn, A.R., Weaver, P.P., Billet, D.S.M., van den Hove, S., Murdock, A.P., Doneghan, G.B. & Le Bas, T. (2012) Human Activities on the Deep Seafloor in the North East Atlantic: An Assessment of Spatial Extent. PLoS ONE, 5, e12730

Bleck, R. (2002) An oceanic general circulation model framed in hybrid isopycnic-cartesian coordinates. Ocean Modelling, 4, 55–88

Bolker, B.M., Brooks, M.E., Clark, C.J., Geange, S.W., Poulsen, J.R., Stevens, M.H.H. & White, J.-S.S. (2009) Generalized linear mixed models: a practical guide for ecology and evolution. Trends in Ecology & Evolution, 24, 127-135

Boyce, M.S., Vernier, P.R., Nielsen, S.E. & Schmiegelow, F.K.A. (2002) Evaluating resource selection functions. Ecological Modelling, 157, 281-300

Brink, K.H. (1995) Tidal and lower frequency currents above Fieberling Guyot. Journal of Geophysical Research, 100, 10817-10832

Brown, C.J., Sameoto, J.A. & Smith, S.J. (2012) Multiple methods, maps, and management applications: purpose made seafloor maps in support of Ocean Management. Journal of Sea Research, 72

Brown, C.J., Smith, S.J., Lawton, P. & Anderson, J.T. (2011) Benthic habitat mapping: A review of progress towards improved understanding of the spatial ecology of the seafloor using acoustic techniques. Estuarine, Coastal and Shelf Science, 92, 502-520

Bryan, T.L. & Metaxas, A. (2007) Predicting suitable habitat for deep-water gorgonian corals on the Atlantic and Pacific Continental Margins of North America. Marine Ecology Progress Series, 330, 113-126

Burnham, K.P. & Anderson, D.R. (1998) Model Selection and Multimodel Inference: A Practical Information-Theoretic Approach. New York: Springer-Verlag.

Busby, J.R. (1991) BIOCLIM - a bioclimate analysis and prediction system. Nature Conservation: Cost Effective Biological Surveys and Data Analysis, 64 - 68

Cacchione, D.A., Pratson, L.F. & Ogston, A.S. (2002) The shaping of continental slopes by internal tides. Science, 296, 724-727

Carpenter, G., Gillison, A.N. & Winter, J. (1993) DOMAIN: a flexible modelling procedure for mapping potential distributions of plants and animals. Biodiversity and Conservation, 2, 667 - 680

Carroll, C. (2010) Role of climatic niche models in focal-species-based conservation planning: Assessing potential effects of climate change on Northern Spotted Owl in the Pacific Northwest, USA. Biological Conservation, 143, 1432-1437

Carton, J.A., Giese, B.S. & Grodsky, S.A. (2005) Sea level rise and the warming of the oceans in the Simple Ocean Data Assimilation (SODA) ocean reanalysis. Journal of Geophysical Research, 110, 1955–1959

Chefaoui, R.M. & Lobo, J.M. (2008) Assessing the effects of pseudo-absences on predictive distribution model performance. Ecological Modelling, 210, 478-486

Clark, M.R., Tittensor, D., Rogers, A.D., Brewin, P., Schlacher, T., Rowden, A.A., Stocks, K. & Consalvey, M. (2006) Seamounts, deep-sea corals and fisheries: vulnerability of deep-sea corals to fishing on seamounts beyond areas of national jurisdiction. UNEP-WCMC, Cambridge, UK.

Clark, M.R. & Tittensor, D.P. (2010) An index to assess the risk to stony corals from bottom trawling on seamounts. Marine Ecology, 31, 200-211

Cogan, C.B., Todd, B.J., Lawton, P. & Noji, T.T. (2009) The role of marine habitat mapping in ecosystem-based management. ICES Journal of Marine Science, 66, 2033-2042

Costello, M.J., McCrea M., Freiwald, A., Lundälv, T., Jonsson, L., Bett, B.J., van Weering, T.C.E., de Haas, H., Roberts, J.M. & Allen, D. (2005) Role of cold-water Lophelia pertusa coral reefs as fish habitat in the NE Atlantic. Cold-water Corals and Ecosystems (ed. by A. Freiwald and J.M. Roberts), pp. 771-805. Springer-Verlag, Berlin, Heidelberg.

Crawley, M. (2007) The R Book. Wiley.

Curtin, R. & Prellezo, R. (2011) Understanding marine ecosystem based management: A literature review. Marine Policy, 34, 821-830

Davies, A., Duineveld, G. & Roberts, M.J. (2009) Downwelling and deep-water bottom currents as food supply mechanisms to the cold-water coral Lophelia pertusa (Scleractinia) at the Mingulay Reef complex. Limnology and Oceanography, 54, 620-629

Davies, A.J. & Guinotte, J.M. (2011) Global Habitat Suitability for Framework-Forming Cold-Water Corals. PLoS ONE, 6, e18483

Davies, A.J., Roberts, J.M. & Hall-Spencer, J. (2007) Preserving deep-sea natural heritage: Emerging issues in offshore conservation and management. Biological Conservation, 138, 299-312

Davies, A.J., Wisshak, M., Orr, J.C. & Roberts, M.J. (2008) Predicting suitable habitat for the cold-water coral Lophelia pertusa (Scleractinia). Deep Sea Research Part I: Oceanographic Research Papers, 55, 1048 - 1062

De Leo, F.C., Smith, C.R., Rowden, A.A., Bowden, D.A. & Clark, M.R. (2010) Submarine canyons: hotspots of benthic biomass and productivity in the deep sea. Proceedings of the Royal Society B: Biological Sciences, 277, 2783–2792

De Mol, B. (2009) The HERMES cold-water coral database. In. PANGAEA. download: http://doi.pangaea.de/10.1594/PANGAEA.728313

De Mol, B., Van Rensbergen, P., Pillen, S., Van Herreweghe, K., Van Rooij, D., McDonnell, A., Huvenne, V., Ivanov, M., Swennen, R. & Henriet, J.P. (2002) Large deep-water coral banks in the Porcupine Basin, southwest of Ireland. Marine Geology, 188, 193-231

De Mol, L., Van Rooij, D., Pirlet, H., Greinert, J., Frank, N., Quemmerais, F. & Henriet, J.-P. (2010) Cold-water coral habitats in the Penmarc'h and Guilvinec Canyons (Bay of Biscay): Deep-water versus shallow-water settings. Marine Geology, 282, 40-52

De'Ath, G. & Fabricius, K.E. (2000) Classification and Regression Trees: A Powerful Yet Simple Technique for Ecological Data Analysis. Ecology, 81, 3178-3192

Degraer, S., Verfaillie, E., Willems, W., Adriaens, E., Vincx, M. & Van Lancker, V. (2008) Habitat suitability modelling as a mapping tool for macrobenthic communities: An example from the Belgian part of the North Sea. Continental Shelf Research, 28, 369-379

Deng, Y. (2007) New trends in digital terrain analysis: landform definition, representation, and classification. Progress in Physical Geography, 31, 405-419

Deng, Y., Wilson, J.P. & Bauer, B.O. (2007) DEM resolution dependencies of terrain attributes across a landscape. International Journal of Geographical Information Science, 21, 187-213

Dickson, R.R. & McCave, I.N. (1986) Nepheloid layers on the continental slope west of Porcupine Bank. Deep Sea Research Part I: Oceanographic Research Papers, 33, 791-818

Dodds, L.A., Roberts, J.M., Taylor, A.C. & Marubini, F. (2007) Metabolic tolerance of the cold-water coral Lophelia pertusa (Scleractinia) to temperature and dissolved oxygen change. Journal of Experimental Marine Biology and Ecology, 349, 205-214

Dolan, M.F.J., Grehan, A.J., Guinan, J.C. & Brown, C. (2008) Modelling the local distribution of cold-water corals in relation to bathymetric variables: Adding spatial context to deep-sea video data. Deep Sea Research Part I: Oceanographic Research Papers, 55, 1564-1579

Doney, S.C., Ruckelshaus, M., Emmett Duffy, J., Barry, J.P., Chan, F., English, C.A., Galindo, H.M., Grebmeier, J.M., Hollowed, A.B., Knowlton, N., Polovina, J., Rabalais, N.N., Sydeman, W.J. & Talley, L.D. (2012) Climate Change Impacts on Marine Ecosystems. Annual Review of Marine Science, 4, 11-37

Dormann, C.F., McPherson, J.M., Araùjo, M.B., Bivand, R., Bolliger, J., Carl, G., Davies, R.G., Hirzel, A., Jetz, W., Kissling, D., Kuehn, I., Ohlemueller, R., Peres-Neto, P.R., Reineking, B., Boris Schroeder, Schurr, F.M. & Wilson, R. (2007) Methods to account for spatial autocorrelation in the analysis of species distributional data: a review. Ecography, 30, 609-628

Dorschel, B., Hebbeln, D., Rüggeberg, A., Dullo, W.-C. & Freiwald, A. (2005) Growth and erosion of a cold-water coral covered carbonate mound in the Northeast Atlantic during the Late Pleistocene and Holocene. Earth and Planetary Science Letters, 233, 33-44

Dorschel, B., Wheeler, A.J., Monteys, X. & Verbruggen, K. (2011) Atlas of the Deep-Water Seabed: Ireland. Springer Verlag, New-York.

Douvere, F. (2008) The importance of marine spatial planning in advancing ecosystem-based sea use management. Marine Policy, 32, 762-771

Duineveld, G., Lavaleye, M.S.S. & Berghuis, E.M. (2004) Particle flux and food supply to a seamount coldwater coral community (Galicia Bank, NW Spain). Marine Ecology Progress Series, 277, 13-23

Duineveld, G.C.A., Jeffreys, R.M., Lavaleye, M.S.S., Davies, A.J., Bergman, M.J.N., Watmough, T. & Witbaard, R. (2012) Spatial and tidal variation in food supply to shallow cold-water coral reefs of the Mingulay Reef complex (Outer Hebrides, Scotland). Marine Ecology Progress Series, 444, 97-115

Dunn, D.C. & Halpin, P.N. (2009) Rugosity-based regional modeling of hard-bottom habitat. Marine Ecology Progress Series, 377, 1–11

Duran Munoz, P., Sayago-Gil, M., Cristobo, J., Parra, S., Serrano, A., Diaz del Rio, V., Patrocinio, T., Sacau, M., Murillo, F.J., Palomino, D. & Fernandez-Salas, L.M. (2009) Seabed mapping for selecting cold-water coral protection areas on Hatton Bank, Northeast Atlantic. ICES Journal of Marine Science, 66, 2013-2025

Durski, S.M., Glenn, S.M. & Haidvogel, D.B. (2004) Vertical mixing schemes in the coastal ocean: Comparison of the level 2.5 Mellor-Yamada scheme with an

enhanced version of the K profile parameterization. Journal of Geophysical Research, 109, C01015

Egbert, G.D. & Erofeeva, S.Y. (2002) Efficient inverse modeling of barotropic ocean tides. Journal of Atmospheric and Oceanic Technology, 19, 183-204

Ehler, C. & Douvere, F. (2009) Marine Spatial Planning: a step-by-step approach toward ecosystem-based management. Intergovernmental Oceanographic Commission and Man and the Biosphere Programme. IOC Manual and Guides No 53, ICAM Dossier No. 6. UNESCO, Paris, 99 pp

Elith, J., Graham, C.H., Anderson, R.P., Dudík, M., Ferrier, S., Guisan, A., Hijmans, R.J., Huettmann, F., Leathwick, J.R., Lehmann, A., Li, J., Lohmann, L.G., Loiselle, B.A., Manion, G., Moritz, C., Nakamura, M., Nakazawa, Y., Overton, J.M.M., Peterson, A.T., Phillips, S.J., Richardson, K., Scachetti-Pereira, R., Schapire, R.E., Soberón, J., Williams, S., Wisz, M.S. & Zimmermann, N.E. (2006) Novel methods improve prediction of species' distributions from occurrence data. Ecography, 29, 129-151

Elith, J. & Leathwick, J.R. (2009a) Conservation prioritisation using species distribution modelling. Spatial Conservation Prioritization: Quantitative Methods and Computational Tools (Oxford Biology) (ed. by A. Moilanen, K.A. Wilson and H. Possingham).

Elith, J. & Leathwick, J.R. (2009b) Species Distribution Models: Ecological Explanation and Prediction Across Space and Time. Annual Review of Ecology, Evolution, and Systematics, 40, 677-697

Elith, J., Leathwick, J.R. & Hastie, T. (2008) A working guide to boosted regression trees. Journal of Animal Ecology, 77, 802-813

Elith, J., Phillips, S.J., Hastie, T., Dudík, M., Chee, Y.E. & Yates, C.J. (2011) A statistical explanation of MaxEnt for ecologists. Diversity and Distributions, 17, 43-57

Engler, R. & Guisan, A. (2009) MigClim: Predicting plant distribution and dispersal in a changing climate. Diversity & Distributions, 15, 590-601

Etnoyer, P. & Morgan, L.E. (2007) Predictive habitat model for deep gorgonians needs better resolution: Comment on Bryan & Metaxas (2007). Marine Ecology Progress Series, 339, 311–312

FAO (2009) International Guidelines for the Management of Deep-Sea Fisheries in the High Seas. Food and Agricultural Organization of the United Nations, Food and Agriculture Organization of the United Nations, Rome, Italy. 73pp.

Feely, R.A., Doney, S.C. & Cooley, S.R. (2009) Ocean acidification - present conditions and future changes in a high-CO_2 world. Oceanography, 22, 36-47

Fielding, A.H. & Bell, J.F. (1997) A review of methods for the assessment of prediction errors in conservation presence/absence models. Environmental Conservation 24, 38–49

Fisher, P., Wood, J. & Cheng, T. (2004) Where is Helvellyn? Fuzziness of multi-scale landscape morphometry. Transactions of the Institute of British Geographers, 29, 106-128

Foley, M.M., Halpern, B.S., Micheli, F., Armsby, M.H., Caldwell, M.R., Crain, C.M., Prahler, E., Rohr, N., Sivas, D., Beck, M.W., Carr, M.H., Crowder, L.B., Emmett Duffy, J., Hacker, S.D., McLeod, K.L., Palumbi, S.R., Peterson, C.H., Regan, H.M., Ruckelshaus, M.H., Sandifer, P.A. & Steneck,

R.S. (2010) Guiding ecological principles for marine spatial planning. Marine Policy, 34, 955-966

Forbes, E. (1844) Report on the Mollusca and Radiata of the Aegean Sea, and on their distribution, considered as bearing on geology. Report of the British Association for the Advancement of Science for 1843. 129–193

Foster-Smith, R., Connor, D. & Davies, J.S. (2007) What is habitat mapping. MESH Guide to Habitat Mapping, MESH Project, 2007. available at http://www.searchmesh.net/pdf/GMHM1%20What%20is%20habitat%20mapping.pdf.

Foubert, A., Beck, T., Wheeler, A.J., Opderbecke, J., Grehan, A., Klages, M., Thiede, J., Henriet, J.-P. & Polarstern ARK-XIX/3a Shipboard Party (2005) New view of the Belgica Mounds, Porcupine Seabight, NE Atlantic: preliminary results from the Polarstern ARK-XIX/3a ROV cruise. Cold-water Corals and Ecosystems (ed. by A. Freiwald and J.M. Roberts), pp. 403-415. Springer-Verlag, Berlin, Heidelberg.

Franklin, J. (2009) Mapping Species Distributions - Spatial inference and prediction. Cambridge University Press.

Frederiksen, R., Jensen, A. & Westerberg, H. (1992) The distribution of the scleractinian coral Lophelia pertusa around the Faroe Islands and the relation to internal tidal mixing. Sarsia 77, 157–171

Freiwald, A., Fosså, J.H., Grehan, A., Koslow, T. & Roberts, J.M. (2004) Cold-water Coral Reefs. UNEP-WCMC, Cambridge, UK.

Friedman, J.H. (1991) Multivariate adaptive regression splines. Annals of Statistics, 19, 1–141

Gage, J.D. & Bett, B.J. (2005) Deep-Sea Benthic Sampling. Methods for the Study of Marine Benthos (Third Edition) (ed. by A.D. Mcintyre and A. Eleftheriou), pp. 273 - 325. Blackwell Science Ltd, Oxford.

Gallant, J.C. & Hutchinson, M.F. (1996) Towards an understanding of landscape scale and structure. In: Proceedings, Third International Conference/Workshop on Integrating GIS and Environmental Modeling. National Center for Geographic Information and Analysis, Santa Fe, NM

Galparsoro, I., Borja, Á., Bald, J., Liria, P. & Chust, G. (2009) Predicting suitable habitat for the European lobster (Homarus gammarus), on the Basque continental shelf (Bay of Biscay), using Ecological-Niche Factor Analysis. Ecological Modelling, 220, 556-567

Garcia, H.E., Locarnini, R.A., Boyer, T.P., Antonov, J.I., Zweng, M.M., Baranova, O.K. & Johnson, D.R. (2010a) World Ocean Atlas 2009 Volume 4: Nutrients (phosphate, nitrate, silicate) (ed. by S. Levitus). NOAA Atlas NESDIS 71, U.S. Government Printing Office, Washington, D.C., 398 pp.

Garcia, H.E., Locarnini, R.A., Boyer, T.P., Antonov, J.I., Zweng, M.M., Baranova, O.K. & Johnson, D.R. (2010b) World Ocean Atlas 2009, Volume 3: Dissolved Oxygen, Apparent Oxygen Utilization, and Oxygen Saturation (ed. by S. Levitus). NOAA Atlas NESDIS 70, U.S. Government Printing Office, Washington, D.C., 344 pp.

GEBCO (2009) General Bathymetric Chart of the Oceans (GEBCO). Hom. http://www.bodc.ac.uk/data/online_delivery/gebco/.

Genin, A., Dayton, P.K., Lonsdale, P.F. & Spiess, F.N. (1986) Corals on seamount peaks provide evidence of current acceleration over deep-sea topography. Nature, 322, 59-61

Glover, A.G. & Smith, C.R. (2003) The deep-sea floor ecosystem: current status and prospects of anthropogenic change by the year 2025. Environmental Conservation, 30, 219–241

Goldner, D.R. & Chapman, D.C. (1997) Flow and particle motion induced above a tall seamount by steady and tidal background currents. Deep Sea Research Part I: Oceanographic Research Papers, 44, 719-744

GOTECH (2002) Report of the Survey in Zone 3 of the Irish National Seabed Survey: Volume 1 - Describing the results and the methods used. In. The Geological Survey of Ireland

Grehan, A. & Shipboard Party (2010) Deep water coral and fish interaction off the west coast of Ireland, CE10014 Cruise Report. Earth and Ocean Sciences, School of Natural Sciences, NUI, Galway.

Grehan, A. & Shipboard Party (2009) A multidisciplinary investigation of ecosystem hotspots and their importance as fish habitat along the Irish and Biscay continental margins. CE0908 Cruise Report. Earth and Ocean Sciences, School of Natural Sciences, NUI, Galway.

Grehan, A., Unnithan, V., Olu-Le Roy, K. & Opderbecke, J. (2005) Fishing Impacts on Irish Deepwater Coral Reefs: Making a Case for Coral Conservation. Benthic Habitats and the Effects of Fishing (ed. by P.W. Barnes and J.P. Thomas), pp. 819-832. American Fisheries Society

Grehan, A.J., van den Hove, S., Armstrong, C.W., Long, R., Van Rensburg, T., Vikki, G., Mikkelsen, E., Mol, B. & Hain, S. (2009) Promoting Ecosystem-Based Management and the Sustainable Use and Governance of Deep-Water Resources. Oceanography, 22, 154

Guinan, J., Brown, C., Dolan, M.F.J. & Grehan, A.J. (2009a) Ecological niche modelling of the distribution of cold-water coral habitat using underwater remote sensing data. Ecological Informatics, 4, 83-92

Guinan, J., Grehan, A., Wilson, M.F.J. & Brown, C. (2009b) Quantifying relationships between video observations of cold-water coral and seafloor terrain in Rockall Trough, west of Ireland. Marine Ecology Progress Series, 375, 125-138

Guinan, J. & Leahy, Y. (2010) Habitat Mapping of Geogenic Reef Offshore Ireland. Report prepared by the Marine Institute, Galway, Ireland and Geological Survey of Ireland to the Department of the Environment, Heritage and Local Government's National Parks and Wildlife Service.

Guinotte, J.M., Davies, A.J. & Ardron, J. (2009) Global habitat suitability for reef forming coldwater corals. Report to Pew Charitable Trusts.

Guinotte, J.M. & Fabry, V.J. (2008) Ocean Acidification and Its Potential Effects on Marine Ecosystems. Annals of the New York Academy of Sciences, 1134, 320-342

Guinotte, J.M., Orr, J., Cairns, S., Freiwald, A., Morgan, L. & George, R. (2006) Will human-induced changes in seawater chemistry alter the distribution of deep-sea scleractinian corals? Frontiers in Ecology and the Environment, 4, 141-146

Guisan, A., Edwards, T.C. & Hastie, T. (2002) Generalized linear and generalized additive models in studies of species distributions: setting the scene. Ecological Modelling, 157, 89 - 100

Guisan, A., Graham, C.H., Elith, J. & Huettmann, F. (2007) Sensitivity of predictive species distribution models to change in grain size. Diversity and Distributions, 13, 332-340

Guisan, A. & Thuiller, W. (2005) Predicting species distribution: offering more than simple habitat models. Ecology Letters, 8, 993-1009

Guisan, A. & Zimmermann, N.E. (2000) Predictive habitat distribution models in ecology. Ecological Modelling, 135, 147-186

Hall-Spencer, J.M., Allain, V. & Fosså, J.H. (2002) Trawling damage to Northeast Atlantic ancient coral reefs. Proceedings of the Royal Society London, 269, 507-511

Halpern, B.S., McLeod, K.L., Rosenberg, A.A. & Crowder, L.B. (2008a) Managing for cumulative impacts in ecosystem-based management through ocean zoning. Ocean & Coastal Management, 51, 203-211

Halpern, B.S., Walbridge, S., Selkoe, K.A., Kappel, C.V., Micheli, F., D'Agrosa, C., Bruno, J.F., Casey, K.S., Ebert, C., Fox, H.E., Fujita, R., Heinemann, D., Lenihan, H.S., Madin, E.M.P., Perry, M.T., Selig, E.R., Spalding, M., Steneck, R. & Watson, R. (2008b) A Global Map of Human Impact on Marine Ecosystems. Science, 319, 948-952

Hannah, C.G., Shore, J.A., Loder, J.W. & Naimie, C.E. (2001) Seasonal Circulation on the Western and Central Scotian Shelf. Journal of Physical Oceanography, 31, 591-615

Henry, L.-A. & Roberts, J.M. (2007) Biodiversity and ecological composition of macrobenthos on cold-water coral mounds and adjacent off-mound habitat in the bathyal Porcupine Seabight, NE Atlantic. Deep Sea Research Part I: Oceanographic Research Papers, 54, 654-672

Hirzel, A.H., Hausser, J., Chessel, D. & Perrin, N. (2002) Ecological-niche factor analysis: How to compute habitat-suitability maps without absence data? Ecology, 83, 2027-2036

Holmes, K.W., Van Niel, K.P., Radford, B., Kendrick, G.A. & Grove, S.L. (2008) Modelling distribution of marine benthos from hydroacoustics and underwater video. Continental Shelf Research, 28, 1800-1810

Hovey, R.K., Van Niel, K.P., Bellchambers, L.M. & Pember, M.B. (2012) Modelling Deep Water Habitats to Develop a Spatially Explicit, Fine Scale Understanding of the Distribution of the Western Rock Lobster, Panulirus cygnus. PLoS ONE, 7, e34476

Howell, K.L. & Davies, J.S. (2010) Deep-sea species image catalogue. Marine Biology and Ecology Research Centre, Marine Institute at the University of Plymouth. On-line version http://www.marlin.ac.uk/deep-sea-species-image-catalogue/.

Howell, K.L., Davies, J.S. & Narayanaswamy, B.E. (2010) Identifying deep-sea megafaunal epibenthic assemblages for use in habitat mapping and marine protected area network design. Journal of the Marine Biological Association of the United Kingdom, 90, 33-68

Howell, K.L., Holt, R., Endrino, I.P. & Stewart, H. (2011) When the species is also a habitat: Comparing the predictively modelled distributions of Lophelia

pertusa and the reef habitat it forms. Biological Conservation, 144, 2656-2665

Huang, Z., Brooke, B. & Li, J. (2011) Performance of predictive models in marine benthic environments based on predictions of sponge distribution on the Australian continental shelf. Ecological Informatics, 6, 205-216

Hutchinson, G.E. (1957) Concluding remarks. Population studies: animal ecology and demography. Cold Spring Harbor Symposia on Quantitative Biology, 22, 415-427

Huthnance, J.M. (1974) On the diurnal tidal currents over Rockall Bank. Deep Sea Research and Oceanographic Abstracts, 21, 23-35

Huthnance, J.M. (1981) Waves and currents near the continental shelf edge. Progress In Oceanography, 10, 193-226

Huthnance, J.M. (1986) The Rockall slope current and shelf-edge processes. Proceedings of the Royal Society of Edinburgh Section B: Biology, 88, 83-101

Huvenne, V.A.I., Beyer, A., de Haas, H., Dekindt, K., Henriet, J.P., Kozachenko, M., Olu-Le Roy, K., Wheeler, A.J., TOBI/Pelagia & 197 CARACOLE cruise participants (2005) The seabed appearance of different coral bank provinces in the Porcupine Seabight, NE Atlantic: results from sidescan sonar and ROV seabed mapping. Cold-water corals and ecosystems (ed. by A. Freiwald and J.M. Roberts), pp. 535–569. Springer, Berlin Heidelberg New York.

Huvenne, V.A.I., Tyler, P.A., Masson, D.G., Fisher, E.H., Hauton, C., Huehnerbach, V., Le Bas, T.P. & Wolff, G.A. (2011) A Picture on the Wall: Innovative Mapping Reveals Cold-Water Coral Refuge in Submarine Canyon. PLoS ONE, 6, e28755

Jiménez-Valverde, A. & Lobo, J.M. (2007) Threshold criteria for conversion of probability of species presence to either-or presence-absence. Acta Oecologica, 31, 361-369

Jiménez-Valverde, A., Lobo, J.M. & Hortal, J. (2008) Not as good as they seem: the importance of concepts in species distribution modelling. Diversity and Distributions, 14, 885-890

JNCC (2009) The Habitats Directive: selection of Special Areas of Conservation in the UK. JNCC Report, 33 pp. www.jncc.gov.uk/SACselection.

Katsanevakis, S., Stelzenmüller, V., South, A., Sørensen, T.K., Jones, P.J.S., Kerr, S., Badalamenti, F., Anagnostou, C., Breen, P., Chust, G., D'Anna, G., Duijn, M., Filatova, T., Fiorentino, F., Hulsman, H., Johnson, K., Karageorgis, A.P., Kröncke, I., Mirto, S., Pipitone, C., Portelli, S., Qiu, W., Reiss, H., Sakellariou, D., Salomidi, M., van Hoof, L., Vassilopoulou, V., Vega Fernández, T., Vöge, S., Weber, A., Zenetos, A. & ter Hofstede, R. (2011) Ecosystem-based marine spatial management: Review of concepts, policies, tools, and critical issues. Ocean & Coastal Management, 54, 807-820

Kendall, M.S. & Miller, T. (2008) The Influence of Thematic and Spatial Resolution on Maps of a Coral Reef Ecosystem. Marine Geodesy, 31, 75 - 102

Kenny, A.J., Cato, I., Desprez, M., Fader, G., Schuttenhelm, R.T.E. & Side, J. (2003) An overview of seabed-mapping technologies in the context of marine habitat classification. ICES Journal of Marine Science, 60, 411-418

Kenyon, N.H., Akhmetzhanov, A.M., Wheeler, A.J., Van Weering, T.C.E., De Haas, H. & Ivanov, M.K. (2003) Giant carbonate mud mounds in the southern Rockall Trough. Marine Geology, 195, 5-30

Key, R.M., Kozyr, A., Sabine, C.L., Lee, K., Wanninkhof, R., Bullister, J.L., Feely, R.A., Millero, F.J., Mordy, C. & Peng, T.H. (2004) A global ocean carbon climatology: Results from Global Data Analysis Project (GLODAP). Global Biogeochemical Cycles, 18, GB4031

Kienzle, S. (2004) The Effect of DEM Raster Resolution on First Order, Second Order and Compound Terrain Derivatives. Transactions in GIS, 8, 83-111

Kostylev, V.E. & Hannah, C.G. (2007) Process-Driven Characterization and Mapping of Seabed Habitats. Mapping the Seafloor for Habitat Characterization: Geological Association of Canada, Special Paper 47 (ed. by B.J. Todd and H.G. Greene), pp. 171-184.

Kostylev, V.E., Todd, B.J., Fader, G.B.J., Courtney, R.C., Cameron, G.D.M. & Pickrill, R.A. (2001) Benthic habitat mapping on the Scotian Shelf based on multibeam bathymetry, surficial geology and sea floor photographs. Marine Ecology Progress Series, 219, 121–137

Kunze, E. & Smith, S.G.L. (2004) The role of small-scale topography in turbulent mixing of the global ocean. Oceanography, 17, 55-64

Lavaleye, M.S.S. & Shipboard Party (2010) CoralFish-HERMIONE cruise report 64PE324, Texel-Vigo 10 Sept – 2 Oct 2010. NIOZ cruise report, 49pp

Lavelle, J.W. & Mohn, C. (2010) Motion, commotion, and biophysical connections at Deep Ocean Seamounts. Oceanography, 23, 90-103

Le Danois, E. (1948) Les Profondeurs de la Mer. Payot, Paris, 303 pp.

Le Goff-Vitry, M.C., Pybus, O.G. & Rogers, A.D. (2004) Genetic structure of the deep-sea coral Lophelia pertusa in the northeast Atlantic revealed by microsatellites and internal transcribed spacer sequences. Molecular Ecology, 13, 537-549

Leathwick, J., Moilanen, A., Francis, M., Elith, J., Taylor, P., Julian, K., Hastie, T. & Duffy, C. (2008) Novel methods for the design and evaluation of marine protected areas in offshore waters. Conservation Letters, 1, 91-102

Legg, S. & Klymak, J. (2008) Internal Hydraulic Jumps and Overturning Generated by Tidal Flow over a Tall Steep Ridge. Journal of Physical Oceanography, 38, 1949-1964

Lek, S. & Guègan, J.F. (1999) Artificial neural networks as a tool in ecological modelling, an introduction. Ecological Modelling, 120, 65-73

Leverette, T. & Metaxas, A. (2005) Predicting habitat for two species of deep-water coral on the Canadian Atlantic continental shelf and slope. Cold-Water Corals and Ecosystems (ed. by A. Freiwald and J.M. Roberts), pp. 467-479.

Levin, L. (2006) Recent progress in understanding larval dispersal: new directions and digressions. Integrative and Comparative Biology, 46, 282-297

Lima, F.P., Ribeiro, P.A., Queiroz, N., Xavier, R., Tarroso, P., Hawkins, S.J. & Santos, A.M. (2007) Modelling past and present geographical distribution of the marine gastropod Patella rustica as a tool for exploring responses to environmental change. Global Change Biology, 13, 2065-2077

Liu, C., Berry, P.M., Dawson, T.P. & Pearson, R.G. (2005) Selecting thresholds of occurrence in the prediction of species distributions. Ecography, 28, 385-393

Lobo, J.M., Jimènez-Valverde, A. & Real, R. (2007) AUC: a misleading measure of the performance of predictive distribution models. Global Ecology and Biogeography, 17, 145-151

Locarnini, R.A., Mishonov, A.V., Antonov, J.I., Boyer, T.P., Garcia, H.E., Baranova, O.K., Zweng, M.M. & Johnson, D.R. (2010) World Ocean Atlas 2009, Volume 1: Temperature (ed. by S. Levitus). NOAA Atlas NESDIS 68, U.S. Government printing office,Washington, D.C., 184 pp.

Long, R. & Grehan, A. (2002) Marine Habitat Protection in Sea Areas under the Jurisdiction of a Coastal Member State of the European Union: The Case of Deep-Water Coral Conservation in Ireland. The International Journal of Marine and Coastal Law, 17, 235-261

Longley, P.A., Goodchild, M.F., Maguire, D.J. & Rhind, D.W. (2005) Geographic Information Systems and Science. John Wiley & Sons Ltd.

Lundblad, E.R., Wright, D.J., Miller, J.R., Larkin, E.M., Rinehart, R., Naar, D.F., Donahue, B.T., Anderson, S.M. & Battista, T. (2006) A Benthic Terrain Classification Scheme for American Samoa. Marine Geodesy, 29, 89-111

MacKey, B.G. & Lindenmayer, D.B. (2001) Towards a Hierarchical Framework for Modelling the Spatial Distribution of Animals. Journal of Biogeography, 28, 1147-1166

Marine Institute (2012) Northeast Atlantic Operational Model, accessible at www.marine.ie/home/services/operational/oceanography/OceanForecast.htm

Marks, K. & Smith, W. (2006) An Evaluation of Publicly Available Global Bathymetry Grids. Marine Geophysical Researches, 27, 19-34

Marshall, C.E. (2012) Species distribution modelling to support marine conservation planning. PhD Thesis. University of Plymout, UK.

Mienis, F., de Stigter, H.C., White, M., Duineveld, G., de Haas, H. & van Weering, T.C.E. (2007) Hydrodynamic controls on cold-water coral growth and carbonate-mound development at the SW and SE Rockall Trough Margin, NE Atlantic Ocean. Deep Sea Research Part I: Oceanographic Research Papers, 54, 1655-1674

Mienis, F., van Weering, T., de Haas, H., de Stigter, H., Huvenne, V. & Wheeler, A. (2006) Carbonate mound development at the SW Rockall Trough margin based on high resolution TOBI and seismic recording. Marine Geology, 233, 1-19

Mohn, C. & Beckmann, A. (2002) Numerical studies on flow amplification at an isolated shelfbreak bank, with application to Porcupine Bank. Continental Shelf Research, 22, 1325-1338

Morrison, C.L., Ross, S.W., Nizinski, M.S., Brooke, S., Järnegren, J., Waller, R.G., Johnson, R.L. & King, T.L. (2011) Genetic discontinuity among regional populations of Lophelia pertusa in the North Atlantic Ocean. Conservation Genetics, 12, 713-729

NEAFC (2010) Information on the protection of biodiversity and mitigating impact of fisheries in the North-East Atlantic. A report prepared by the NEAFC Secretariat forCBD COP 10 Agenda item 5.2 and 5.4, Nagoya; October 2010.

New, A.L. & Smythe-Wright, D. (2001) Aspects of the circulation in the Rockall Trough. Continental Shelf Research, 21, 777-810

Nycander, J. (2005) Generation of internal waves in the deep ocean by tides. Journal of Geophysical Research, 110, C10028

O'Hara, T.D. & Tittensor, D.P. (2010) Environmental drivers of ophiuroid species richness on seamounts. Marine Ecology, 31, 26-38

O'Leary, B.C., Brown, R.L., Johnson, D.E., von Nordheim, H., Ardron, J., Packeiser, T. & Roberts, C.M. (2012) The first network of marine protected areas (MPAs) in the high seas: The process, the challenges and where next. Marine Policy, 36, 598-605

Olu-Le Roy, K., Caprais, J.-C., Crassous, P., Dejonghe, E., Eardley, D., Freiwald, A., Galeron, J., Grehan, A., Henriet, J.P., Huvenne, V., Lorance, P., Noel, P., Opderbecke, J., Pitout, C., Sibuet, M., Unnithan, V., Vacelet, J., van Weering, T., Wheeler, A. & Zibrowius, H. (2002) Caracole Cruise, N/O Atalante and ROV Victor, 1+2. In. Ifremer, Brest

Orejas, C., Gori, A., Lo Iacono, C., Puig, P., Gili, J.M. & Dale, M.R.T. (2009) Cold-water corals in the Cap de Creus canyon, northwestern Mediterranean: spatial distribution, density and anthropogenic impact. Marine Ecology Progress Series, 397, 37-51

Orr, J.C., Fabry, V.J., Aumont, O., Bopp, L., Doney, S.C., Feely, R.A., Gnanadesikan, A., Gruber, N., Ishida, A., Joos, F., Key, R.M., Lindsay, K., Maier-Reimer, E., Matear, R., Monfray, P., Mouchet, A., Najjar, R.G., Plattner, G.-K., Rodgers, K.B., Sabine, C.L., Sarmiento, J.L., Schlitzer, R., Slater, R.D., Totterdell, I.J., Weirig, M.-F., Yamanaka, Y. & Yool, A. (2005) Anthropogenic ocean acidification over the twenty-first century and its impact on calcifying organisms. Nature, 437, 681-686

OSPAR (2010) 2009/10 Status Report on the OSPAR Network of Marine Protected Areas. Biodiversity Series 2010, 62 pp.

Otero. P., Ruiz-Villareal, M. & Peliz, A. (2008) Variability of river plumes off Northwest Iberia in response to wind events. Journal of Marine Systems 72, 238 – 255.

Pearce, J.L. & Boyce, M.S. (2006) Modelling distribution and abundance with presence-only data. Journal of Applied Ecology, 43, 405-412

Pearson, R.G. & Dawson, T.P. (2003) Predicting the impacts of climate change on the distribution of species: are bioclimate envelope models useful? Global Ecology & Biogeography, 12, 361-371

Penven, P., Debreu, L., Marchesiello, P. & McWilliams, J.C. (2006) Evaluation and application of the ROMS 1-way embedding procedure to the central California upwelling system. Ocean Modelling, 12, 157-187

Peterson, A.T. (2003) Predicting the Geography of Species' Invasions via Ecological Niche Modeling. The Quaterly Review of Biology, 78, 419-433

Phillips, S.J. (2005) A brief tutorial on Maxent. AT&T Research, Florham Park, New Jersey. Available at: http://www.cs.princeton.edu/schapire/maxent/tutorial/tutorial.doc (last accessed February 2012).

Phillips, S.J. (2008) Transferability, sample selection bias and background data in presence-only modelling: a response to Peterson et al. (2007). Ecography, 31, 272-278

Phillips, S.J., Anderson, R.P. & Schapire, R.E. (2006) Maximum entropy modeling of species geographic distributions. Ecological Modelling, 190, 231-259

Phillips, S.J., Dudìk, M., Elith, J., Graham, C.H., Lehmann, A., Leathwick, J. & Ferrier, S. (2009) Sample selection bias and presence-only distribution

models: implications for background and pseudo-absence data. Ecological Applications, 19, 181-197

Pingree, R.D., Sinha, B. & Griffiths, C.R. (1999) Seasonality of the European slope current (Goban Spur) and ocean margin exchange. Continental Shelf Research 19, 929-975

Pingree, R.D. & Le Cann, B. (1990) Structure, strength and seasonality of the slope currents in the Bay of Biscay region. Journal of the Marine Biological Association of the United Kingdom, 70 (4), 857 – 885Pingree, R.D., Sinha, B. & Griffiths C.R. (1999) Seasonality of the European slope current (Goban Spur) and ocean margin exchange. Continental Shelf Research 19, 929-975

Pittman, S.J., Christensen, J.D., Caldow, C., Menza, C. & Monaco, M.E. (2007) Predictive mapping of fish species richness across shallow-water seascapes in the Caribbean. Ecological Modelling, 204, 9-21

Purser, A., Bergmann, M., Lundälv, T., Öntrup, J. & Nattkemper, T.W. (2009) Use of machine-learning algorithms for the automated detection of cold-water coral habitats: a pilot study. Marine Ecology Progress Series, 397, 241-251

Ramirez-Llodra, E., Brandt, A., Danovaro, R., Escobar, E., German, C.R., Levin, L.A., Arbizu, P.M., Menot, L., Buhl-Mortensen, P., Narayanaswamy, B.E., Smith, C.R., Tittensor, D.P., Tyler, P.A., Vanreusel, A. & Vecchione, M. (2010) Deep, diverse and definitely different: Unique attributes of the world's largest ecosystem. Biogeosciences Discussions, 7, 2361-2485

Ramirez-Llodra, E., Tyler, P.A., Baker, M.C., Bergstad, O.A., Clark, M.R., Escobar, E., Levin, L.A., Menot, L., Rowden, A.A., Smith, C.R. & Van Dover, C.L. (2011) Man and the Last Great Wilderness: Human Impact on the Deep Sea. PLoS ONE, 6, e22588

Reiss, H., Cunze, S., König, K., Neumann, H. & Kröncke, I. (2011) Species distribution modelling of marine benthos: a North Sea case study. Marine Ecology Progress Series, 442, 71-86

Rengstorf, A., Grehan, A., Yesson, C. & Brown, C. (2012) Towards high resolution habitat suitability modelling of vulnerable marine ecosystems in the deep-sea: resolving terrain attribute dependencies. Marine Geodesy, 35, 343-361

Rengstorf, A., Yesson, C., Brown, C. & Grehan, A. (in press) High resolution habitat suitability modelling can improve conservation of vulnerable marine ecosystems in the deep sea. Journal of Biogeography

Rhines, P. (1970) Edge-, bottom-, and Rossby waves in a rotating stratified fluid. Geophysical and Astrophysical Fluid Dynamics, 1, 273-302

Roberts, J.M., Henry, L.-A., Longand, D. & Hartley, J.P. (2008) Cold-water coral reef frameworks, megafaunal communities and evidence for coral carbonate mounds on the Hatton Bank, north east Atlantic. Facies, 54, 297-316

Roberts, J.M., Wheeler, A.J. & Freiwald, A. (2006) Reefs of the Deep: The Biology and Geology of Cold-Water Coral Ecosystems. Science, 312, 543-547

Roberts, J.M., Wheeler, A.J., Freiwald, A. & Cairns, S. (2009) Cold-Water Corals - The Biology and Geology of Deep-Sea Coral Habitats. Cambridge University Press, New York.

Robertson, R. (2006) Modeling internal tides over Fieberling Guyot: resolution, parameterization, performance. Ocean Dynamics, 56, 430-444

Robinson, L.M., Elith, J., Hobday, A.J., Pearson, R.G., Kendall, B.E., Possingham, H.P. & Richardson, A.J. (2011) Pushing the limits in marine species

distribution modelling: lessons from the land present challenges and opportunities. Global Ecology and Biogeography, 20, 789–802

Rodolfo-Metalpa, R., Houlbreque, F., Tambutte, E., Boisson, F., Baggini, C., Patti, F.P., Jeffree, R., Fine, M., Foggo, A., Gattuso, J.P. & Hall-Spencer, J.M. (2011) Coral and mollusc resistance to ocean acidification adversely affected by warming. Nature Climate Change, 1, 308-312

Rogers, A.D. (1999) The biology of Lophelia pertusa (Linnaeus 1758) and other deep-water reef-forming corals and impacts from human activities. International review of hydrobiology, 84, 315-406

Rogers, A.D., Clark, M.R., Hall-Spencer, J.M. & Gjerde, K.M. (2008) The Science behind the Guidelines: A Scientific Guide to the FAO Draft International Guidelines (December 2007) For the Management of Deep-Sea Fisheries in the High Seas and Examples of How the Guidelines May Be Practically Implemented. IUCN, Switzerland.

Ross, S.W., Carlson, M.C.T. & Quattrini, A.M. (2012) The utility of museum records for documenting distributions of deep-sea corals off the southeastern United States. Marine Biology Research, 8, 101-114

Schmidt, J. & Andrew, R. (2005) Multi-scale landform characterization. Area, 37, 341-350

Schoening, T., Bergmann, M., Ontrup, J., Taylor, J., Dannheim, J., Gutt, J., Purser, A. & Nattkemper, T.W. (2012) Semi-Automated Image Analysis for the Assessment of Megafaunal Densities at the Arctic Deep-Sea Observatory HAUSGARTEN. PLoS ONE, 7, e38179

Segurado, P. & Araújo, M.B. (2004) An evaluation of methods for modelling species distributions. Journal of Biogeography, 31, 1555-1568

Seo, C., Thorne, J.H., Hannah, L. & Thuiller, W. (2009) Scale effects in species distribution models: implications for conservation planning under climate change. Biol. Lett., 5, 39–43

Shchepetkin, A.F. & McWilliams, J.C. (2003) A method for computing horizontal pressure-gradient force in an oceanic model with a nonaligned vertical coordinate. Journal of Geophysical Research, 108, 3090

Shchepetkin, A.F. & McWilliams, J.C. (2005) The regional oceanic modeling system (ROMS): a split-explicit, free-surface, topography-following-coordinate oceanic model. Ocean Modelling, 9, 347-404

Smith, K.L., Ruhl, H.A., Bett, B.J., Billett, D.S.M., Lampitt, R.S. & Kaufmann, R.S. (2009) Climate, carbon cycling and deep-ocean ecosystems. Proceedings of the National Academy of Sciences, 106, 19211-19218

St. Laurent, L. & Garrett, C. (2002) The role of internal tides in mixing the deep ocean. Journal of Physical Oceanography, 32, 2882-2899

Stigall, A.L. (2009) Using ecological niche modelling to evaluate niche stability in deep time. Journal of Biogeography, 39, 772-781

Stockwell, D. & Peters, D. (1999) The GARP modelling system: problems and solutions to automated spatial prediction. International Journal of Geographical Information Science, 13, 143-158

Sutton, T., de Giovanni, R. & Ferreira de Siqueira, M. (2007) Introducing openModeller - A fundamental niche modelling framework. OSGeo Journal, 1, 1-6

Symmons, C. (2000) Ireland and the law of the sea. Round Hall Sweet & Maxwell, Dublin (Ireland), September 2000, 485pp

Sørensen, R. & Seibert, J. (2007) Effects of DEM resolution on the calculation of topographical indices: TWI and its components. Journal of Hydrology, 347, 79-89

Thiem, Ø., Ravagnan, E., Fosså, J.H. & Berntsen, J. (2006) Food supply mechanisms for cold-water corals along a continental shelf edge. Journal of Marine Systems, 60, 207-219

Thomas, C.D., Cameron, A., Green, R.D., Bakkenes, M., Beaumont, L.J., Collingham, Y.C., Erasmus, B.F.N., de Siqueira, M.F., Grainger, A., Hannah, L., Hughes, L., Huntley, B., van Jaarsveld, A.S., Midgley, G.F., Miles, L., Ortega–Huerta, M.A., Peterson, A.T., Phillips, O.L. & Williams, S.E. (2004) Extinction risk from climate change. Nature, 427, 145–148

Thomson, C.W. (1873) The Depths of the Sea. 57 pp

Thuiller, W., Lafourcade, B., Engler, R. & Araùjo, M.B. (2009) BIOMOD - a platform for ensemble forecasting of species distributions. Ecography, 32, 369-373

Tittensor, D.P., Baco, A.R., Brewin, P.E., Clark, M.R., Consalvey, M., Hall-Spencer, J., Rowden, A.A., Schlacher, T., Stocks, K.I. & Rogers, A.D. (2009) Predicting global habitat suitability for stony corals on seamounts. Journal of Biogeography, 36, 1111-1128

Tittensor, D.P., Baco, A.R., Hall-Spencer, J.M., Orr, J.C. & Rogers, A.D. (2010a) Seamounts as refugia from ocean acidification for cold-water stony corals. Marine Ecology, 31, 212-225

Tittensor, D.P., Mora, C., Jetz, W., Lotze, H.K., Ricard, D., Berghe, E.V. & Worm, B. (2010b) Global patterns and predictors of marine biodiversity across taxa. Nature, 466, 1098-1101

Tong, R., Purser, A., Guinan, J. & Unnithan, V. (2012) Modeling the habitat suitability for deep-water gorgonian corals based on terrain variables. Ecological Informatics

Tracey, D.M., Rowden, A.A., Mackay, K.A. & Compton, T. (2011) Habitat-forming cold-water corals show affinity for seamounts in the New Zealand region. Marine Ecology Progress Series, 430, 1-22

Tyberghein, L., Verbruggen, H., Pauly, K., Troupin, C., Mineur, F. & De Clerck, O. (2012) Bio-ORACLE: a global environmental dataset for marine species distribution modelling. Global Ecology and Biogeography, 21, 272-281

Ullgren, J.E. & White, M. (2010) Water mass interaction at intermediate depths in the southern Rockall Trough, northeastern North Atlantic. Deep Sea Research Part I: Oceanographic Research Papers, 57, 248-257

UNEP (2007) Deep-Sea Biodiversity and Ecosystems: A scoping report on their socio-economy, management and governance. 88 pp

UNEP (2011) Taking Steps toward Marine and Coastal Ecosystem-Based Management - An Introductory Guide. UNEP Regional Seas Reports and Studies No. 189.

UNGA (2006) UNGA, 2006. Sustainable fisheries, including through the 1995 agreement for the implementation of the provisions of the United Nations Convention on the Law of the Sea of 10 December 1982 relating to the conservation and management of straddling fish stocks and highly migratory

fish stocks, and related instruments. Ref. A/RES/61/105, 21. New York: United Nations.

van der Wal, J., Shoo, L.P., Graham, C. & Williams, S.E. (2009) Selecting pseudo-absence data for presence-only distribution modeling: How far should you stray from what you know? Ecological Modelling, 220, 589-594

van Oevelen, D., Duineveld, G., Lavaleye, M., Mienis, F., Soetaert, K. & Heipa, C.H.R. (2009) The cold-water coral community as a hot spot for carbon cycling on continental margins: A food-web analysis from Rockall Bank (northeast Atlantic). Limnological Oceanography, 54, 1829–1844

Van Rooij, D., De Mol, B., Huvenne, V., Ivanov, M. & Henriet, J.P. (2003) Seismic evidence of current-controlled sedimentation in the Belgica mound province, upper Porcupine slope, southwest of Ireland. Marine Geology, 195, 31-53

van Weering, T.C.E., de Haas, H., de Stigter, H.C., Lykke-Andersen, H. & Kouvaev, I. (2003) Structure and development of giant carbonate mounds at the SW and SE Rockall Trough margins, NE Atlantic Ocean. Marine Geology, 198, 67-81

Veloz, S.D. (2009) Spatially autocorrelated sampling falsely inflates measures of accuracy for presence-only niche models. Journal of Biogeography, 36, 2290-2299

Verfaillie, E., Du Four, I., Van Meirvenne, M. & Van Lancker, V. (2008) Geostatistical modeling of sedimentological parameters using multi-scale terrain variables: application along the Belgian Part of the North Sea. International Journal of Geographical Information Science, 23, 135-150

Vertino, A., Savini, A., Rosso, A., Di Geronimo, I., Mastrototaro, F., Sanfilippo, R., Gay, G. & Etiope, G. (2010) Benthic habitat characterization and distribution from two representative sites of the deep-water SML Coral Province (Mediterranean). Deep Sea Research Part II: Topical Studies in Oceanography, 57, 380-396

Wade, P.R. (2000) Bayesian methods in conservation biology. Conservation Biology, 14, 1308–1316

Waller, R. & Tyler, P. (2005) The reproductive biology of two deep-water, reef-building scleractinians from the NE Atlantic Ocean. Coral reefs, 24, 514-522

Walters, R.A., Goring, D.G. & Bell, R.G. (2001) Ocean tides around New Zealand. New Zealand Journal of Marine and Freshwater Research, 35, 567-579

Watts, M.E., Ball, I.R., Stewart, R.S., Klein, C.J., Wilson, K., Steinback, C., Lourival, R., Kircher, L. & Possingham, H.P. (2009) Marxan with Zones: Software for optimal conservation based land- and sea-use zoning. Environmental Modelling & Software, 24, 1513-1521

Weaver, P.P.E., Benn, A., Arana, P.M., Ardron, J.A., Bailey, D.M., Baker, K., Billett, D.S.M., Clark, M.R., Davies, A.J. & Duran Munoz, P. (2011) The impact of deep-sea fisheries and implementation of the UNGA Resolutions 61/105 and 64/72.

Weiss, A.D. (2001) Topographic Position and Landforms Analysis. Poster presentation, ESRI User Conference, San Diego, CA.

Wheeler, A., Beyer, A., Freiwald, A., de Haas, H., Huvenne, V., Kozachenko, M., Olu-Le Roy, K. & Opderbecke, J. (2007) Morphology and environment of cold-water coral carbonate mounds on the NW European margin. International Journal of Earth Sciences, 96, 37-56

Wheeler, A.J., Bett, B.J., Billett, D.S.M., Masson, D.G. & Mayor, D. (2005) The impact of demersal trawling on NE Atlantic deepwater coral habitats: the case of the Darwin Mounds, United Kingdom. Benthic habitats and the effects of fishing (ed. by P. Barnes), pp. 807-817. American Fisheries Society, Bethesda MD, USA, .

White, M. (2007) Benthic dynamics at the carbonate mound regions of the Porcupine Sea Bight continental margin. International Journal of Earth Sciences, 96, 1-9

White, M. & Dorschel, B. (2010) The importance of the permanent thermocline to the cold water coral carbonate mound distribution in the NE Atlantic. Earth and Planetary Science Letters, 296, 395-402

White, M., Mohn, C., Stigter, H. & Mottram, G. (2005) Deep-water coral development as a function of hydrodynamics and surface productivity around the submarine banks of the Rockall Trough, NE Atlantic. Cold-Water Corals and Ecosystems, pp. 503-514.

White, M., Roberts, J. & van Weering, T. (2007) Do bottom-intensified diurnal tidal currents shape the alignment of carbonate mounds in the NE Atlantic? Geo-Marine Letters, 27, 391-397

Wiens, J.A. (2002) Predicting species occurrences: progress, problems, and prospects. Predicting species occurrences: issues of accuracy and scale (ed. by J.M. Scott, P.J. Heglund, F. Samson, J. Haufler, M. Morrison, M. Raphael and B. Wall), pp. 739–749. Island Press, Covelo, California.

Williams, S.B., Pizarro, O., Webster, J.M., Beaman, R.J., Mahon, I., Johnson-Roberson, M. & Bridge, T.C.L. (2010) Autonomous underwater vehicle–assisted surveying of drowned reefs on the shelf edge of the Great Barrier Reef, Australia. Journal of Field Robotics, 27, 675-697

Wilson, K.A., Westphal, M.I., Possingham, H.P. & Elith, J. (2005) Sensitivity of conservation planning to different approaches to using predicted species distribution data. Biological Conservation, 122, 99-112

Wilson, M.F.J., O'Connell, B., Brown, C., Guinan, J.C. & Grehan, A.J. (2007) Multiscale Terrain Analysis of Multibeam Bathymetry Data for Habitat Mapping on the Continental Slope. Marine Geodesy, 30, 3–35

Wisz, M.S., Hijmans, R.J., Li, J., Peterson, A.T., Graham, C.H. & Guisan, A. (2008) Effects of sample size on the performance of species distribution models. Diversity and Distributions, 14, 763-773

WOA (2009) downloaded from http://www.nodc.noaa.gov/OC5/WOA09/pr_woa09.html

Wolock, D.M. & McCabe, G.J. (2000) Differences in topographic characteristics computed from 100- and 1000-m resolution digital elevation model data. Hydrological Processes, 14, 987-1002

Wood, J. (1996) The geomorphological characterisation of digital elevation models. PhD thesis. University of Leicester (http://www.soi.city.ac.uk/~jwo/phd).

Woodby, D., Carlile, D. & Hulbert, L. (2009) Predictive modeling of coral distribution in the Central Aleutian Islands, USA. Marine Ecology Progress Series, 397, 227-240

Yesson, C., Taylor, M.L., Tittensor, D.P., Davies, A.J., Guinotte, J., Baco, A., Black, J., Hall-Spencer, J.M. & Rogers, A.D. (2012) Global habitat suitability of cold-water octocorals. Journal of Biogeography, 39, 1278-1292